eM-Brace: Development of an Autonomous Wrist Splint with an Integrated Massage System for Alleviating Muscle Weakness Related to Carpal Tunnel Syndrome

A Senior Design Project

Presented to the Faculty of the Engineering Department

College of Science, Information Technology, and Engineering

ATENEO DE ZAMBOANGA UNIVERSITY

by:

Chezter P. Vargas

Mark Vincent G. Salupado

Rosen Gabriel Garcia, ECE

Adviser

November 2025

TABLE OF CONTENTS

LIST OF FIGURES

LIST OF TABLES

ACKNOWLEDGEMENTS

The successful completion of this thesis would not have been possible without the support, advice, and encouragement of numerous individuals and institutions. We take this opportunity to express our sincere appreciation to all those who played a role in our research, whether through direct involvement, guidance, or moral support.

First and foremost, we extend our deepest gratitude to God Almighty, whose unwavering guidance and blessings have given us the strength, wisdom, and perseverance to complete this research. Throughout moments of difficulty and uncertainty, His grace has provided clarity and resilience, allowing us to overcome the many challenges we encountered. His divine presence has been a constant source of motivation, pushing us to strive for excellence and to trust in the process, even when the path seemed unclear. It is through His wisdom and blessings that we have reached this milestone, and we dedicate this accomplishment to Him.

Our deepest gratitude also goes to our adviser, Sir Rosen Gabriel Garcia, whose expertise, dedication, and thoughtful guidance have been vital to the success of this study. His insights and constructive feedback have sharpened our research direction and strengthened the quality of our work. His support throughout the development of this project has inspired us to maintain a high standard of rigor and innovation. We would also like to acknowledge Ma'am Mudznalyn B. Usama, BME, for her invaluable technical guidance and support, which greatly contributed to the refinement of this research.

We would also like to extend our sincere gratitude to Mr. Roel Rojas and the Biomedical Engineering Team at Zamboanga City Medical Center for their generosity in lending us their time,

expertise, and equipment throughout the development of our prototype. Their technical knowledge and hands-on guidance played a crucial role in refining our design and improving the functionality of our device.

We would also like to extend our deepest appreciation to Mr. Dave Vargas and Mrs. Anabel Vargas, parents of Chezter Vargas, and Mr. Elmer Salupado and Mrs. Rhodora Salupado, parents of Mark Vincent Salupado for their heartfelt encouragement and words of support. Their kindness and unwavering belief in our abilities helped us push forward during moments of struggle. Their comforting words and reassurance provided the emotional strength needed to continue, reminding us that we were never alone in this journey. Their support, though unexpected, has left a lasting impact, and for that, we are truly grateful.

We also extend our heartfelt gratitude to Joan Doris Bazan for her invaluable moral support and for introducing us to her father, Mr. Jose Bazan, whose guidance and insightful advice have been incredibly helpful throughout this journey. As such, we would also like to express our appreciation to Francis Jerus Rabaca for his assistance in building the prototype, which played a crucial role in bringing our project to life.

We are immensely grateful to our research panelists, Ms. Abigail Joy C. Subido, Ms. Carmellie Anne A. Plaza, and Sir Abdul Hadi Nograles, for their critical insights and valuable recommendations, which significantly refined both our thesis and prototype. In particular, we extend special thanks to Sir Hadi Nograles, our thesis coordinator, whose unwavering commitment and guidance ensured we remained on track throughout the research process; his dedication and willingness to provide direction at every stage were invaluable in strengthening

the technical aspects and methodology of our work.

We also extend our heartfelt thanks to Ma'am Janet G. Tan, Chair of the School of Engineering and Architecture, and Ma'am Joselyn D. Partosa, our Dean, for fostering an environment that promotes research excellence and continuous learning. Their leadership and commitment to academic development have provided us with the resources and opportunities necessary to carry out our study successfully.

Last but not the least, we would like to express our sincere gratitude to Ateneo de Zamboanga University for equipping us with the knowledge, facilities, and academic foundation needed to pursue this research. The institution's unwavering support has played a fundamental role in the realization of this study, and we are honored to be part of its academic community.

ABSTRACT

Carpal Tunnel Syndrome (CTS) is a prevalent musculoskeletal disorder caused by median nerve compression, leading to pain, numbness, and weakened grip strength. Conventional wrist splints often restrict wrist motion and lack therapeutic functions that promote recovery. This study introduces the eM-Brace, an autonomous wrist splint that integrates a surface electromyography (sEMG)-activated myofascial release massage system. sEMG sensors positioned on the Abductor Pollicis Brevis muscle detect rest conditions, triggering the massage mechanism only when the wrist is inactive. The device includes an Integrated Massager calibrated to deliver 1.36 kPa of therapeutic pressure, an Auto-Fit Module maintaining consistent support pressure of approximately 3.68 kPa, and a Motion Support Module that loosens during activity, allowing up to 10° flexion and 30° extension. Functional testing verified 100 % accuracy in classifying muscle states and 80 % accuracy in delivering target pressure. In beta testing with 15 participants subjected to induced CTS symptoms, 73 % showed grip strength improvements exceeding 2.2 kg, and mean pain scores dropped from 3.27 to 0.33. The eM-Brace demonstrates a lightweight, non-invasive, and adaptive alternative to static splints.

Keywords: Carpal Tunnel Syndrome, sEMG, Myofascial Release, Wrist Splint, Rehabilitation

CHAPTER I
INTRODUCTION

Background of the Study

The median nerve is a motor-sensory mixed nerve critical in controlling movement and sensation of the first three fingers (the thumb, index, and middle finger) and the wrist. It originates from the lateral and medial cords of the brachial plexus by nerve roots C6-T1 and passes through various canals, such as the carpal tunnel [1], [2]. Furthermore, its structure is made more complex by anatomical variations, such as branches or median-ulnar communicating branches, as well as its delicate fascicular microanatomy and intricate blood supply. As such, these factors increase the nerve's susceptibility to compression and complicate treatment when injury occurs [1].

In addition, this vulnerability is often exacerbated by modern daily activities that place repeated strain on the wrist, such as typing, drawing, playing sports like basketball, or performing manual labor (e.g., carpentry, assembly line work, or construction). Over time, these repetitive motions can inflame the wrist, increasing pressure in the carpal tunnel and compressing the median nerve, ultimately leading to a condition known as Carpal Tunnel Syndrome (CTS) [1], [2], [3].

Given the widespread nature of these activities, it is no surprise that CTS has a high incidence rate. Recent studies [4], [5] report that CTS is most common among adults aged 40 to 60, affecting approximately 8.0% of the general population while being markedly higher in women. Additionally, the condition was shown to be particularly prevalent in individuals whose

professions or daily routines require frequent wrist use, such as secretaries, gamers, laborers, doctors, and nurses. Despite this, individual susceptibility to CTS still varies, leading to differences in how frequently the condition occurs across different groups [2]. In addition to varying susceptibility, the symptoms of CTS can also differ significantly from person to person.

As previously discussed, the pathophysiology of CTS is due to compression and traction of the median nerve within the carpal tunnel, causing mechanical trauma, increased pressure, and ischemic damage [2]. However, evidence from another study [6] questions the traditional view and suggests that small-fiber degeneration, intraneural inflammation, and remote mechanisms may also be involved. Moreover, genetic predisposition, rheumatoid inflammation, repetitive wrist activity, obesity, and pregnancy are all risk factors for CTS [2]. Common symptoms also include numbness, pain, and tingling in the affected fingers, which may impact grip strength and overall hand function [2].

Diagnosis primarily relies on clinical symptoms and signs, confirmed by electrodiagnostic studies and high-resolution ultrasonography [7], [8]. Ultrasonography provides the advantages of being noninvasive, quick, and able to visualize tissue dynamics, whereas electrodiagnostic testing has been the gold standard for diagnosis and grading [8]. Diagnosis is then further supported by physical examination findings such as the flick sign, Phalen maneuver, and median nerve compression tests [9]. Additionally, electrodiagnostic studies classify CTS severity into mild, moderate, and severe. The cross-sectional area (CSA) of the median nerve at the carpal tunnel inlet is a valuable tool for assessing the severity of CTS by ultrasonography. Mean CSA values of 11.64 mm^2, 13.74 mm^2, and 16.80 mm^2 for mild, moderate, and severe CTS are reported by meta-

analysis [10]. Another study [11] states that a CSA ≥14 mm² is highly probable to be reported as moderate to severe CTS.

Fortunately, various treatments are available to address CTS and help restore normal wrist function. Treatment options are categorized into administrative, personal, and engineering interventions based on the guidelines provided by the National Institute of Occupational Safety and Health (NIOSH) [12]. Administrative interventions include changes to work processes, such as job rotations, to reduce musculoskeletal stress. Personal interventions center on worker behavior and may include ergonomics training, biofeedback, and various exercise programs, which are usually subjective to worker compliance. Lastly, engineering interventions involve modifying tools and workstations, such as using ergonomic mice and keyboards and designing wrist splints to alleviate wrist strain.

Review of Previous Research

Among the various treatment options for CTS, wrist splints offer a more targeted and objective means of support by stabilizing the wrist and reducing strain. This is possible because using wrist splints prevents frequent wrist flexion and extension, which causes more pressure on the median nerve. Moreover, this helps to move the lumbricals distally, reducing the pressure felt upon the median nerve and potentially alleviating most symptoms in an average of six weeks [13], [14]. Furthermore, studies [13], [15] support that the most effective method for relieving muscle weakness and other CTS symptoms is through the use of a "neutral splint" or a static wrist orthosis following the neutral position, or the "loose pack position," and should be worn full-time rather than just wearing the splint at night to prevent patients from flexing or extending their

wrists unconsciously. However, full-time usage of wrist splints is often limited due to patients' intolerance to prolonged wear. To address this, some studies [16], [17] have incorporated Kinesio taping as a supplementary treatment, allowing individuals to use wrist splinting during the day with increased long-term use.

Additionally, myofascial release massage has been shown to be effective in addressing tendon swelling associated with CTS. According to another study [18], this technique works through three primary mechanisms: breaking down collagen adhesions, facilitating drainage of excess fluid, and increasing blood flow. These actions help reduce tendon restrictions, alleviate fluid pressure, and promote the healing of damaged tissues in the affected area. Moreover, massage therapy, particularly myofascial release, has also been noted for its ability to improve blood circulation and relieve muscle tension, thus improving muscle strength, and should be considered a preferred treatment for mild to moderate-severe cases [15], [19]. Ms. Frencie Quintin Z. Purol, an interviewed Physical Therapist as referenced in Appendix A, had also suggested myofascial release as a massage technique for CTS. The interviewee suggested that myofascial release can be delivered above the flexor retinaculum by applying two circular movement near but not directly above the median nerve, to help release pressure in the tissues in the wrist. A case study [19] further supports the benefits of myofascial release, reporting significant symptom relief in a patient who had previously used a wrist orthosis for tendonitis and muscle strain. Despite using splinting for these conditions, CTS symptoms had progressed. However, due to myofascial release being utilized, the patient's symptoms rapidly alleviated in 2 months, and they no longer experienced burning pain or numbness [19].

Statement of the Problem

Despite its widespread use, wrist splints exhibit significant limitations. One such limitation of conventional splints is that conventional motorized massagers are bulky and heavy, making them unsuitable for wrist splints despite evidence suggesting that massage therapy shows significant change in symptom severity and functional status from two weeks [20]. As a result, users are often compelled to seek additional devices or external assistance, introducing further inconvenience and potential costs. Moreover, wrist splints may be intolerable for some users and may cause complications such as skin irritation [16]. Even though splints may provide temporary relief, the benefits are often short-lived, and symptoms may recur [21]. Additionally, many splints lack the sufficient support for the allowable range of motion, limiting the user's range of motion and adaptability during daily activities and having a less positive effect than when patients only use it at night [16]. As such, this limitation may prevent the splint from effectively accommodating varying levels of wrist movement and strain, especially for individuals who need to use it full-time.

Limitations in Integrating Mechanical Massagers with Conventional Wrist Splints for Carpal Tunnel Syndrome

The integration of massage therapy into wrist splints for Carpal Tunnel Syndrome (CTS) is essential because professionally administered massage provides better therapeutic outcomes compared to self-administered techniques. As noted by Ms. Purol in Appendix A, professional massage delivery ensures uniform pressure and technique, which is vital for achieving the full benefits of therapy. Inconsistent self-administration may result in ineffective treatment,

undermining the potential of even the best-designed mechanical massagers. This has driven the development of wrist splints with integrated massage features. However, most existing products, rely solely on vibration and heat therapy, such as the Komec wrist massager, marketed for CTS relief, which studies suggest may not be suitable for addressing the condition [9], [10]. Despite claims of efficacy, vibration therapy poses risks such as exacerbating inflammation and increasing pressure within the carpal tunnel, particularly when improperly regulated [22], [23], [24]. Occupational exposure to hand-arm vibration, for example, has been linked to an increased risk of developing CTS 2-3 times higher than usual, suggesting that the duration and intensity of vibration therapy must be carefully controlled to avoid exacerbating the condition [23], [25]. Heat therapy is also not recommended for CTS treatment, as the heat sensitivity of sensory fibers in CTS patients can cause conduction block in demyelinated neurons [9], [10].

The integration of mechanical massagers into wrist splints is further complicated by the bulky and heavy design of conventional massagers. This challenge makes it difficult to incorporate larger mechanical components without compromising the splint's functionality or user comfort. Devices like the CarpalRx, while offering therapeutic benefits, are impractical for continuous, multi-purpose use due to their cumbersome design [18]. Other alternatives, such as the CINCOM Hand Massager or Lunix LX7, provide portability but still face integration challenges because their size and form factor are not optimized for simultaneous immobilization and massage therapy [26], [27].

Moreover, for massagers to be effective, synchronization with the muscle's state of relaxation is needed. As referenced in Appendix A, Ms. Frencie Quintin Z. Purol has shown that

massage therapy for CTS is most effective when the muscle is at rest, as the primary goal is to release muscle tension. If the muscle is Active during massage, it can counteract the benefits, as the pressure may exacerbate rather than alleviate the tension. This highlights a key limitation of existing mechanical massagers as they lack the ability to monitor muscle activity through Electromyography (EMG) signals. Without this functionality, the device cannot automatically adjust to ensure that massage therapy is performed only when the muscle is in a relaxed state, potentially reducing the therapeutic effect. Furthermore, the inability to set specific massage intervals, such as twice a day as recommended by Ms. Purol, further limits the practical application of these devices for consistent therapy.

Lack of Wrist Splints That Automatically Adjust Tightness for a Proper Fit

A proper fit is essential for wrist splints to effectively treat CTS and encourage patient adherence. A well-fitted splint achieves its primary goals of immobilizing the wrist, maintaining a neutral position, and reducing inflammation, thereby alleviating symptoms [13], [28]. However, the immobilization required for symptom relief can hinder manual tasks, underscoring the need to balance support with functionality when determining the splint's position and level of rigidity [29].

Patient compliance with splint use is influenced by the perceived benefits, such as symptom relief and wrist stability, as well as challenges, including discomfort and reduced ability to perform certain activities [30]. To maximize adherence and therapeutic outcomes, close follow-up care is crucial. As such, monitoring and adjusting splint fit not only addresses patient concerns but also ensure the splint provides consistent support without causing additional

complications [28]. By incorporating these considerations into splint design and patient education, healthcare providers can optimize its effectiveness.

Research highlights the critical role of wrist position and external compression in influencing median nerve morphology and intracarpal pressure, which are key factors in managing CTS. A neutral wrist position minimizes median nerve compression over time, while extended positions cause nerve flattening at the proximal carpal tunnel, exacerbating symptoms [31]. Orthotic wrist splints are widely prescribed to maintain this neutral position, aiming to reduce inflammation and alleviate CTS symptoms [13]. Ultrasound studies further illustrate the impact of wrist deviation on median nerve morphology wherein, deviations alter the nerve's cross-sectional area at the proximal carpal tunnel, affecting the nerve function [32]. Additionally, applying a radioulnar compressive force across the wrist can increase the carpal arch's height and area while reducing its width. This biomechanical change causes the median nerve to shift radially and become more rounded, which may relieve nerve compression and improve symptoms for CTS patients [33].

However, improperly applied wrist splints can result in significant complications, underscoring the need for proper application and oversight. Studies report that up to 93% of pediatric splints are incorrectly positioned, with 40% leading to complications such as excessive edema (28%) and direct skin injury (6%) [34]. Errors in splint application are also prevalent in adult cases, with 61% of splints applied incorrectly. Common issues include inappropriate length (29%) and direct contact between ACE bandages and skin (25%), which can exacerbate discomfort and lead to soft tissue damage [35].

Complications are even more frequent when splints are applied by non-orthopedic services or in non-trauma settings, highlighting the need for specialized training and standardized protocols [35]. While supervised therapy and home programs show comparable outcomes in uncomplicated fractures [36], errors in splint application during complex cases, such as wrist arthroplasty, can lead to severe complications. For instance, wrist arthroplasty has a reported 51% overall complication rate, with 39% of cases requiring revision surgery [37]. These findings emphasize the importance of proper splint application to minimize risks and improve patient outcomes.

Lack of Wrist Splints That Allow Controlled Movement While Supporting CTS

Recent studies [16], [38] show that although wrist splints are generally advised for nighttime use, they can also be worn throughout the day, especially when symptoms aggravate. The same study [38] shows that day-night splinting is an effective way to improve pain ($p = 0.001$, $p = 0.015$), functionality ($p = 0.004$, $p = 0.020$), and quality of life ($p = 0.001$, $p = 0.003$) compared to no splinting or night-only splinting, respectively. Additionally, day-night splinting reduces nocturnal symptoms and pain levels and results in greater improvements in pain related quality of life and functionality than both approaches [38]. Furthermore, the study [38] has also shown that distal motor latency (DML) and compound muscle action potentials (CMAP) to have improved with splinting.

However, another study [39] noted variability in adherence to splint wearing instructions among patients, which may affect treatment comparisons. In only 46% of hands, was strict compliance with prescribed splint use reported, and the rest of the participants showed partial

adherence. Nighttime wear compliance was very high, with 85% of the night only group and 100% of the full-time group completely or almost completely adherent. However, among the full-time group, daytime compliance was much lower, with just 27% of hands reporting consistent daytime use.

Interestingly, 23% of the night-only group reported occasional daytime use of splints, highlighting a tendency for some participants to extend their splinting regimen beyond the prescribed nighttime use [39]. This behavior suggests that some patients recognize the importance of wrist alignment in managing CTS. By maintaining the wrist in a neutral position during sleep, when the user is unconscious and unable to control wrist posture, nighttime splints help prevent poor positioning that could exacerbate CTS symptoms. However, according to a study [38], misalignment during sleep can occur and increase pressure within the carpal tunnel, compressing the median nerve and worsening pain. The occasional daytime use of splints by some participants suggests that they may recognize the benefits of maintaining proper wrist positioning beyond just nighttime, potentially seeking additional relief from pressure during waking hours to better manage their symptoms.

However, while offering static support to the wrist, conventional wrist splints fail to accommodate the need for allowable motion required for daily activities [40]. It is also discussed that splints are designed to immobilize the wrist to prevent any flexion or extension to allow the lumbricals to move distally [13]. This mismatch between the static design and the wrist's dynamic demand often leads to skin irritation, and reduced user compliance [40].

Ms. Purol (Appendix B) suggested that while wrist splints are commonly used to

immobilize the hand in the treatment of Carpal Tunnel Syndrome (CTS), they do not necessarily have to completely immobilize the wrist. Instead, the splints can be designed to allow for specific degrees of movement, particularly during work tasks or daily activities. For instance, a splint may restrict motion by limiting wrist flexion to around 10 degrees and extension to about 30 degrees, rather than preventing all movement [41]. This approach provides support while still permitting some motion within a controlled range, which can be beneficial for individuals who need to use their hands during the day, without exacerbating the symptoms of CTS. This type of motion restriction helps manage the condition effectively while maintaining some functional mobility.

The restricted movement in conventional wrist splints highlights the need for solutions that promote functionality during daily activities. Rigid splints severely restrict wrist movement, making it difficult for individuals to perform tasks such as typing or driving that require flexibility [42]. In contrast, non-rigid splints, such as soft splints and wrist braces, provide partial immobilization, offering stabilization while allowing limited motion. This feature is particularly advantageous for individuals with chronic conditions like Carpal Tunnel Syndrome (CTS), enabling them to engage in essential activities with greater ease [43].

According to a study [42], rigid splints are useful for acute conditions or post-surgery recovery but fail to accommodate movements needed for everyday tasks. On the other hand, soft splints and braces are specifically designed to limit unwanted motion while maintaining sufficient mobility, making them better suited for chronic conditions like CTS [42]. Another study [43] further emphasizes that wrist braces allow for essential mobility while still providing the necessary stabilization, making them ideal for managing conditions where both support and

flexibility are critical [43].

Objective of the Study

The study aims to develop and evaluate an autonomous wrist splint equipped with an integrated massage system to help alleviate muscle weakness related to CTS and assess the improvements by measuring the grip strength before and after wearing the device. Specifically, the study aims 1.) To detect the muscle's state by acquiring electromyography (EMG) signals from the Abductor Pollicis Brevis muscle. Furthermore, it seeks 2.) To develop and implement a signal processing module that minimizes noise and identifies the muscle's resting and active states using advanced filtering techniques. Additionally, the study intends 3.) To design and integrate a lightweight massage system that activates at specified time intervals when the muscle is at rest. 4.) To implement an auto-fitting feature that automatically adjusts the wrist splint's pressure to ensure a proper fit for any wrist size. 5.) To create a motor-based motion support system that automatically adjusts strap tension to accommodate the allowable range of wrist movement, providing consistent motion support. Lastly, it aims 6.) To evaluate the device's effectiveness through testing on 15 female participants aged 18–25 from Ateneo de Zamboanga University who frequently use keyboards for at least four hours daily.

Significance of the Study

This study offers an improved solution for alleviating muscle weakness related to CTS. By offering a non-invasive solution, this study provides a novel approach to symptom management by using surface electromyography (EMG) signals, amplified and processed for accuracy,

contributing to a more precise assessment of muscle activity and allowing for targeted interventions. Moreover, its focused massage system promotes healing, potentially leading to better long-term outcomes. As such, the following are the beneficiaries of the study:

CTS Patients. This study will benefit patients by reducing muscle weakness and improving hand function through a wrist splint that combines immobilization with massage therapy to address CTS-related weakness. As such, it can enhance daily activity performance and potentially delay or avoid surgery, minimizing associated risks and recovery time. The splint will also be designed to be worn full-time for patients with moderate symptoms and other exceptional cases.

Orthopedic Specialists. This development represents a significant advancement in CTS management, potentially revolutionizing care, driving future innovations in wearable technology in CTS prevention, and raising awareness among healthcare professionals. It also provides an effective aid for alleviating muscle weakness, exemplifying the integration of medical devices with advanced features like massage therapy and opening new avenues for tailored treatment solutions. Moreover, the study also analyzes the limitations of existing options for CTS, giving healthcare professionals a comprehensive review of other available options.

Future Researchers. This study contributes to the advancement of Biomedical Engineering by developing and evaluating an improved solution for CTS. Its findings can be valuable for researchers in medical-related fields who are interested in the Musculoskeletal system. Furthermore, the developed system could be adapted and improved upon in future studies to address the limitations discovered in this study.

The Scope and Delimitation

This study aims to develop eM-Brace, an autonomous wrist splint with an integrated massage system to reduce muscle weakness caused by Carpal Tunnel Syndrome (CTS) in patients with moderate symptoms. The device aims to improve hand grip strength following myofascial release therapy. Grip strength will be measured at three stages: (1) before temporarily simulating median nerve compression to establish a baseline, (2) after temporarily simulating median nerve compression to observe any reduction in grip strength, and (3) after using the device to determine its effectiveness in restoring grip strength. The expected improvement is an increase of at least 2.2 kg, returning grip strength to the typical range for adult females, which averages 35.4 kg [44].

Additionally, eM-Brace uses a surface electromyographic (sEMG) sensor with three electrodes placed below the sensor, positioned above the Abductor Pollicis Brevis near the thumb, to autonomously deliver massage at 12-hour intervals when the muscle is at rest. The use of the sEMG sensor is crucial because muscle contractions or stiffness during non-resting states can reduce the effectiveness of myofascial release, which aims to relax muscle tissues and reduce tension [45]. While accelerometers track movement, they cannot provide biofeedback on muscle activity, making them unsuitable for this device, which requires the muscle to be at rest before delivering a massage.

This study will involve 15 female students, aged 18 to 25, from the Fr. Eusebio Salvador campus of Ateneo de Zamboanga University, who frequently use keyboards for at least four hours a day. This criterion was chosen because prolonged keyboard use can lead to deformation in the median nerve region, potentially contributing to CTS [46]. Moreover, female

students are more prone to CTS, as noted by an interviewed physical therapist and in the previous studies [4], [5], making them ideal participants.

Furthermore, the study will ensure the wrist splint uses a standardized pressure range of approximately 1.36 kPa on the contact area, which is comparable to the pressure usually applied by therapists to the wrist tendon [47]. Moreover, this pressure level is also optimized for the chosen age group having the same pain tolerance. Participants with lower pressure tolerance, which could affect the therapy's effectiveness or cause discomfort, will be excluded. Additionally, athletes, individuals with sports-related wrist injuries, previous wrist surgeries, or conditions like peripheral neuropathy or rheumatoid arthritis, which may mimic CTS symptoms, will be excluded. While the device can detect early signs of CTS, it is not intended for pre-diagnostic purposes; the primary focus is to support individuals with muscle weakness due to CTS.

CHAPTER II
REVIEW OF RELATED LITERATURE

Background and Context

According to a study [48], Sir James Paget first described carpal tunnel syndrome (CTS) in 1854, and although he described two cases of median nerve compression at the wrist, the term ‘carpal tunnel syndrome’ did not come into use until much later. Similar symptoms in the late 19th and early 20th centuries were referred to as "acroparesthesia," as stated in a recent study [49]. The modern understanding of CTS was then described in the late 1940s with a description of median nerve compression at the wrist [50]. As also previously discussed [4], [5], CTS has shown to be more common in women, and especially in adults aged 40 to 60, affecting approximately 8.0% of the general population. Furthermore, electrodiagnostic studies, such as electromyography and nerve conduction studies, have significantly aided in the diagnosis of CTS [7], [50].

Treatment options have also evolved, but the earliest documented treatment for CTS was wrist immobilization, as first described by Paget [48]. This later on became known as wrist splinting, and until today, there are various conservative treatment options, such as splinting, steroid injections, non-steroidal anti-inflammatory drugs (NSAIDs), or rehabilitation modalities [51], [52]. Splinting and corticosteroid injections may afford a short-term improvement but lack benefit in the long term [52]. Additionally, it was also discovered in a study [53] that diuretics, pyridoxine, NSAIDs, yoga, and laser acupuncture are simply ineffective for short-term relief of symptoms. Moreover, progressive functional deficits and significant pain remain the indications

of the need for surgery [52].

In terms of CTS treatment, local corticosteroid injections (LCI) are superior to placebo with regard to short-term benefits and clinical outcomes of up to six months [54], [55]. In the short term, LCI is also more effective than oral steroids, and higher doses may yield better midterm results [55]. However, the long-term efficacy of LCI is uncertain, as 41.6% of patients eventually require surgery [56]. Nevertheless, the median time to surgery is from 128 to 446 days, which can be delayed or prevented with LCI [56]. Another study [54] also noted that adverse effects of LCI are generally mild and uncommon, which include temporary pain and swelling. LCI is a low-risk procedure with the potential to improve symptoms; however, its benefits are not sustained in the long term, and more high-quality research is needed to evaluate its long-term effectiveness fully [55], [56].

On the other hand, the standard for conservative treatment for CTS has always been wrist splints or immobilization, as first documented by Paget [48], [57]. As such, the evolution of splinting has also been influenced by factors such as diseases, war, technological advancements, and medical progress [57]. CTS splints differ in design and effectiveness compared to other wrist splints, as modified designs incorporating metacarpophalangeal (MCP) joint support have been compared to traditional wrist-only splints. As such, these MCP-inclusive splints are more effective in reducing pain and improving function in CTS patients [58], [59]. Recent studies [59], [60] showed that these splints significantly improved grip strength, pinch strength, and pain reduction more than wrist-only splints. Dorsal lock wrist hand orthoses have also been promising for maintaining a neutral wrist position and have improved pain and neurological symptoms [61].

Moreover, nighttime use of splints is typically recommended; however, some designs also allow for daytime use [13].

CTS treatment may also depend on the position of MCP joints and should be taken into account when prescribing splints [60]. Compared to traditional wrist-only designs, CTS-specific splints that support both the wrist and MCP joints have superior outcomes. Additionally, splinting has also been shown in long-term studies to be efficacious, and 43% of patients were successfully treated using splints alone over a 36-month period [62]. In primary care settings, wrist splinting is still a standard of care as a noninvasive first-line treatment of CTS [62]. However, the basis for the results in the previous study has been purely subjective, as stated in its limitations, and a more recent research suggests that because there are no precise positioning guidelines for these splints, they may only be effective in the short term and may not offer the best symptom relief [62], [63]. Additionally, its efficacy in preventing CTS is limited because it mainly treats symptoms rather than underlying causes such as repetitive strain [64]. Concerns about insufficient protection during high-impact activities, and potential complications from incorrect use all highlight the need for more thorough preventive measures than splinting.

Research Questions

How can a massage alleviate muscle weakness in Carpal Tunnel Syndrome?

Massage therapy has been suggested as an effective treatment for CTS, where regular massage session studies have shown significant improvements in symptom severity and performance status [20], [65]. According to a study [65], grip strength improved with general and targeted massage techniques, with more significant gains seen with the targeted massage

protocol, leading to improvements in subjective measures associated with CTS. When combined with splint wear, the "Madenci" hand massage technique has significantly decreased pain and increased grip strength compared to splint wear alone [66].

Additionally, soft tissue massage, such as myofascial release, along with joint and nerve mobilization techniques, has shown effectiveness in reducing symptom severity, improving blood circulation, and alleviating muscle tension in CTS patients [15], [19], [67]. Research has shown that myofascial release can also alleviate pain, paresthesia, and dysesthesias, as well as enhance hand dexterity of CTS sufferers [19], [68]. Self-stretching myofascial release techniques have been used in combination and have been known to enhance the carpal tunnel's cross-sectional area as captured by Magnetic Resonance Imaging (MRI) scans as suggested by [19]. These increases in canal size are linked to better clinical results, such as more favorable altered nerve conduction tests. Furthermore, by using myofascial release, CTS was treated successfully during pregnancy, and better electrophysiological and clinical aspects were obtained than splinting [68].

The immediate effects of myofascial release on the body are noticeable, such as a reduction in pain due to changes in blood flow and temperature, metabolism, and the autonomic system [69]. Additionally, it affects the activity of fibroblasts or the production of collagen during the healing process in people with CTS. This is possible because myofascial release stretches the fascia and loosens the connections between the fascia and the skin, muscles, and bones, aiming to alleviate pain, improve joint flexibility, and bring the body into balance. Another study [15] stated that this single, simple wrist self-stretching maneuver may improve sensation (numbness and tingling), strength, and overall symptom severity.

Figure 1 Operator applies upward dorsal wrist pressure while thumbs press along carpal ligament borders [19].

However, the majority of manual therapies, including myofascial release, are still administered by trained clinicians for maximum effectiveness, albeit being self-performed by patients, thus necessitating access to specialized healthcare for proper treatment [15]. Moreover, because some of the treatments were self-administered, adherence could have varied, and the study's limited scope failed to account for other treatments that participants may have sought, potentially influencing the results [13]. The previous study [15] also reported that self-stretching of the carpal ligament, despite leading to improvements in numbness, tingling, and pinch strength, had ANOVA analyses that were inconclusive about group differences. These studies suggest that while self-massage and stretching may offer some benefits, their effectiveness may be limited for certain CTS symptoms.

How long can wrist splints for Carpal Tunnel Syndrome be worn continuously without adverse side effects?

Although wrist splinting is an effective conservative treatment for CTS, the duration and wear schedule of this treatment remain debated. While a study [14] suggests that 6 weeks of splinting may be sufficient for symptom improvement with no benefit for extending to 12 weeks; many patients still do not experience complete relief of symptoms even after 6 weeks of treatment. In addition, as previously discussed in another study [62], long-term follow-up revealed that 43% of patients were successfully treated with splinting alone after 36 months. Moreover, while combining wrist splinting with steroid injections gave long-term relief in only about 10% of patients, better outcomes were reported in those who had a shorter symptom duration and less sensory impairment [70].

Physiological improvements were also better with full-time splint wear than with night-only wear, with some varying degrees of patient compliance [71]. Despite this, night splinting alone, even for patients with more severe degrees of CTS, can sometimes be as beneficial as full-time splint wear instructions, which results in better physiological improvements than night-only [71], [72], [73]. This is because night splinting reduces pain and paresthesia, especially in patients with night-only symptoms [73]. In addition, although splinting may have potential benefits, patient compliance with wear instructions may still pose limitations [71]. Furthermore, an 8-week full-time splinting program and education were combined in a randomized controlled trial and found to reduce symptom severity and functional status in CTS patients [74]. Daytime splinting has been proposed to benefit both neural and vascular CTS by preventing wrist movement and

excessive gripping to alleviate compression of arteries and the median nerve [75].

While a study [76] suggests that splinting may offer short-term relief over no treatment at all, its long-term benefits still remain unclear. However, adverse effects from splint use are sometimes reported by some patients and are generally minor [76]. As reported in a study [77], the most effective treatment for moderate CTS cases still appears to be splinting, especially when distal motor latency is less than 8 milliseconds. However, it has been noted that some patients using specialized splints, such as the C-Trac, have developed side effects of De Quervain's tenosynovitis and basal joint arthritic pain [78]. However, a study [60] showed that MCP wrist splints were better than wrist-only splints in reducing pain and improving grip strength and functional capacity. Overall, splinting has been shown to be beneficial for CTS with the caveat that limited long-term efficacy data and inconsistent evidence for the superiority of particular splint designs exist [76].

How can a motion support system account for the allowable range of motions of the wrist during daily activities?

Despite immobilization being considered the most effective initial conservative treatment method, treating CTS may sometimes involve movement [79], [80]. According to previous studies [80], [81], the long-term benefits of neurodynamic techniques, which promote median nerve gliding, have been shown in CTS patients with improved nerve conduction, pain reduction, and increased muscle strength. Neurodynamic modulation is also shown by a meta-analysis of randomized controlled trials to significantly reduce symptom severity, pain, and motor latency and increase nerve conduction velocities [80], [81]. Additionally, electrodiagnostic tests can be

inconclusive in diagnosing CTS, and provocative exercises and sonographic evaluation can be combined to increase sensitivity and specificity in diagnosing CTS [82]. Moreover, although both corticosteroid injection and carpal tunnel release do improve clinical outcomes, median nerve mobility was not significantly improved [83].

Similarly, a previous study [84] showcased a soft, wearable robotic sleeve designed to actively adjust wrist position in real-time to prevent or alleviate CTS-related strain. The device consisted of two airbags, one assisting in wrist flexion. At the same time, the other elevates the wrist to a height similar to that of a keyboard, ensuring ergonomic comfort during tasks such as typing. The airbags are regulated by a microcontroller system that monitors wrist positioning and internal airbag pressure [84]. Additionally, elastic and inextensible straps are incorporated into the design to secure the sleeve and prevent radial expansion of the airbags when pressurized. However, the design is limited by its degrees of freedom due to the integration of the airbags and lacks clinical confirmation of the relief of CTS [84].

As discussed previously, one study [85] on the development of a similar device called the C-Trac assessed its efficacy in treating CTS in patients who failed conservative therapy. The C-Trac is designed to fit loosely onto the wrist of the person to address skin-related issues that may arise when wearing the device for prolonged periods. The C-Trac device is worn, and as the bladder on the back of the hand inflates, it generates a three-point traction force that separates the thenar and hypothenar regions, creating traction on the flexor retinaculum [85]. However, instead of using a microcontroller to pressurize the airbag, the C-TRAC only utilizes a manometer and bulb to pump air manually and has been reported to have developed side effects of De Quervain's

tenosynovitis and basal joint arthritic pain in patients [78], [85].

Synthesis of Literature

How can a massage alleviate muscle weakness in Carpal Tunnel Syndrome?

A. Smart splint using shape memory alloys (SMA) wires

Recent literature investigates new methods of integrating massage techniques with splint therapy for several musculoskeletal disorders. One study [86] for instance, developed a continuous local massage delivered by an intelligent splint using shape memory alloy (SMA) wires, which showed significant improvement in muscle recovery, with a percentage of qualified muscle recovery increasing by more than 70% compared to traditional splints. The study also found that the temperature inside the splint varied between 33-36.3°C, and the humidity values changed over time. The pressure applied to the fracture area by the cast was 58 gf/cm^2, which is necessary to stabilize the bone and joint [86]. The fundamental difference between the study's proposed splint and other splints is that the proposed device can detect and monitor all the different vital changes and greater fixation of a fracture in addition to maintaining the permanence of the internal movement of the muscles and surrounding tissues through the use of the SMA wires as shown in Figure 2.2, which led to a shortening of the process of rehabilitation for the injured area after recovery in a record time, which makes it suitable for optimal use by athletes and people who need quick rehabilitation to practice their daily activities [86].

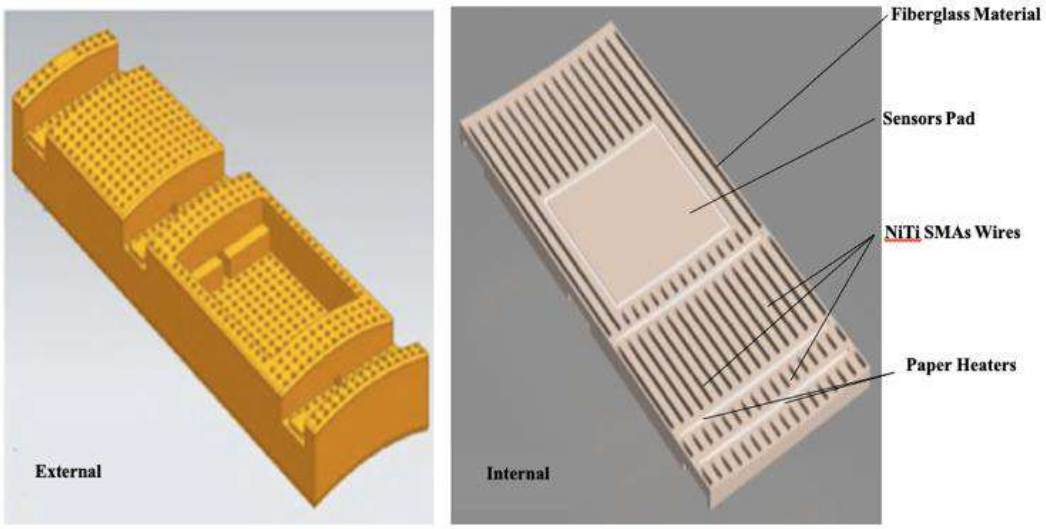

Figure 2 The internal and external shape of the proposed smart splint

Additionally, the purpose of the inclusion of paper heaters in the device was to control the temperature within the cast itself [86]. The nickel-titanium wires were used to expand and contract automatically when they undergo thermal transformations, and temperature adjustment was critical to activating the nickel-titanium wires. Moreover, the pressure from this process supports the muscles and tissues around the fracture site and delivers a continuous massaging effect on the affected area [86].

Furthermore, it had been discussed that the smart splint was designed using nickel-titanium-shaped memory alloy wires, a microcontroller, and pressure, temperature, and humidity sensors [86]. The wires were placed on the splint in a square shape, and the microcontroller was used to monitor and analyze the data from the sensors. However, the study [86] stated that the SMA wires gave different results from each other, which depended on the radius of the cross-section of the wire through the ability of the memory of the alloy to restore its original shape after the removal of external influence, in addition to a group of paper heaters

that are used to balance the temperature or humidity inside the cast according to the patient. Thus, due to this, the proponents had to use three types of wires with different diameters.

This study [86] introduced a design for an intelligent splint capable of sensing changes in temperature, humidity, and pressure in the injured area over a period of time as specified by a doctor. The sensor data can be collected, stored, and compared to a database to monitor the progression of the injury. Moreover, the main feature of the splint is in its nickel-titanium alloy wires of differing diameters, which activate and stimulate the surrounding tissues and muscles, using the alloy's memory effect to return to its original shape after deformation [86]. However, the study's main limitations also lie with the measurement of the temperature of the wire due to its small diameter, and the condition surrounding the wire was a challenge. Aside from that, the study does not mention any other limitations [86].

B. The mechanical hand of Thai massage

Another study [87] developed a standardized and programmable massage therapy that was provided through a mechanical model of a traditional Thai massage integrated with a massage chair system, which was widely accepted by users. As stated in the study [87], three fundamental principles of Thai massage, namely pull, press, and pin, were incorporated into the mechanics of Thai massage and analyzed. Moreover, a mathematical model was devised to describe a mechanical hand's dynamics and design criteria. As such, the mechanical hand model is presented in Figure 2.3. The key findings of the study were that users were satisfied with the treatment and felt that it was similar to that performed by human hands, and they were likely to utilize the mechanical hand as an alternative to traditional massage.

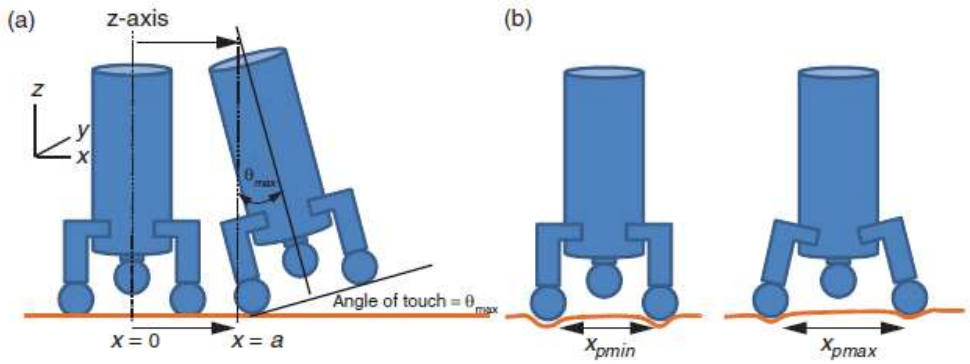

Figure 3 Model of the mechanical hand for Thai massage's pull, press, and pin actions.

Moreover, in the study [87], the initial effort to mechanically replicate a fundamental and standardized form of Thai massage involved rotational and translational motion, and mechanical fingers were used to perform the pull, press, and pin techniques. However, this approach was limited, as the proponents have noted in the study's introduction that Thai massage is a complex art form that should be further studied scientifically and that the developed mechanical hand could not have perfectly captured the complex movements of the actual massage.

This study [87] also presented a limitation on the performance testing of the prototype massage chair. Participants were asked simple questions and given positive feedback. Still, it was unclear whether the participants actually liked the system or would purchase a Thai massage system if it was commercially available. Medical imaging techniques, such as MRI scans, could also provide a more objective assessment of the therapeutic effects of the participants in the study [87].

C. Electro-mechanical device manipulator for CTS

Similarly, one patent [88] also discussed a device and method for treating CTS and other tendon-related disorders by manipulating the affected tendons with a three-dimensional motion, thereby reducing compression of the median nerve and alleviating symptoms. As presented in Figure 2.4, this manipulation utilizes myofascial release and helps reduce inflammation and pressure, alleviating pain and other associated symptoms. When further used with an orthopedic device, it allows the affected limb to remain stationary, promoting rest and recovery between treatments [88].

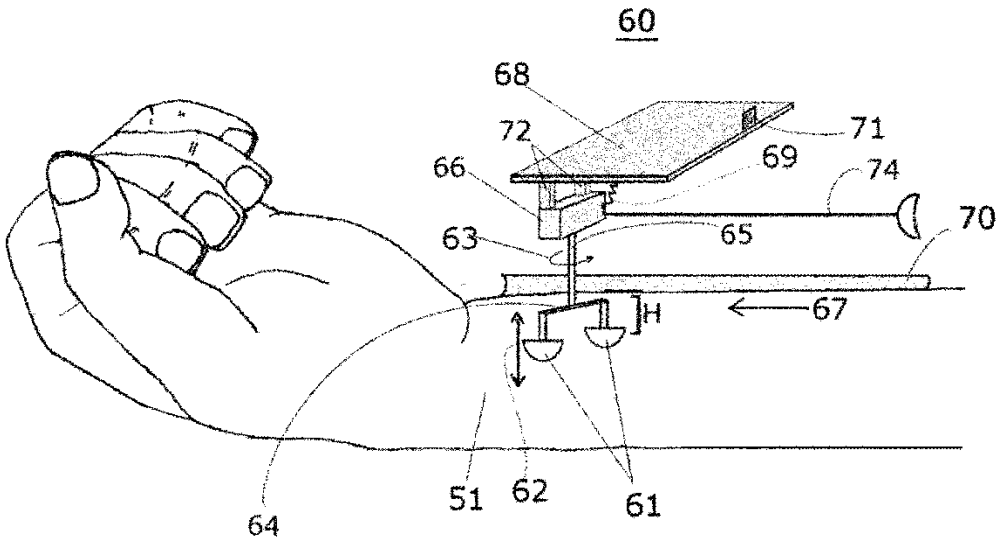

Figure 4 Massage delivery of mechanical motions over the wrist

The inventors have found through experimentation that the three-dimensional mechanical motions produced over the wrists and forearms are effective for symptomatic relief of wrist tenosynovitis, wrist tendonitis, and CTS [88]. This involved attaching the affected limb with a limb-engaging component, including the relevant tendons. This component can be

temporarily attached to a manipulator that manipulates the underlying tendons effectively by performing movements close to the skin [88]. Moreover, the device has been found to reduce hand pain and improve the suppleness of the tissues.

The mentioned patent [88] also has unveiled some flaws, indicating that although the integrated massage system can alleviate the symptoms, it cannot do right away with the root causes, which might include anatomical factors or severe nerve compression. The device may present limitations regarding the specific conditions and tendon regions that can be treated and the potential for adverse effects or interactions with other treatments [88]. It would also be essential to note that the system's success may depend on the patient's state and the body's anatomy [88]. Moreover, this probably causes the long-term utilization of mechanical devices to underutilize other possible practical therapeutic strategies, including physiotherapy or surgery, which might be necessary for some patients.

On the other hand, the device can be used in a clinical setting or at home and powered by a battery [88]. The device can treat conditions such as CTS, flexor tendonitis, Achilles tendonitis, and plantar fasciitis. It can also provide massage therapy to the user's arm, hand, wrist, foot, or ankle. However, as previously discussed, the device may have limitations regarding the particular conditions and tendon areas it can address and the possibility of adverse effects or interactions with other therapies [88].

How long can wrist splints for Carpal Tunnel Syndrome be worn continuously without adverse side effects

Various devices are designed to facilitate long-term usage for symptom relief in CTS, with

each offering unique benefits in terms of usability, adaptability, and sustained symptom management. Three notable examples of such devices include the C-TRAC splint, Beta Wrist Brace (BWB), and soft robotic wrist braces with origami-patterned actuators, each providing distinctive advantages for long-term application in CTS management.

A. C-trac splint

The C-TRAC Splint, designed to stretch the transverse carpal ligament, provides an effective non-invasive alternative to surgical decompression, as well as a feasible solution for long-term use. In studies comparing it to other bracing solutions, C-TRAC was associated with significant reductions in pain, numbness, and sleep interruptions due to CTS symptoms, with benefits lasting up to a year for many users [85]. Patients also experienced minimal maintenance requirements post-initial intensive phase, typically needing only occasional use for symptom management. The primary advantage of C-TRAC lies in its ability to serve as a long-term intervention that minimizes the need for surgery or frequent clinical visits, thereby lowering the overall cost and physical risks associated with operative treatments.

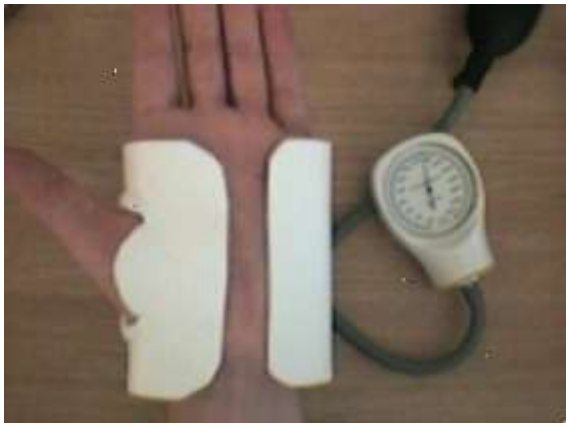

Figure 5 C-TRAC on left hand applies three-point traction via dorsal bladder expansion,

stretching the flexor retinaculum

In a separate evaluation of the C-TRAC device as a standalone intervention, a non-comparative outcome study was performed. The study targeted patients unresponsive to standard conservative therapies, such as nonsteroidal anti-inflammatory drugs (NSAIDs) and nighttime hand splints [85]. Patients were instructed to use the C-TRAC device for a four-week intensive period with thrice-daily application, followed by an "as-needed" schedule for maintenance. Outcome measures included symptom relief, reduction in nighttime awakenings, and patient-reported satisfaction scores. Patient assessments were performed both during and after the intensive period, allowing researchers to gauge the device's long-term utility and the reduction in symptom recurrence with intermittent usage.

The study targeted patients unresponsive to conventional treatments, focusing on the effectiveness of C-TRAC as a standalone intervention [85]. Although this study effectively fills a gap by addressing a population that might otherwise consider surgical intervention, its credibility is limited by the lack of a control group and non-randomized design, which restricts its ability to rule out placebo effects or natural symptom variation. This limitation is partially offset by the specific patient population—those who had previously shown resistance to other treatments—suggesting that observed improvements are more likely due to the intervention. However, the study's relatively short primary intervention period (four weeks) also limits conclusions on its long-term benefits. As a preliminary exploration, it provides valuable insight, though its findings should ideally be confirmed in larger, controlled studies to strengthen credibility.

B. Beta wrist brace (BWB)

Conversely, the Beta Wrist Brace (BWB) is a more traditional splint that focuses on limiting wrist movement to minimize compression of the median nerve, effectively providing relief from CTS symptoms [78]. Although not specifically engineered to stretch the carpal ligament, BWB is lightweight and accessible, making it a practical choice for long-term use. In comparative trials, both C-TRAC and BWB demonstrated comparable efficacy. Still, the C-TRAC's ability to stretch the carpal ligament provides a potential advantage in addressing ligament tightness, which can contribute to chronic CTS [85]. Additionally, BWBs are economically advantageous, costing significantly less than C-TRAC, although they may require more frequent replacements over extended periods.

In the C-TRAC study, researchers employed a randomized controlled trial (RCT) design to compare the device's effectiveness against that of the BWB in treating mild to moderate CTS. Forty-nine patients, confirmed through clinical and neurophysiological assessment to have CTS, were randomized into two treatment groups: one using the C-TRAC and the other using the BWB [78]. Clinical evaluations, including symptom assessments and grip strength measurements, were conducted at multiple intervals over one year to track both primary outcomes, such as symptom improvement, and secondary outcomes, such as patient satisfaction and side effects. Patients received follow-up calls at two and six weeks, with clinic visits scheduled at zero, four, eight, 26, and 52 weeks. This setup allowed researchers to determine the clinical efficacy and safety of each splint type across long-term usage.

The C-TRAC splint study implemented a randomized controlled trial (RCT), which is a

rigorous design often considered the “gold standard” in clinical research due to its ability to minimize bias and establish causation through randomization [78]. This study’s one-year follow-up period adds credibility, allowing researchers to capture long-term effects and sustainability of the intervention. However, the sample size of 49 participants, although adequate for a pilot study, limits the generalizability of the findings to a broader population. Additionally, while the RCT design strengthens internal validity, the study was unblinded, which could introduce observational bias, particularly in subjective measures such as patient-reported symptom relief. Nevertheless, the rigorous follow-up schedule and use of both primary and secondary outcome measures provide credible evidence for the C-TRAC splint’s long-term efficacy compared to BWB.

C. Soft robotic (SR) brace with soft origami actuators

Soft Robotic Wrist Braces, particularly those using soft origami-patterned actuators, represent a newer approach to CTS therapy. These devices offer unique benefits due to their lightweight design and adaptability, which are crucial for sustained usage [89]. Unlike rigid braces, the soft robotic brace conforms to the user’s wrist, offering controlled assistance for wrist motion while reducing discomfort associated with prolonged wear. By providing a low-profile, soft material structure, this robotic brace supports safe human-robot interaction, allowing users to perform a wide range of wrist motions, including extension, flexion, and radial/ulnar deviation. The modular design also facilitates long-term wear as it can adjust to changes in wrist dimensions, which may be especially beneficial in patients with fluctuating wrist inflammation common in CTS. Furthermore, the device's customizable pressure levels support tailored therapy intensity, which can be scaled based on user needs and symptom progression, fostering sustained symptom

relief.

Researchers utilized a technical and mechanical testing framework for the soft robotic wrist brace study to assess the device's engineering design and efficacy in supporting CTS management. This study introduced a wrist brace incorporating eight origami-patterned pneumatic actuators arranged in modular units, which were tested for controlled bidirectional wrist motion, flexibility, and comfort [89]. The methodology included several experimental stages: 1.) material testing to validate the actuators' performance in terms of range of motion and output force; 2.) a user-wear trial to observe device adaptability to wrist size variations and to examine long-term wearability; and [89] simulated motion tasks to evaluate control performance and load-bearing capacity. Tests were performed under varied pressure conditions to assess both flexion/extension and ulnar/radial deviation. Researchers collected quantitative data on output force and angular displacement, which were then analyzed to determine the device's suitability for extended use in therapeutic settings.

The soft robotic wrist brace study relies on technical performance testing and engineering assessments, which lends credibility to its findings on the mechanical efficacy and adaptability of the device. This approach enables a detailed evaluation of device reliability, flexibility, and long-term usage viability by applying quantitative metrics such as output force, angular displacement, and adaptability to wrist size [89]. The study's emphasis on repeatable mechanical performance and modular design testing provides a strong foundation for evaluating the device's long-term potential. However, the absence of a clinical testing phase with actual CTS patients limits the applicability of the findings to real-world contexts. Further, while the study thoroughly assesses

engineering aspects, the lack of patient-centered outcomes like symptom relief or comfort levels introduces a gap in understanding the device's effectiveness from a user's perspective. Although this study effectively establishes the device's feasibility, clinical trials with CTS patients are needed to substantiate its therapeutic claims.

Overall, each study contributes meaningful data for long-term CTS device management, though future research would benefit from larger sample sizes, control groups, and integration of clinical testing where applicable. The combination of rigorous RCT designs, outcome-based engineering assessments, and patient-centered trials will enhance the evidence base for sustainable CTS therapy devices.

How can a motion support system account for the allowable range of motions of the wrist during daily activities?

A. Exos wrist brace with BOA fit system for adjustable wearables

Radioulnar wrist compression (RWC) is one of the non-invasive treatment methods considered for managing carpal tunnel syndrome (CTS). Despite CTS being caused by compression in the median nerve, previous research has shown that RWC can increase the carpal arch space, which in turn will enhance the median nerve mobility and decrease nerve flattening [90], [91], [92]. When implementing the RWC intervention for four weeks, patient outcomes showed significant improvements and symptoms of numbness and tingling were reported to be less severe by the patients. Furthermore, RWC was identified to reduce median nerve cross-sectional area and distal motor latency, as well as improve nerve sliding in CTS subjects [91], [92]. Such enhancements were noted even after two weeks of treatment and were sustained even at the

end of the intervention duration. It is assumed that the positive outcomes of RWC for CTS are due to the ability to intermittently decompress the median nerve by augmenting the carpal arch. Consequently, it can be assumed that RWC is a feasible approach to treat mild to moderate CTS, particularly for sensory dysfunction prognosis [91], [92].

The methodology used for the referenced studies on wrist compression therapy involves developing a portable, wearable wrist device replicating a laboratory-based system's biomechanical specifications [92]. The device includes a thermoformable Exos Wrist Brace with Boa, an air bladder, and an inflation system to apply wrist compression. This method shows promise in providing personalized wrist support in various settings. One of its weaknesses, however, is that it was unsuitable for long-term use due to its bulky brace design and bulb configuration. Nevertheless, the use of a Boa fit system is proven to increase the user's wearability and provides easy adjustability to the splint while in use [92], [93], [94].

The study on radioulnar wrist compression for carpal tunnel syndrome demonstrates significant improvements in sensory symptoms, emphasizing a patient-centric and noninvasive approach to treatment. This study highlights the potential benefits of static support modules in enhancing patient-reported outcomes, particularly regarding numbness and tingling. By prioritizing comfort and usability, the design of the wrist splint can improve compliance and effectiveness. The study's protocol, involving thrice-daily sessions over four weeks, suggests that the splint should accommodate extended wear while allowing for easy adjustments. However, further investigation into long-term efficacy is needed to support widespread adoption of these non-surgical options in clinical practice [92].

The paper's credibility in [69] is well-supported by its publication in the Journal of Orthopaedic Research. This reputable, peer-reviewed journal confirms it is a formally recognized academic publication. The study's focus on morphological changes in patients with carpal tunnel syndrome (CTS) provides valuable insights into this specific medical condition, and its defined methodology—utilizing compressive forces and ultrasound imaging—enhances the reliability of its findings. Additionally, the paper's indexing in PubMed, a highly regarded database for biomedical literature, further establishes its credibility and visibility within the scientific community.

The study in [70] presents findings on the effectiveness of splinting for carpal tunnel syndrome (CTS). However, its credibility is limited by a small sample size of only 11 patients, which restricts the generalizability of the results. The authors conclude that the evidence supporting splinting for CTS is insufficient, indicating a low degree of certainty regarding its effectiveness. Although there were reports of minor, transient adverse events associated with splinting, these did not significantly impact the study's findings. Overall, the study contributes valuable preliminary insights into CTS treatment, but the limited sample size and lack of conclusive evidence reduce the robustness of its conclusions, suggesting a need for further research to validate its claims.

B. Soft robotic (SR) brace with soft origami actuators

Another study focuses on the use of dynamic movement devices in rehabilitation, particularly for individuals with upper limb motor impairments caused by conditions like stroke. The soft origami actuator (SOA) is of particular interest because it provides smooth contraction

and extension to improve the control and performance of the device. The refined design of the actuator makes it highly suitable for rehabilitation exercises, particularly in conditions requiring precision in wrist movements, such as carpal tunnel syndrome. The device's high-level control system processes pressure feedback, allowing it to estimate wrist motion and adapt for flexion-extension and deviation, which are critical motions for patients with carpal tunnel syndrome.

In conjunction with the SOA, the soft robotic (SR) brace allows the wrist to bend up to 30 degrees while maintaining user comfort. This is particularly beneficial for carpal tunnel syndrome rehabilitation, as it enables the device to mimic natural wrist movements without causing additional strain or pain—critical factors for those with wrist discomfort. These features suggest that the device could provide significant advantages over traditional, non-dynamic therapies, offering a more effective solution for managing carpal tunnel syndrome by promoting natural movement and supporting motor recovery [89].

The study on Compact Soft Robotic Wrist Brace highlights several methodological issues related to the design and use of rehabilitation robots. One major challenge is kinematic compatibility, as existing devices often struggle to align with the human body's natural movements, which can reduce the effectiveness of therapy. Additionally, discomfort experienced by users while using these robotic devices can hinder participation and decrease compliance, posing a barrier to successful rehabilitation. Another key issue is misalignment, where improper alignment between the robotic device and the user's limb can not only reduce the efficacy of the therapy but also increase the risk of injury [89].

C. Self-lacing shoe technology

The concept of self-adjusting devices has been explored in various studies, particularly in wearable technologies that enhance user comfort and functionality. For instance, [95] investigated the impact of self-lacing technology on foot containment, demonstrating that dynamically adjusting straps could significantly enhance the fit and responsiveness of wearable devices by adapting to the user's needs in real time [95]. This principle can be applied to developing wrist splints with auto-adjusting straps, which utilize EMG sensors to detect muscle activity and adjust tension based on pain signals. Such an approach could allow for personalized adjustments that respond dynamically to the user's discomfort or movement requirements, potentially improving support and comfort by reducing manual adjustments and promoting optimal alignment.

Figure 2.6 illustrates generic models of foot bones and a shoe positioned at three distinct stages of the shuttle cut task, using three-dimensional coordinates obtained from stereo radiography of metal beads in the foot and shoe. The contour plot on the shoe's surface displays the foot's movement relative to the anterior and medial aspects of the shoe. The experimental Adapt BB shoe's foot motion under the preferred tension condition is contrasted with the motion observed in the Control shoe. Radiographic images of each shoe at 100% of the cut motion, taken at the peak measurement moment, are displayed on the right side of the figure [95].

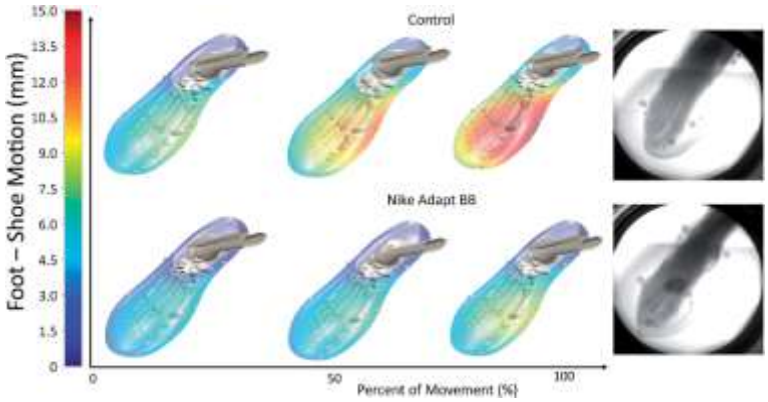

Figure 6 Relation of foot shoe motion to Percent of Movement

Participants in the study on the impact of self-lacing technology included twenty healthy athletes (average age 23.6), each regularly engaged in sports involving dynamic movements, such as basketball. After ethical approval from the University of Denver Institutional Review Board and informed consent, participants were assigned two footwear types: a standard-lace basketball shoe (Nike Hyperdunk) and a self-lacing shoe (Nike Adapt BB), the latter controlled by a smartphone app to adjust lace tension across different conditions [95]. High-speed stereo radiography (HSSR) instrumentation involving X-ray generators, image intensifiers, and high-speed cameras was used for submillimeter accuracy in capturing three-dimensional foot motion. A 14-camera motion capture system collected kinematic data on the knee, shank, and foot, while small and large radio-opaque beads tracked relative foot-shoe motion precisely [95]. Testing included static measurements, lateral shuttle cuts, and forward jab steps, with foot-shoe motion measured along the medial-lateral (ML) axis for cuts and the anterior-posterior (AP) axis for jab steps. Data analysis using XMA software and statistical significance assessment through ANOVA, with Bonferroni post-hoc adjustments, provided a comprehensive evaluation of motion control

and containment for each footwear condition [95].

The paper's credibility on self-lacing technology can be assessed through several vital factors. First, the expertise and academic backgrounds of the authors contribute significantly to the study's reliability, as those with solid credentials in biomechanics or wearable technology are likely to provide well-informed insights. The journal's reputation also plays an important role; publications in peer-reviewed and widely respected journals suggest the study has undergone rigorous evaluation, enhancing its validity. Furthermore, the methodology used in the study should be scrutinized for clarity, sample size adequacy, and statistical rigor, as these aspects impact the quality of the findings. Lastly, the study's credibility is reinforced if it has garnered citations from other researchers, indicating its acceptance and impact in the academic field. Taken together, these factors suggest that the paper offers a credible foundation for exploring dynamic adjustments in wearable devices, such as auto-adjusting straps for wrist splints that respond to EMG-detected pain [95].

Conceptual Framework/Theoretical Framework

The design and development of a wrist splint with an integrated massage system to alleviate CTS-related muscle weakness were based on several key concepts and theories. These concepts inform the selection of the most critical features that address the challenges associated with current wrist splint designs to enhance its overall efficacy.

Key Concepts and Theories

A. Massage and Soft Tissue Mobilization

Some promise is shown that massage therapy can help reduce muscle weakness and soreness. In the previous study, massage has been shown to reduce delayed onset muscle soreness (DOMS) and to improve muscle performance following strenuous exercise [96]. Massage also helps improve circulation and assists with lymphatic drainage to alleviate numbness and pain [15]. Additionally, combining massage with programmable mechanical devices that evoke massage movements, such as pressing, pulling, and pinning, enhances the therapeutic effect [87]. These movements stretch the fascia and muscle fibers around the wrist and stretch the tissue, improving the pliability of the tissue and supporting muscle recovery [15]. This approach utilizes principles of soft tissue mobilization to improve blood flow and reduce tissue stiffness to address the effects of CTS.

Another study highlights that 3 second per rotation ensures a steady and controlled application of pressure, contributing to a light, soothing massage. This speed strikes a balance between effective muscle relaxation and user comfort, avoiding overstimulation. The 3-second interval per rotation supports a gentle rhythm, which is ideal for stress reduction and comfort without inducing discomfort or fatigue [97]. The design of 1 rotation every 3 seconds corresponds to a pace that translates to 20 RPM.

$$RPM = \frac{60}{Sec} = \frac{60}{3} = 20RPM$$

This interval emphasizes a steady, rhythmic motion that aligns with the principles of light massage, offering a comfortable and relaxing experience. The calculated RPM (20) ensures that

the system operates slowly enough to avoid overstimulation while providing a consistent, soothing effect, which is ideal for promoting relaxation and muscle relief in non-intrusive therapeutic settings [97].

B. Massage Pressure standards

In determining the optimal pressure for the massager, it is first crucial to consider both the physiological effects of various pressures, and the standards established in massage and ergonomic research. Studies on massage pressures have demonstrated that different intensities can trigger distinct physiological responses. For instance, a study [98] found that moderate pressures of 20-40 mm Hg in rats resulted in blood pressure reduction and autonomic changes, highlighting the potential benefits of light to moderate pressure for therapeutic effects. Similarly, another study [99] reported that light pressing at 3.55 kg/cm² improved foot skin blood flow in diabetic patients, suggesting that lower pressures might be more suitable for enhancing circulation without causing discomfort or potential harm. In contrast, it had been observed that pressures such as 1.25 kPa and 2.50 kPa, inhibited spinal motoneuron excitability, emphasizing the therapeutic role of higher pressures in addressing muscular tension and pain [100].

Further research underscores the need for precision in pressure application. For example, a study [101] reported that physiotherapists typically apply an average pressure of 2.317 kg/cm² during deep friction massage, with higher pressures leading to faster analgesia onset. This suggests that moderate to deep pressures may be more effective in providing pain relief, though care must be taken to avoid exceeding individual tolerance thresholds. Regarding wrist-specific applications, a study [102] found that limiting wrist extension and flexion to 32.7° and 48.6°,

respectively, protected most individuals from reaching damaging pressures (30 mmHg). Similarly, another study [47] found that optimal pressure for the wrist tendon area was 1.36 kPa and 1.71 kPa for the muscle area, which can serve as a guide for setting pressure levels that both enhance circulation and avoid excessive strain on the wrist tendons.

Additionally, the pattern of pressure application plays a significant role in the muscle's response. A study [103] investigating the effects of pressure on the rectus femoris muscle found that applying deep pressure without prior conditioning resulted in increased muscle activity, whereas gradual pressure increases led to a more controlled response. This pattern suggests that a gradual increase in pressure, starting with light to moderate intensity, may be beneficial for the wrist massager to prevent overstimulation and ensure that the muscle and soft tissues respond effectively to the massage.

Considering the physiological responses observed in the literature, a balanced approach to pressure is recommended for the wrist massager in this thesis. Since most of the pressure values discussed in the studies are focused on leg muscles, apart from 1.36 kPa for the wrist tendon area, it would be advisable to focus on a pressure around 1.36 kPa for the wrist tendon region. This pressure is moderate enough to stimulate circulation and provide therapeutic relief without causing excessive strain or discomfort, especially for individuals with Carpal Tunnel Syndrome.

C. Ergonomics of Long-Term Use

From an ergonomic perspective, the design of wrist splints must ensure user comfort for prolonged wear without causing discomfort or skin irritation. The principles of ergonomics stress

the importance of adjustable fit, lightweight materials, and breathable fabrics to ensure that the device can be worn continuously, even during extended periods or overnight. This is similar to the C-TRAC device wherein the flexor retinaculum experiences traction as the bladder in the hand's dorsum expands, separating the thenar and hypothenar plates with a three-point traction force [85]. Furthermore, long-term usability is enhanced by devices that adjust to different wrist sizes and activity levels, reducing discomfort and promoting compliance. Ergonomics also emphasizes that the splint should not restrict regular wrist movements, ensuring users can perform daily activities without added strain or pain.

D. Wrist Splints and Discomfort Over Time

Wrist splints are commonly used to manage various conditions, but their long-term comfort and effectiveness can vary. Restricted movement associated with the long-term use of wrist splints can lead to discomfort, skin irritation, and reduced grip strength. This has been observed in a study that suggests a significant number of patients experience discomfort over time, leading to reduced use or discontinuation of the splint [104]. The solution to this problem is the motion support concept, which provides flexibility for wrist movement while still providing support without long-term stiffness and discomfort. This is crucial since full-time wear instructions have shown superior physiological improvements compared to night-only wear in carpal tunnel syndrome patients. However, adherence to specific wearing instructions can be limited [71].

E. Biomechanics of Wrist Motion

The wrist is a complex joint connecting the forearm and hand, allowing multidirectional motion while maintaining stability [105], [106]. It comprises the radiocarpal, midcarpal, and distal radioulnar joints, involving eight carpal bones and the radius and ulna [107]. Wrist motion primarily occurs in two planes: flexion-extension and radial-ulnar deviation, with the center of motion located in the capitate [89], [90], [91], [106]. As such, adequate wrist support must accommodate the natural motions of the wrist, such as flexion, extension, and radial-ulnar deviation, while simultaneously preventing excessive strain on the wrist structures. A motion support system, therefore, should not immobilize the wrist completely but allow for controlled movements, which are essential for daily functional tasks. Moreover, the study on soft robotic actuators and origami-patterned designs suggests that such systems, when integrated with pressure-feedback controls, can adapt to the varying needs of the user, providing support without restricting necessary motion [89].

F. CTS Compression Tests

Phalen's test, a widely used diagnostic tool for carpal tunnel syndrome (CTS), involves placing the backs of the hands together with fingers pointing downward and holding the position for approximately 60 seconds [41], [108]. This maneuver flexes the wrists into full flexion, creating pressure on the median nerve as it passes through the carpal tunnel. In individuals with CTS, this compression can provoke symptoms such as tingling, numbness, or pain in the fingers. However, in healthy individuals, the test generally causes only temporary discomfort due to the compression of soft tissues and nerves, which does not result in lasting harm [108].

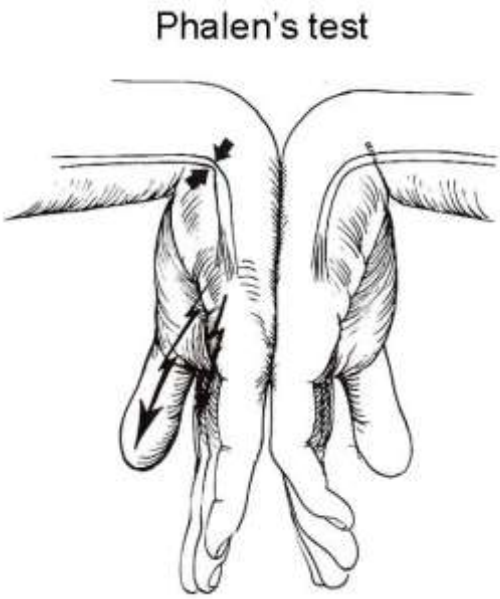

Figure 7 A visual representation of Phalen's Test

Research has shown that Phalen's test exhibits high specificity in healthy individuals, with false positives being rare [109], [110]. In these individuals, the discomfort experienced during the test is typically transient, dissipating once the wrist position is relieved. This makes the test a safe and non-invasive method for detecting median nerve irritation in patients with CTS without causing permanent damage. However, it is important to note that the test can affect grip strength temporarily, as the compression may induce some weakness in the hand muscles during the maneuver. This temporary reduction in grip strength, while discomforting, is generally reversible and does not cause any lasting effects.

According to Ms. Purol (Appendix B), although Phalen's test can induce temporary symptoms in healthy individuals, such as mild discomfort, or a reduction in grip strength, it is considered safe. The discomfort and loss of strength usually resolve shortly after the position is released, indicating that no significant harm is done. This characteristic makes it a useful tool in

clinical settings, especially when evaluating patients for CTS, while posing minimal risk to healthy individuals.

G. Range of Wrist Flexion Across Different People

The range of wrist flexion varies among individuals due to factors such as age, gender, and daily activities, making it a key consideration when conducting diagnostic tests like the Phalen's test. Normal wrist flexion spans reported ranges of 68.3 degrees to 74.2 degrees, and these values are influenced by age, with younger individuals typically exhibiting greater flexibility, while those over 60 show reduced motion [111], [112]. Gender differences further underscore variability, as females generally produce 76.3% of male flexion force, potentially affecting their ability to achieve and sustain the full 90-degree flexion required during the Phalen's test [113], [114]. On the other hand, healthy individuals with naturally flexible wrists may not feel sufficient compression on the median nerve at 90 degrees of flexion, as their anatomical structures can accommodate the position without inducing discomfort or nerve irritation. In such cases, extending beyond 90 degrees could be necessary to elicit a diagnostic response.

This concept aligns with findings from a study [115] that nerve conduction changes are more pronounced under prolonged or exaggerated wrist flexion in individuals with CTS, suggesting that modifying the angle may enhance the test's sensitivity in certain populations. Moreover, another study [116] emphasizes that adjustments to the Phalen's test, such as combining flexion with direct median nerve compression, yield higher diagnostic accuracy. Therefore, a tailored approach that accounts for individual differences in wrist flexibility may improve the reliability of the Phalen's test, particularly when applied to individuals with greater

ranges of motion who might otherwise present false-negative results at the standard angle.

H. Grip Strength

A handheld dynamometer, such as the Jamar Hydraulic Hand Dynamometer, is commonly used to measure maximum isometric grip strength, which refers to the maximal force a person can exert using their hand without any movement. The assessment procedure typically involves the patient being seated with their elbow flexed at 90 degrees, the forearm in a neutral position (with the palm facing the body), and the wrist slightly extended at an angle of 15–30 degrees. This standardized posture helps to ensure that the measurements are accurate and consistent across different individuals and testing sessions. The positioning minimizes the influence of compensatory muscle activity and ensures that the force measured comes predominantly from the hand and forearm muscles [44].

Threshold values for hand-grip strength measured using a dynamometer vary across demographic groups and contexts. General averages indicate maximal grip strength of approximately 43.7 ± 12.4 kg for adults, with men averaging 55.0 ± 10.2 kg and women 35.4 ± 5.2 kg. In older adults, a grip strength below 28.3 pounds (12.8 kg) for women over 75 years is considered subaverage. Clinically, a grip strength below 5 kg is strongly predictive of frailty and increased mortality risk in older populations. Testing conditions often standardize participant posture and use specific dynamometer settings, such as Handle Position 2 on a Jamar dynamometer, to ensure consistency and reliability in measurements [44].

I. The Patient-Rated Wrist Evaluation (PRWE)

The Patient-Rated Wrist Evaluation (PRWE) can be utilized alongside Phalen's test to assess the impact of wrist nerve compression on pain and function. While Phalen's test is a diagnostic tool designed to elicit symptoms of nerve compression, particularly in conditions such as carpal tunnel syndrome [117], the PRWE offers a quantitative measure of patient-reported pain and functional limitations [118]. By administering the PRWE every 15 to 20 seconds of performing Phalen's test, an evaluation on any immediate changes in pain levels or functional capacity can be made, thereby quantifying the test's effect on wrist nerve compression.

1. PAIN											
Rate the **average** amount of pain in your wrist over the past week by circling the number that best describes your pain on a scale from 0-10. A zero **(0)** means that you **did not** have any pain and a **ten (10)** means that you had the **worst pain you have ever experienced** or that **you could not do the activity because of pain.**											
RATE YOUR PAIN: Sample Scale ☞	0 No Pain	1	2	3	4	5	6	7	8	9	10 Worst Ever
At rest	0	1	2	3	4	5	6	7	8	9	10
When doing a task with a repeated wrist movement	0	1	2	3	4	5	6	7	8	9	10
When lifting a heavy object	0	1	2	3	4	5	6	7	8	9	10
When it is at its worst	0	1	2	3	4	5	6	7	8	9	10
How often do you have pain?	0 Never	1	2	3	4	5	6	7	8	9	10 Always

Figure 8 Pain Subscale of the PRWE

This combined approach integrates objective diagnostic findings with subjective patient-reported outcomes, providing a more comprehensive assessment of the clinical impact of nerve compression. For instance, if Phalen's test exacerbates pain or functional limitations as indicated by a higher PRWE score post-test, it reinforces the utility of the test in identifying clinically significant nerve compression. Additionally, the high reliability and validity of the PRWE across diverse patient populations, as demonstrated in various translations and studies [119], [120], ensure that the findings are robust and applicable in clinical and research settings. This

methodology bridges the gap between diagnostic tests and outcome measures, offering insights into the immediate and functional implications of wrist nerve compression.

J. Wrist splint Pressure tests

Research indicates the average baseline carpal tunnel pressure in healthy individuals averages 8 ± 4 mmHg (1.07 ± 0.53 kPa). To avoid worsening CTS symptoms or causing additional injuries, pressure splints must be designed to maintain or reduce pressure to within these thresholds. Additionally, the ideal wrist positioning for minimizing carpal tunnel pressure is approximately 2 ± 9 degrees of extension and 2 ± 6 degrees of ulnar deviation. Maintaining this position reduces strain on the median nerve, highlighting the importance of splints that promote proper wrist alignment [121].

Testing should include static and dynamic evaluations of pressure distribution across the wrist. Materials must be assessed for durability and comfort, ensuring they provide uniform pressure without causing discomfort or excessive localized force. Long-term testing under varied activity levels is necessary to confirm that the splint retains its structural integrity and efficacy over time. Regulatory requirements, such as FDA or CE compliance, mandate thorough safety and performance evaluations before approval for medical use [121].

Key Features for the Ideal Solution

An effective wrist splint for preventing Carpal Tunnel Syndrome (CTS) weakness should combine targeted relief, comfort, and flexibility. Key features include an integrated massage system to reduce tension around the median nerve, comfortable materials for extended wear, and a motion support system that adapts to natural wrist movements. Together, these elements

create a splint that not only helps alleviate muscle weakness but also supports long-term comfort and usability.

A. EMG Sensor

The EMG sensor measures electrical activity in muscles, and in clinical settings, it is often used with the Biopac system to assess muscle function. To calibrate the EMG sensor in Biopac, the sensor is placed on the target muscle, and the amplifier settings are adjusted for optimal signal quality. The process begins with a baseline measurement while the muscle is relaxed to capture any background noise. Next, a Maximum Voluntary Contraction (MVC) is performed, where the subject contracts the muscle as hard as possible. The highest signal recorded during this effort is used as a reference point to calibrate the system. This allows future readings to be normalized, making it easier to compare muscle activity across different individuals or trials. Proper calibration ensures that the system accurately reflects the muscle's electrical activity, aiding in reliable assessments of muscle strength and recovery.

B. Resting EMG Threshold

The abductor pollicis brevis (APB) muscle exhibits varying EMG amplitudes depending on its state and the subject's condition. In resting diabetic patients, EMG amplitudes for the right and left APB muscles are significantly lower in males showing 8.67 ± 1.15 µV and 5.00 ± 0.00 µV, respectively, compared to females showing 10.00 ± 0.00 µV [122]. Thus, a threshold of 0-10 microvolts (µV) can be taken as a reference for the resting state of the muscle. During moderate voluntary contraction however, the mean R1 response amplitude in healthy subjects is 1.17 mV (SD 0.79 mV) [123]. Nevertheless, it can be implied that an amplitude greater than 10 µV generally

implies muscle contraction.

Moreover, the APB's EMG activity is influenced by various factors, including intracortical inhibition, which can modulate muscle activation during specific tasks [124]. The APB functions in coordination with the abductor pollicis longus muscle, contributing to thumb and hand movements [125]. As such, these studies highlight the complexity of APB activation and the importance of considering various factors when interpreting EMG data.

C. Integrated Massage System

A wrist splint that would help prevent the muscle weakness due to CTS should possess some key features, whereby an incorporated massager system is very sensitive. A massage mechanism focuses on the wrist and forearm because this is essential in relieving muscle tension and increasing blood flow around the median nerve, which remains essential for alleviating muscle weakness and other CTS-related symptoms. It emphasizes the weakness of soft tissues in providing nerve release. Some factors that influence the efficiency of the massage system are the nature of the massage, for instance, kneading, pressing, or pulling massage, duration of the therapy, frequency of treatment, and temperature during the massage process.

It can also be developed by emulating mechanisms such as pressing, pulling, and pinning, which have been applied to the integrated massage system to ease the tissues' stiffness and the muscles' flexibility. Moreover, a programmable system implies the possibility of changing the massage intensity and is suitable for any phase of CTS. This feature fits the concept of soft tissue mobilization, which calls for frequent massaging of the affected tissues to decongest them and thus provide relief to CTS patients.

The pressure for the massager will be conducted by assessing the individual's pain tolerance and adjusting the pressure accordingly, with guidance and validation from a physical therapist (PT). The process will begin with the lightest pressure, as this is generally the most universally tolerable and can still provide effective therapeutic outcomes. The PT will monitor the individual's response to ensure that the pressure does not exceed their comfort level.

Since pressure is typically measured manually, through techniques like applying force with the thumb, no specific value will be assigned to terms like "moderate" or "deep pressure," as strength and tolerance can vary between practitioners. The PT will gauge the individual's tolerance and adjust the pressure gradually, starting with the lightest and increasing only if it is well tolerated.

D. Auto-fit System

Patients with CTS must always wear a wrist splint, especially during sleep, but constant wearing may cause skin rash and joint rigidity. For a device to encompass wearability, it suggests that the design of a product intended for long-term use needs to be comfortable and use material that allows the wearer to breathe and be eminently adjustable. Aspects such as the soft texture and the ability to allow air are essential when it comes to preventing the generation of rashes as people wear the splint for many hours. Another factor is the feasibility of the strap or fit adjustment since they also contribute to increased comfort to make the splint fit perfectly to the size and shape of a wrist of every user.

To ensure optimal comfort and effectiveness, pressure thresholds in splints for Carpal Tunnel Syndrome (CTS) must align with safe physiological limits. Research indicates that the average carpal tunnel pressure in healthy individuals is 8 ± 4 mmHg (1.07 ± 0.53 kPa), serving as a benchmark for splint designs. Exceeding these pressure levels can exacerbate symptoms or contribute to additional complications [121].

The splint for wear over long periods should be lightweight and moisture-resistant to minimize skin friction, thus not causing discomfort to the patient. Precautions must be taken to observe the principles of keeping the object as ergonomic as possible; the splint should not prove to be too tight but should be securely fixed simultaneously. Some of these may include customizable straps or the Boa fit systems, which help the user attain optimal fit without compromising comfort. This part accommodates the design decision and facilitates the user's ability to wear the splint undisturbed throughout the duration without such side effects.

E. Motion Support System

A motion support system in a wrist splint should follow the natural movements of the wrist while providing support during activities such as typing, gripping, or lifting. This system aligns with the Biomechanics of Wrist Motion by reducing compression without restricting motion. The splint should allow the wrist to move freely in flexion-extension and radial-ulnar deviation, which are necessary for performing everyday tasks without discomfort.

To achieve flexible, motion support, the motion wrist system incorporates an auto-lace mechanism controlled by EMG sensors, which monitor muscle activity in real time. This system responds automatically based on the user’s muscle engagement levels, delivering stability and

comfort without requiring manual adjustments. When the EMG sensors detect that the wrist muscles are at rest, such as during tasks requiring minimal wrist movement, the auto-lace mechanism contracts and provides firm support. This function stabilizes the wrist, reducing strain and offering the necessary bracing for activities like typing, where a steady wrist position can improve efficiency and comfort. This support helps prevent fatigue and strain, especially during repetitive motions, by maintaining the wrist in an optimal posture.

According to Ms. Purol (Appendix B), The allowable motion of 10 degrees flexion and 30 degrees extension provide a controlled and functional range, essential for tasks like rehabilitation or therapeutic support. This degree of motion balances joint mobility and stability, preventing excessive strain while allowing sufficient movement for functional activities. For instance, a splint may restrict motion by limiting wrist flexion to around 10 degrees and extension to about 30 degrees, rather than completely immobilizing the joint.

The system also incorporates a timed relaxation feature programmed to gradually reduce tension after a specific rest period. This time-based release prevents excessive pressure from building up, allowing for increased comfort over extended wear. Notably, the relaxation phase does not entirely detach the support, ensuring the splint remains in place and continues to offer mild stabilization. This slight tension reduction relieves the user from feeling overly restricted and helps prevent discomfort from prolonged immobility.

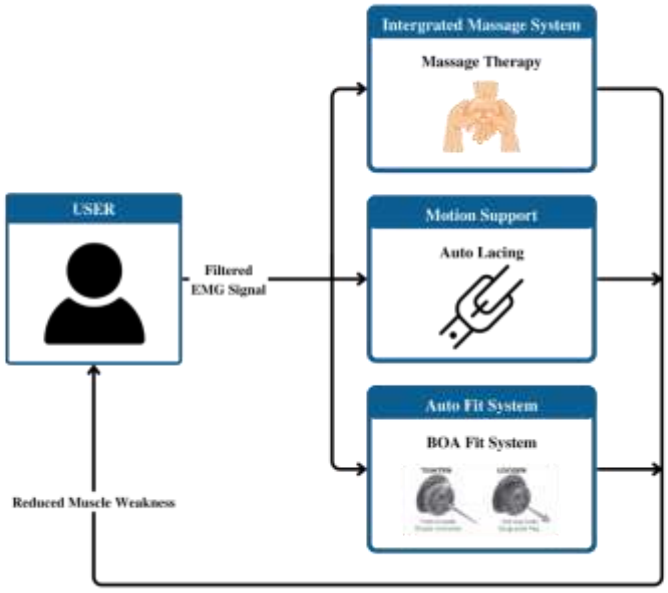

Figure 9 Conceptual Framework of the Related Literature

The conceptual framework presented in Figure 2.7 describes the interrelation among the main features critical to an ideal wrist splint for alleviating CTS-related muscle weakness. It encapsulates the three main components: A motion support system, an integrated massage system, long-term usability, and comfort. The massage system emphasizes soft tissue mobilization of the soft tissue around the median nerve, reducing muscle tension associated with CTS weakness. Breathable, adjustable materials such as the auto-lacing concept are highlighted for long-term usability, as they are necessary for long-wear comfort. The motion support system aligns with wrist biomechanics and provides motion support that maintains flexibility and prevents stiffness during repetitive wrist activities. Overall, these elements aid in a design that balances efficacy, patient comfort, and adaptability.

Theoretical Foundation and Practical Application

The theoretical foundation for this study is derived from biomechanical and ergonomic theories supporting selected features of motion support, long-term usability, and integrated massage. The biomechanical theory stresses the need to maintain natural wrist movements while providing enough stabilization to reduce nerve compression. Ergonomic principles, in parallel, seek to achieve compliance by designing the device to provide comfort to the user during extended use.

Thus, motion support systems, which adapt to natural wrist movements, are part of the optimal solution, providing the necessary stability. Furthermore, programmable massage mechanisms are integrated to help alleviate CTS-related muscle weakness. These features, when combined, address the most significant problems listed in the literature: discomfort in prolonged use, lack of wrist support, and lack of integrated massage systems in CTS. The proposed wrist splint with an integrated massage system incorporates these elements and, with its ability to alleviate muscle weakness, represents a comprehensive approach to managing CTS symptoms.

Summary and Conclusion

This review demonstrates promising noninvasive methods to treat Carpal Tunnel Syndrome (CTS), such as radioulnar wrist compression (RWC), various splints, and motion support systems to alleviate symptoms and improve patient comfort. RWC has been shown to increase the carpal arch space effectively, increase median nerve mobility, and reduce symptoms such as tingling and numbness. Intermittent and nighttime use of the C-TRAC and BWB studies provide substantial relief and minimal common side effects of continuous immobilization, including joint

stiffness and skin irritation. Soft robotic braces, which include soft origami actuators, support dynamic wrist movements necessary for daily activities, including flexion-extension and radial-ulnar deviation, addressing the functional needs of CTS patients more effectively than static devices.

Additionally, massage therapy has been identified to be beneficial in slowing the progression of CTS symptoms by promoting blood flow, decreasing muscle tension, and assisting in the healing of tissue around the median nerve. Targeted therapeutic effects are obtained from programmable mechanical devices that mimic massage techniques such as pressing, pulling, and pinning, which may alleviate muscle weakness and other CTS symptoms over time. Further research on adaptable wearable technologies, such as the Boa fit system, highlights the importance of adaptable and responsive designs that respond in real-time to the user's movements and discomfort.

Study	Integrated Massage System	Long-Term Usability	Motion Support
Smart splint using shape memory alloys (SMA) wires	✓	×	×
The mechanical hand of Thai massage	✓	×	×
Electro-mechanical device manipulator for CTS	✓	×	×
C-trac splint	×	✓	×
Beta wrist brace (BWB)	×	✓	×

Soft robotic (SR) brace with soft origami actuators	×	✓	✓
Exos wrist brace with BOA fit system for adjustable wearables	×	×	✓
Self-lacing shoe technology	×	✓	✓
eM-Brace	✓	✓	✓

Table 1 Summary of Related Literature

Table 2.1 compares various existing studies and devices to the proposed device based on three key features of an ideal solution for alleviating muscle weakness in CTS: the integration of a massage system, long-term usability, and motion support. While several studies highlight one or two of these features, none comprehensively address all three aspects. For instance, devices like the Smart Splint using Shape Memory Alloys (SMA) and the Mechanical Hand of Thai Massage integrate a massage system but neither support long-term usability nor dynamic movement. Similarly, while the Soft Robotic (SR) Brace with Soft Origami Actuators offers motion support and long-term usability, it lacks an integrated massage system.

This gap in the existing research underscores the importance of developing a device that provides a motion support system for wrist movements, incorporates an integrated massage function, and ensures long-term usability. Thus, the proposed device aims to bridge these gaps by addressing all three features simultaneously, offering a holistic and innovative solution to effectively alleviate muscle weakness in CTS.

Implications for Future Research

This comparison of current research reveals significant gaps, especially the absence of devices that combine all three essential features: massage, long-term usability, and motion support. Further research should seek to develop complete solutions that incorporate all these elements to produce more effective and sustainable treatments for CTS. Studies may also delve into enhancing the automatic delivery of massage through the integration of artificial intelligence, along with the automatic fitting system of the splint, to deliver radioulnar wrist compression efficiently. Moreover, the long-term clinical outcomes of such devices need to be studied, and it needs to be ensured that such devices are comfortable and adaptable to the functional demands of users. Such a possibility may provide a new direction for more customized and flexible forms of intervention in CTS management and related musculoskeletal disorders.

CHAPTER III
METHODOLOGY

Conceptual Framework

People suffering from CTS encounter significant difficulties doing their daily tasks requiring wrist movement. If untreated, this can result in a substantial loss of quality of life, reduced productivity, and an increase in long-term disability. However, existing wrist splints face several limitations as presented in Section 1.3 - Statement of the Problem. To address these problems, the proponents aim to develop an autonomous wrist splint equipped with an integrated massage system as shown in the conceptual framework in Figure 3.1 below.

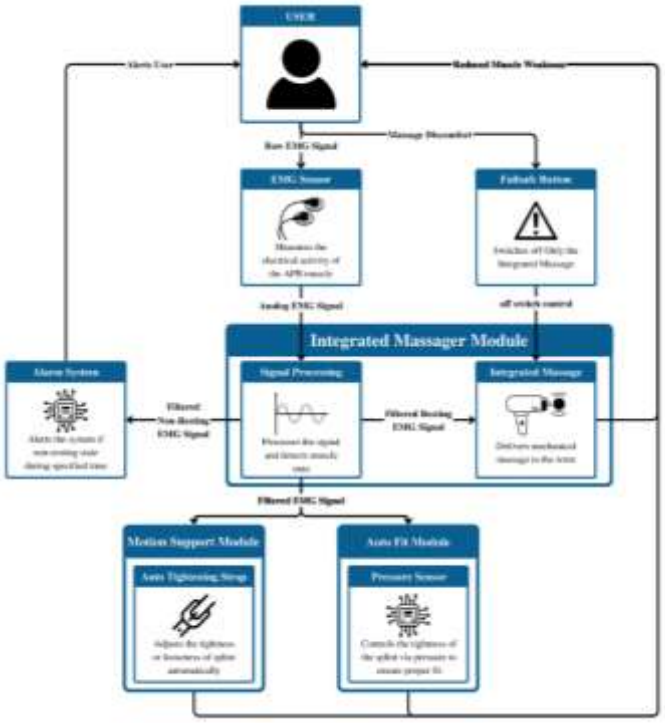

Figure 10 Conceptual Framework of the Proposed Solution

The proposed solution is composed of three modules: Integrated Massager Module,

Motion Support Module, and Auto Fit Module. The Integrated Massager Module is responsible for continuously gathering EMG signals as individuals engage in daily activities. It does so through an EMG sensor equipped with three surface electrodes arranged in a close triangular configuration to ensure accurate and continuous monitoring of muscle activity. These signals are then transmitted to a microcontroller, which filters and processes them, preparing the data for the activation of the system's mechanical components, present in all the three modules.

When the processed EMG signals indicate resting muscle activity, with amplitudes less than 10 μV, the microcontroller activates the integrated massager. Otherwise, the microcontroller will activate the alarm system, alerting the user that they need to be in a resting state at that time. Overall, the integrated massager module ensures that a massage will be automatically performed when muscles are at rest, reducing the need for manual intervention. Furthermore, the microcontroller adjusts the massage duration to 2-3 minutes, with pressure calibrated to a level of 1.36 kPa, ensuring a light tissue engagement to the wrist. The Integrated Massager Module also uses a soft, comfortable surface to maximize comfort and minimize irritation to inflamed tissues. Additionally, the user can also utilize the failsafe button in the case that the integrated massage is too painful for them. This failsafe button will stop the integrated massage only while keeping the rest of the system on.

Next, the Motion Support Module is designed for both flexibility and adjustability, enabling the allowable range of motion for daily tasks while providing essential stability to the wrist joint. It comprises of the auto tightening straps which will tighten the splint when muscles are at rest and loosen the splint when the muscles are moving. As such this will activate

simultaneously with the integrated massage, maximizing the effectiveness of the massage.

Finally, the Auto Fit Module ensures that the user can wear the splint for a prolonged period without compromising comfortability. This module features a pressure sensor that automatically detects the tightness of the splint, adjusting the auto-tightening straps as needed to maintain the correct fit without excessive pressure.

Overall, the integration of these three modules directly addresses the challenges outlined in Section 1.3, resulting in an improved wrist splint aimed at alleviating CTS-related muscle weakness.

Theoretical Framework

Anatomy of The Hand and Wrist

The hand and wrist structures must first describe where the surface electrodes and the massage system should be placed. In particular, which muscles and ligaments are involved in obtaining the myoelectric signals. First, the primary structure, the abductor pollicis brevis (APB), is essential in the thumb abductor, which enables it to move away from the palm [126]. It originates from the flexor retinaculum and the scaphoid tubercle and is inserted on the first phalanx of the thumb. Supplied with the recurrent motor branch of the median nerve, the APB is crucial for griping and controlling objects finely.

Furthermore, the flexor pollicis brevis (FPB) muscle, which is very close to the APB, is responsible for flexing the thumb. It originates from the flexor retinaculum as well as the tubercle of the trapezium, inserted into the lateral aspect of the proximal phalanx of the thumb [126]. It is essential to discuss the FPB muscle because the electrode placement may overlap with the two

muscles, which is expected as they are both near each other.

Figure 11 Anatomy of The Hand and Wrist

Lastly, the Transverse Carpal Ligament or the Flexor Retinaculum serves as the anterior boundary of the carpal tunnel, complemented by the dorsal boundary formed by the carpal bones. Within the carpal tunnel posterior to the flexor retinaculum are the tendons of four Flexor Digitorum Superficialis and Flexor Digitorum Profundus muscles, along with the Flexor Pollicis Longus and the median nerve [127].

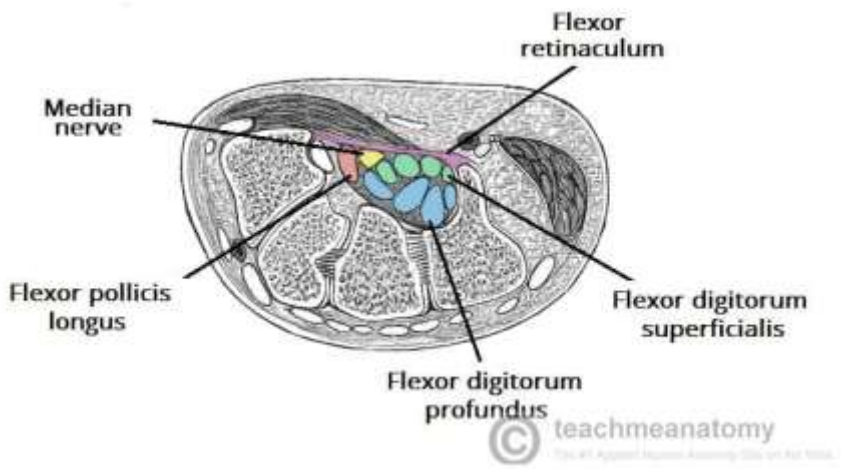

Figure 12 Anatomy of The Carpal Tunnel

During isometric contractions, these tendons become longer while the muscle fibers get shorter and, therefore, cause changes in muscle length [128]. This phenomenon indicates that the frequency of certain frequency content of the surface EMG signal is predominant at short muscle length. Additionally, as mentioned previously, when these tendons are under pressure from the median nerve compression, EMG signals may reveal changes in muscle function, increased co-activation, poor fatiguing, and pain-related patterns. Hence, this sensitivity of ISA to muscle length variations is attributed to the difference in conduction velocities, which is measured in muscles containing fibers of different diameters at varying muscle lengths [128].

EMG Signal Frequency Range

EMG measurements use monopolar or bipolar electrode setups with the ability to combine intramuscular and surface electrodes for more refined measurements [129]. The frequency range of EMG signals varies depending on the specific application and measurement conditions. Surface EMG signals can contain frequencies up to 500 Hz, with muscle activations

typically ranging from 100 Hz to almost 500 Hz [130]. In robotic hand control applications, the optimal myoelectric signal frequency band for muscle contractions was found to be between 60 and 80 Hz [131]. Another key factor in EMG is frequency range, with signal capture in the optimal range being between 50 to 150 Hertz, with full-range EMG analysis from 0.01 Hz to 10 kHz, depending on the type of examination [129].

Fourier Transform

The Fourier transform is a powerful mathematical tool and a fundamental tool in signal processing to decompose complex waveforms into their constituent frequency components. It turns time-domain signals into frequency-domain representations so that spectral analysis and manipulation of signals can be performed [132]. Several papers discuss the fundamental properties and applications of it. In [133], the Fourier transform's basic definition and properties are reviewed, the Plancherel theorem is proved, and the Fourier transform is used to solve wave equations. Another study [134] gave a self-contained study of the Fourier transform when applied to partial differential equations and dynamical systems while also proving the Plancherel formula. In [135], the study introduced a generalization of the Fourier transform, called the Katugampola Fourier transform, and explored its properties and relationship to the classical Fourier transform. An inversion formula and a convolution theorem are provided, and the potential for applying Fourier analysis in this new definition is expanded.

Amplification of Raw EMG Signals

EMG signals from the APB muscle are typically low in amplitude, with a mean amplitude

of only 1.17 mV [123]. Thus, to ensure these signals are usable for subsequent processing and analysis, they must first undergo amplification. A differential amplifier is employed for this purpose, as it enhances the amplitude of the EMG signal while maintaining its waveform integrity. Differential amplifiers are specifically designed to amplify the difference in voltage between two electrode inputs, which is crucial for minimizing interference from external noise sources.

One of the key features of the differential amplifier is its high Common Mode Rejection Ratio (CMRR), which enables it to effectively suppress common-mode noise such as electromagnetic interference from power lines (typically at 50 or 60 Hz). This suppression is essential for capturing the true muscle activity signal, as any noise can obscure the small variations in voltage that correspond to muscle states. Proper amplification is therefore a critical first step in transforming weak raw EMG signals into a format suitable for further filtering and analysis to differentiate between the relaxed and Active states of the muscle.

Signal Filtering Using High-Pass and Low-Pass Filters

To extract meaningful EMG signals from the APB muscle, noise and unwanted frequency components must be effectively removed. This is achieved through the implementation of high-pass and low-pass filters, both designed as active first-order filters operating within a gain range of 2 to 20 dB.

The high-pass filter, with a cutoff frequency of 20.8 Hz, is crucial for eliminating low-frequency noise, such as baseline drift caused by electrode movement or skin motion artifacts. By attenuating signals below the cutoff frequency, the filter ensures that only relevant EMG frequencies, which typically start around 20 Hz, are preserved for analysis. This preprocessing

step enhances the accuracy of subsequent signal interpretation by removing spurious fluctuations that do not represent muscle activity.

The low-pass filter, with a cutoff frequency of 498.4 Hz, is equally essential for attenuating high-frequency noise components. These may include electrical interference and aliasing artifacts, which could otherwise compromise signal clarity. By allowing frequencies below 498.4 Hz to pass while filtering out higher frequencies, the low-pass filter isolates the primary frequency range of surface EMG signals (approximately 20-500 Hz).

Together, the high-pass and low-pass filters create a bandpass effect, isolating the EMG signal's frequency range of interest while suppressing noise from both ends of the spectrum. The use of active filters provides the added benefit of amplification during the filtering process, ensuring that the filtered signals retain sufficient amplitude for subsequent rectification, smoothing, and feature extraction.

Digital Notch Filter Theory

The notch filter is a digital signal processing (DSP) tool to filter a specific narrow frequency band (attenuation or elimination) without distorting other frequencies. Notch filter is often considered a type of band stop filter with a narrow stop band, compared with other types of band-stop filters. A common design of the device is to remove undesired periodic interference or noise, usually 50-60 Hz hum from electrical powerline interference, while preserving nearby signal components.

The Notch filtering theory consists of setting the filter’s frequency response that approaches zero (or near zero) at a given frequency of interest. Poles and zeros in the filter’s

transfer function are used to accomplish this as shown:

$$H(z) = \frac{K(z^2 - 2z\cos\omega_0 + 1)}{z^2 - 2z\cos\omega_0 + r^2}$$

$$\omega_0 = 2\pi\left(\frac{f_0}{f_s}\right)$$

$$r \approx 1 - \frac{BW}{f_s} \times \pi, \text{ best result with } 0.9 \leq r < 1$$

If a zero is placed by a complex plane to a frequency which is unwanted, then the filter will suppress the amplitude of this frequency. This is sometimes implemented in digital filter design, using an infinite impulse response (IIR) filter structure with a pair of complex conjugate zeros and corresponding poles near the unit circle. The closer the poles are to the unit circle, the sharper or "notch depth" of the filter, with more poles yielding a sharper, narrower band attenuation. The difference equation describing the considered IIR filter has the following form:

$$y(n) = K\big(b_0x(n) + b_1x(n-1) + b_2x(n-2)\big) - a_1y(n-1) - a_2y(n-2)$$

$$a_1 = -2r\cos\omega_0$$

$$a_2 = r * r$$

$$b_0 = 1$$

$$b_1 = -2\cos\omega_0$$

$$b_2 = 1$$

Where *x(n)* is the last measurement of the signal, and *x(n-1)* and *x(n-2)* are the two previous measurements, *y(n)* is the current filtered value of the signal, and *y(n-1)* and *y(n -2)* - two previous values of the filtered signal [136].

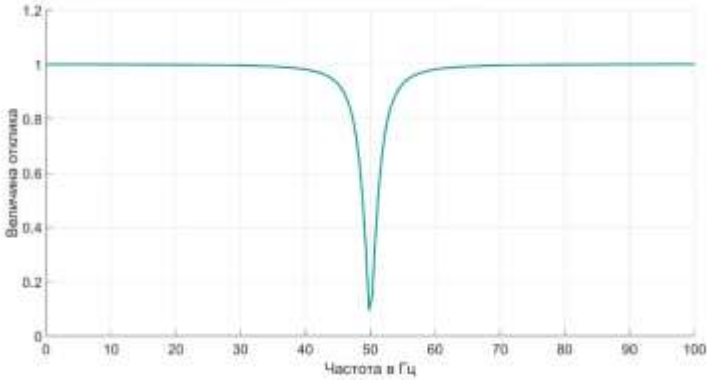

Figure 13 Frequency response of the Notch filter

Methodology

This section summarizes the methodologies used to achieve each specific objective of the study.

Table 2 Specific Objectives and Methodology

Specific Objectives	Methodology
1) To detect the muscle's state by acquiring electromyography (EMG) signals from the Abductor Pollicis Brevis muscle	**A. Integration of Surface EMG (sEMG) electrodes with EMG sensor** **B. Calibration of EMG sensor** **C. Integration of EMG sensor and Microcontroller** **D. Signal Acquisition Algorithm**
2) To develop and implement a signal processing module that minimizes	**E. Signal Processing Algorithm** **F. Implementation of Alarm System**

	noise and identifies the muscle's resting and active states using advanced filtering techniques	**G. Threshold Calibration and Rest Detection Algorithm**
3)	To design and integrate a lightweight massage system that activates at specified time intervals when the muscle is at rest	**H. Integration of DC Motor and Gear System for Myofascial Release** **I. Utilize Stepper Motor Precision for Myofascial Release** **J. Calibration of Integrated Massager** **K. Integration of battery power supply**
4)	To implement an auto-fitting feature that automatically adjusts the wrist splint's pressure to ensure a proper fit for any wrist size	**L. Implementation of Pressure Sensor and Detection Algorithm**
5)	To create a motor-based motion support system that automatically adjusts strap tension to accommodate the allowable range of wrist movement, providing consistent motion support	**M. Implementation of auto-adjusting belt system** **N. Implementation of Tension Adjustment Mechanism**

6) To evaluate the device's effectiveness through testing on 15 female participants aged 18–25 from Ateneo de Zamboanga University who frequently use keyboards for at least four hours daily	**O. Functional Testing** **P. System Testing** **Q. Beta Testing**

A. Integration of Surface EMG (sEMG) electrodes with EMG sensor

The integration of surface EMG (sEMG) electrodes with the EMG sensor will be achieved through a secure connection between the electrodes and the sensor's snap connectors. As such, the EMG sensor will be directly above the electrodes. Silver/silver chloride (Ag/AgCl) sEMG electrodes will be used for their stable conductivity and minimal baseline drift, ensuring reliable capture of low-amplitude EMG signals from the Abductor Pollicis Brevis, where the sEMG electrodes will be attached, as shown in Figure 3.5. The MID electrode will be connected to the middle of the muscle body, with the END electrode aligned in the direction of the muscle's length. Furthermore, the REF electrode will be placed adjacent to the muscle body. These electrodes will offer greater comfort to the user compared to needle electrodes, although they may result in a slight reduction in signal quality. With a diameter of 23.9 mm, the electrodes will be designed to effectively isolate the desired muscle signals while minimizing cross-talk from surrounding muscle activity.

Figure 14 Electrode Placement on the Abductor Pollicis Brevis Muscle

Additionally, to ensure optimal signal quality, the sEMG electrodes that will be used will be pre-gelled, latex-free adhesive pads as shown in Figure 3.6. This specific sEMG electrodes will guarantee stable and consistent skin contact, even on the curved surface of the wrist, and will reduce noise caused by electrode shifting during movement.

Figure 15 Surface EMG Electrodes

B. Calibration of EMG Sensor

The calibration of the EMG sensor using the BIOPAC system starts with the setting up of the equipment. It involves the connection of the EMG sensor securely to the BIOPAC platform, as well as the attachment of disposable adhesive electrodes to the subject's skin. The active electrode is placed over the belly of the *Abductor Pollicis Brevis muscle*, the reference electrode on a neutral bony site like the wrist, and the ground electrode on a neutral area such as the forearm or elbow. After setting up all the hardware, the software for acquiring the signals is configured with the BIOPAC. Parameters such as sampling rate (e.g. 1000 Hz), gain settings, and filtering options (high-pass filter at 20 Hz and low-pass filter at 450 Hz) are optimized to obtain the best signal quality.

The basal signal recording is first carried out with the subject at rest, ensuring stable and low noise. The subject then performs voluntary contractions of the Abductor Pollicis Brevis muscle, such as opposition of the thumb or pushing against resistance. Both contraction and relaxation phases are recorded by the EMG signal to ensure that the sensor discerns the obvious differences in signal amplitude and pattern. This is repeated several times to guarantee that this reading is consistent and reliable.

In case of inconsistencies or noise, changes in electrode placement, gain, or filtering settings are implemented to enhance the quality of the signal. After calibration is confirmed, the ability of the sensor to distinguish between relaxation and contraction of the muscle is confirmed. All data from the calibration and any software settings done and observations/adjustments needed are noted in records for future applications. This whole process guarantees proper EMG

signal acquisition for consequent applications.

C. Integration of EMG sensor and Microcontroller

Following the integration of the sEMG electrodes with the EMG sensor, the next step involves connecting the EMG sensor to the microcontroller for signal transmission, processing, and analysis as shown in Figure 3.7. Specifically, the EMG Sensor will capture the bioelectric signals from the sEMG electrodes and send them to the ESP32 microcontroller. The ESP32 will then convert the analog signals into digital form using its built-in analog-to-digital converter (ADC) for further processing and analysis.

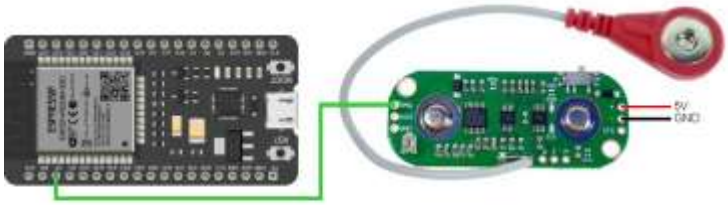

Figure 16 Circuit Diagram of the Integration of EMG Sensor and Microcontroller

This is achieved by connecting the raw input pin of the sensor to one of the ESP32 pins with a built-in ADC. Furthermore, the input voltage (Vin) of the EMG sensor will be connected to the 5V pin of the ESP32 along with the reference pin to the GND pin of the ESP32. This seamless integration between the sensor and microcontroller ensures efficient data collection, conversion, and analysis of muscle activity signals.

D. Signal Acquisition Algorithm

After the electrodes, EMG sensor, and microcontroller are fully integrated, the next step is to design and implement a signal acquisition algorithm using the Arduino Integrated Development Environment (IDE). The raw EMG signals will be captured using the Arduino's built-in analogRead() function, with a default sampling rate of 1000 Hz. Additionally, a delay will be added into the code to prevent the microcontroller from taking readings faster than can be monitored and processed.

During the development process, print statements will be utilized to display the EMG signal readings in the Serial Monitor. This is done to verify the correct acquisition of EMG signals. For instance, when the muscle is clenched, the EMG amplitude should fall >10uV, while when the muscle is at rest, the amplitude should remain lower and stable. This ensures that the system is accurately detecting muscle activity.

E. Signal Processing Algorithm

The signal processing algorithm begins by applying a bandpass filter to focus on the frequency range of interest, specifically between 20-500 Hz, to eliminate low-frequency noise (such as movement artifacts or baseline drift) and high-frequency noise (such as electrical interference). However, this is an already built in feature of the EMG sensor in which will not be included in the code.

Next, a notch filter is applied to eliminate powerline interference at 50 Hz, corresponding to the standard supply voltage frequency in the Philippines. This filter is essential for attenuating

powerline noise that could distort the EMG signal. The notch filter will be implemented using the ELEMYO library, which provides various functions for EMG applications. Specifically, the bandstop function of the library will be used to apply the notch filter, ensuring compact and efficient code. The implementation details of the notch filter are provided in Appendix C.

Once the EMG signal is filtered, the algorithm further processes the data using conditional statements to assess muscle activity patterns. Specifically, the filtered muscle state signal will be analyzed to determine whether the muscle is in a resting state, recorded at 0-10 µV, or in a non-resting state, recorded at any value above 10 µV, which will be further explained in section G.

F. Implementation of Alarm System

The alarm system is designed to ensure that the patient remains in a resting state during their scheduled massage. If the muscle activity exceeds the established threshold, a real-time web display will show the resting/moving state of the patient, notifying the patient that they are not in the resting state.

In addition, the EMG signals will be continuously monitored, as these will be used to control the auto-fit and motion support modules. However, the alarm will only be triggered during the scheduled massage periods, which are set 12 hours apart: once in the morning and once in the evening, as recommended by the licensed physical therapist that was interviewed by the proponents. Outside of these scheduled times, the system will still monitor muscle activity but will not trigger the alarm. This approach ensures that the patient is alerted only during the designated times for the massage, minimizing unnecessary alerts while ensuring the system functions effectively when needed.

The alarm system incorporates a blinking LED to alert the patient when their muscle activity exceeds the dynamic threshold during scheduled massage periods. The EMG sensor continuously monitors the muscle signals, and the ESP32 microcontroller processes the data, determining whether the patient is in a resting state. During designated massage times, set 12 hours apart in the morning and evening, the system activates the blinking LED if muscle activity surpasses the threshold, signaling the patient to relax. Outside of these periods, the EMG continues monitoring but suppresses the alarm to avoid unnecessary alerts.

The system's real-time clock (RTC) module ensures precise time-based scheduling, while the ESP32's processing capabilities provide accurate signal analysis and seamless communication between modules. The blinking LED minimizes power consumption while effectively catching the patient's attention, making it an ideal choice for continuous operation.

G. Threshold Calibration and Muscle State Detection Algorithm

The Muscle State Detection Algorithm begins with a calibration phase designed to determine a personalized dynamic threshold for each user. Calibration is initiated only when the splint is idle, no alarm is active, and the pressure has reached its set threshold, or the stepper motor has stopped moving. Once these conditions are met, the algorithm collects EMG readings for 10 seconds, continuously summing and counting the samples to obtain an average baseline value that represents the user’s resting muscle potential. After the 10-second interval, the baseline is finalized, and a dynamic threshold is computed as twice the baseline value or a minimum of 10 µV, whichever is higher. This adaptive threshold accounts for user-specific EMG characteristics and environmental variations, enhancing accuracy and reducing false activations.

After calibration, the system transitions to normal operation. The algorithm continuously monitors the EMG signal against the computed threshold. When the EMG amplitude remains below this dynamic threshold for an extended period, the system interprets the muscle as being at rest and activates the massager module to perform the myofascial release massage technique for 2 minutes and 30 seconds. If the EMG signal rises above the threshold, indicating active muscle movement, the massage is halted and an visual alarm is triggered to notify the user of resumed muscle activity.

To maintain reliability, a debounce mechanism is implemented that requires the EMG signal to remain below the activation threshold for a continuous 10-second period before the massage function can engage. This prevents false activation caused by transient signal spikes or minor electrical noise, ensuring that the system responds only to genuine muscle relaxation.

System validation and fine-tuning are conducted by having the user alternate between periods of rest and minimal wrist movement. Adjustments to the baseline multiplier or timing criteria are made when misclassifications occur to ensure consistent and accurate triggering of the massage system during true rest states. The complete implementation of this calibration and detection routine is presented in Appendix C.

H. Integration of DC Motor and Gear System for Myofascial Release

The massager module utilizes a DC motor and gear system to provide smooth, controlled motions specifically designed to alleviate muscle weakness related to CTS. The DC motor enables adjustable dynamic movements, ensuring the massage function is tailored to the user's needs, which is crucial for managing CTS caused by continuous strain on the wrist. Additionally, the gear

system efficiently distributes the motor's force across the wrist and hand, ensuring consistent pressure is applied to the most affected points. This precision guarantees that the correct amount of pressure is delivered to sensitive areas commonly impacted by CTS.

In this study, the rotation of the gears, powered by the DC motor, is designed to replicate the myofascial release massage technique through inward rotation along the wrist. Specifically, the gear system, as shown in Figure 3.10, converts the motor's high-speed rotation into a slower, controlled motion at the massage heads, ensuring they follow a precise path and effectively mimic the pressing and circular movements of a massage therapist. This slower motion achieved through the gear mechanism makes it possible to apply sustained, pressing, and circular movements, which is essential for targeting tight fascia and relieving pain.

The massage system operates at a controlled speed of 20 RPM, as illustrated in Figure 3.8, providing steady and consistent pressure for deep tissue therapy. The system delivers a pressure of approximately 1.36 kPa, as referenced in a study, which is effective for targeting tight fascia and relieving pain. This consistent pressure ensures reliability and comfort, making it suitable for therapeutic applications without variations in intensity. The controlled slow rotation maintains a stable force without sudden changes, ensuring user comfort while delivering firm, sustained pressure for effective myofascial release. By mimicking the gradual, targeted pressure progression characteristic of professional massage therapy, the system promotes muscle relaxation, enhances circulation, and reduces tension effectively.

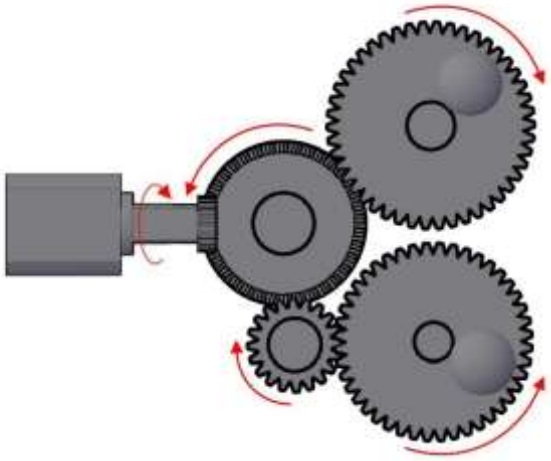

Figure 17 Motor-Based Massage System

I. Utilize Stepper Motor Precision for Myofascial Release

The stepper motor works in conjunction with the previously described gear system to replicate the myofascial release massage technique. While the gear system ensures slow and controlled motion, the stepper motor's high torque ensures that the massage is delivered with sufficient power, and for its low vibration to minimize potential discomfort for the user.

In this study, the 8mm Stepper Motor shown in Figure 3.9 is well-suited for a myofascial release massage system, where slow, controlled rotation and steady pressure are essential. Its friction torque (600–1200 gf.cm) adds resistance to keep the movements smooth, while the pull-in torque (300 gf.cm) ensures reliable engagement without slipping. These characteristics help deliver an effective massage needed to relieve tension at targeted pressure points.

Figure 18 8mm Stepper Motor

The integration of the 5V 8mm stepper motor with the gear system forms the core of the myofascial release massage system, ensuring slow, controlled motion and consistent pressure delivery. Mounted securely to the gear system, the stepper motor achieves the desired output speed of 20 RPM through precise mechanical alignment and a suitable gear reduction ratio. The motor driver interfaces with an ESP32 microcontroller, enabling precise control of speed, torque, and motion. A feedback loop incorporating force sensors or EMG input ensures the motor dynamically adjusts to deliver steady and effective pressure at targeted points, replicating massage techniques.

The ESP32's software controls the motor using feedback-driven algorithms to fine-tune performance based on sensor input. By monitoring real-time force or muscle signals, the system adapts motor behavior to maintain user comfort and achieve optimal therapeutic pressure. Initial testing verifies smooth operation and precise speed control, while calibration aligns feedback sensitivity for consistent performance. The entire system, housed and tested for reliability,

minimizes vibration and enhances user experience. This integrated approach ensures the stepper motor and gear assembly work seamlessly to deliver professional-grade myofascial release therapy.

J. Calibration of Integrated Massager

To evaluate the effectiveness of the massage system, a single-phase calibration protocol will be implemented. The massage pressure will be pre-set to 1.36 kPa, a value chosen based on existing research on effective massage therapy techniques for Carpal Tunnel Syndrome. Calibration will be conducted subjectively by a licensed physical therapist (PT). During this process, the PT will assess whether the applied pressure at 1.36 kPa is sufficient to achieve therapeutic relief and provide feedback on adjustments if necessary.

K. Integration of battery power supply

The integration of a 69800mAh 3.7V Li-ion battery pack ensures a stable and portable power supply for all system components. To meet the voltage requirements of the system, a DC-DC voltage booster is used to step up the nominal 3.7V battery output to a stable 9V. This boosted voltage is then distributed in parallel to power the system components effectively. A 7805-voltage regulator subsequently steps down this boosted 9V output to a stable 5V, powering the ESP32 microcontroller, EMG sensor, and pressure sensors. Meanwhile, the stepper motor is powered directly from the regulated 9V supply through the stepper driver, ensuring efficient operation. This configuration effectively manages power distribution, providing each component with the necessary voltage for reliable performance.

To estimate the system's battery life, its power consumption was analyzed. The ESP32 with sensors typically draws 150-250mA [137], while the 8mm stepper motor regulated by the DRV8825 stepper driver consumes approximately 165mA with both phases active. Without regulation, the motor could draw up to 450mA, but with proper current limiting set at approximately 82.5mA per phase, total consumption remains optimized. Additionally, the pressure sensors add approximately 5-10mA [138], and the EMG sensor contributes another 10-20mA [139].

Given the Li-ion battery pack's rated capacity of 69800mAh at 3.7V, the total effective capacity at the boosted 9V output is approximately 28670mAh, accounting for voltage conversion efficiency. In low-power mode (monitoring only), with an average consumption of around 150mA, the estimated runtime is approximately 191 hours (approximately 8 days). Under full operational load, where current draw increases to approximately 320-500mA, the battery life is estimated to be 57 to 89 hours (approximately 2.4 to 3.7 days) under continuous use.

Figure 19 69800mAh 3.7V Li-ion battery

The combination of the 9V DC-DC voltage booster and the subsequent 7805 voltage regulator ensures stable voltage supply and effectively reduces fluctuations. Capacitors further filter noise to maintain smooth operation and prevent damage to sensitive components. This configuration provides an optimal balance between power efficiency, performance, and operational longevity, enabling reliable and continuous functionality of the wrist splint system within its available battery capacity.

L. Implementation of Pressure Sensor and Detection Algorithm

To implement a pressure sensor, an existing splint will be customized and modified to mount the sensor along with other necessary components. This process will involve adapting the splint's design to accommodate the pressure sensor and ensure it functions seamlessly with the rest of the system.

In addition, the pressure sensor that will be utilized will accurately measure the force the wrist splint exerts on the user's wrist. It will be strategically placed in between the wrist splint and the user's skin to measure real time pressure change as the user wears it to ensure that the wrist splint is snug, but not too tight, or too loose, for smaller or larger wrists. This is a critical step to collect wrist pressure data and feed into the pressure detection algorithm to keep optimal fit.

Specifically, the pressure sensor collects data, and the pressure detection algorithm processes it to make real-time adjustments. It compares the measured pressure with a defined range of acceptable pressure values, which falls at 1.71 kPa for a comfortable and supportive fit. The algorithm alerts the control system if the pressure falls below 1.71 kPa (too loose) or exceeds

the same value (too tight) and adjusts the strap tension as required, automatically tightening or loosening [89]. In this way, the wrist splint adapts to various wrist sizes and maintains the optimal level of support dynamically through this continuous feedback loop.

M. Implementation of auto-adjusting belt system

The implementation of the auto-adjusting belt system in a wrist splint utilizes a stepper motor to provide precise and gradual adjustments to the tension of the belt, ensuring optimal support and comfort for the user. The stepper motor's ability to move in discrete steps allows for small, incremental changes in pressure, preventing sudden movements that could cause discomfort. This motor's high torque at low speeds also ensures the belt tension remains steady, making it ideal for the proposed wrist splint which requires consistent adjustments over time.

In addition, central to the system's functionality is the ESP32 microcontroller, which manages the auto-adjusting mechanism through a Proportional-Integral-Derivative (PID) control loop. This control loop enables real-time adjustments, calculating the necessary motor movements to maintain the appropriate level of support. As the wrist's condition changes, the system adapts, gradually adjusting the belt tension without abrupt shifts.

N. Implementation of Tension Adjustment Mechanism

The tension adjustment mechanism for the wrist splint is housed in a carefully designed 3D-printed housing that securely holds the stepper motor in place, ensuring stability and alignment during operation. This housing is designed to be both lightweight and compact, minimizing any additional bulk to maintain comfort and portability. The 3D-printed material can

be customized to fit the contours of the wrist, providing ergonomic benefits while ensuring that all components are tightly secured. The housing also includes mounting points for the motor and slots or guides for the straps, keeping the motor and belt system aligned and preventing any slippage or misalignment during use.

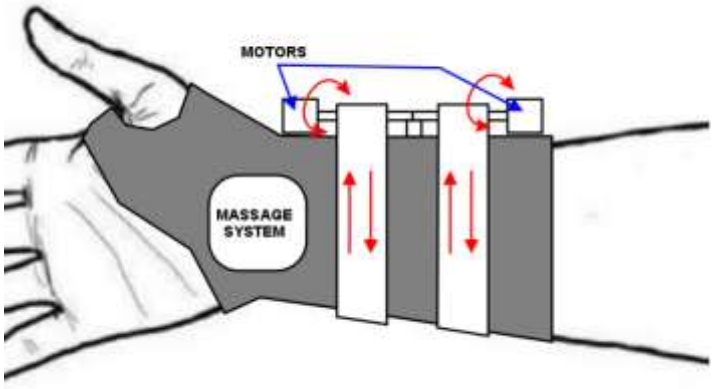

Figure 20 Auto Lacing Mechanism

In this setup, the straps are directly attached to spools or rollers connected to the stepper motor shaft. When the motor is activated, it rotates these spools, effectively winding or unwinding the straps to adjust the tension. This rolling mechanism allows the straps to contract or expand smoothly, dynamically adjusting the support around the wrist based on the tension requirements controlled by the ESP32. The use of a rolling action minimizes wear on the straps, as it avoids direct pulling or stretching, which can lead to material fatigue. The 3D-printed housing, therefore, plays a crucial role in maintaining consistent performance by providing a stable framework that holds all components in place, ensuring reliable, smooth, and responsive

tension adjustments.

O. Functional Testing

Signal Acquisition Module

To ensure that the EMG sensor in the wrist splint system accurately detects muscle activity and can transmit the data to the microcontroller, functional testing was performed on the signal acquisition module. This involved testing the sensor's ability to gather data during both resting and Active states of the target muscle, the Abductor Pollicis Brevis, and verifying that the sensor detected changes in the EMG signals when different muscle activities were performed.

The sensor and electrodes were securely attached to the ESP32 microcontroller. The EMG sensor module was placed on the Abductor Pollicis Brevis muscle of a human subject, with the sensor monitoring the muscle activity. The subject was asked to remain at rest, allowing the baseline muscle activity to be recorded. The subject then Active the muscle voluntarily to test whether the sensor could detect a significant change in muscle activity.

The performance of the sensor was checked by comparing the EMG signal acquired from the sensor module with known muscle activity, ensuring that the sensor detected changes from baseline activity during contraction. The data was reviewed for consistency and reproducibility across multiple trials, confirming that the sensor could reliably detect muscle activity during both resting and Active states.

To evaluate the sensor's durability and reliability, data was gathered from multiple trials under varying conditions to ensure consistent performance. The sensor's ability to transmit data to the microcontroller was also verified, ensuring that the data was captured accurately and sent

for further processing.

Test Condition	Expected Outcome	Number of Trials	Acceptable Accuracy Rate
Resting State	The sensor records EMG signals at rest.	10 trials	≥ 70% accuracy
Active State	The sensor should detect an increase in signal amplitude.	10 trials	≥ 70% accuracy

Table 3 Signal Acquisition Functionality Test

The functional testing results, shown in Table 3.2, indicated that the sensor successfully recorded EMG signals when the Abductor Pollicis Brevis muscle was at rest and during contraction, with 10 trials conducted for each condition. The results were deemed acceptable when the successful detection rate of the sensor was at least 7 out of 10 (70%) for each set of trials.

Signal Processing Module

The functional testing of the signal processing module ensures that the implemented filters and algorithms effectively enhance the clarity of the acquired EMG signals. The process evaluates whether noise components, such as powerline interference and baseline drift, are adequately removed while preserving relevant signal features. The testing involves real EMG

signal data under controlled conditions.

First, the signal processing algorithm is applied to the raw EMG data containing known artifacts, such as baseline drift, high-frequency noise, and powerline interference at 50 Hz. The bandpass filter (20–500 Hz) is tested by observing its ability to retain the relevant frequency components of the EMG signal while suppressing low-frequency motion artifacts and high-frequency interference. The notch filter is then applied to remove the 50 Hz powerline noise. The filtered signal is visually and quantitatively analyzed to ensure effective noise attenuation without significant distortion of the signal's amplitude or shape.

Following the filtering process, the module's ability to classify muscle states (resting vs. non-resting) is evaluated. The conditional logic embedded within the algorithm assesses the amplitude of the filtered signal to determine whether the muscle is at rest or active, as shown in Appendix C. Multiple trials are conducted with different levels of muscle contraction to ensure the algorithm accurately distinguishes between resting and active states, achieving an acceptable classification accuracy rate of ≥ 80%. In addition to classifying muscle states, the system is designed to activate an alarm if the muscle is detected in a Active state and remains off if it is at rest.

For real-time testing, filtered EMG signals are monitored using the Arduino IDE serial plotter to ensure that noise-free signals are transmitted to subsequent modules. The system's performance is evaluated based on two key metrics: signal-to-noise ratio (SNR) improvement and classification accuracy. The SNR improvement is measured by comparing the ratio of the filtered signal's power to the noise power before and after filtering, providing a quantitative measure of

the filtering efficiency. Classification accuracy is determined by the percentage of trials where the muscle state is correctly classified as resting or active.

Test Condition	Expected Signal Amplitude	Expected Outcome	Number of Trials	Acceptable Accuracy Rate
Resting State	< 10 µV or depending on the threshold	The EMG signal of the Abductor Pollicis Brevis is filtered, processed, and classified as resting, while the alarm is off.	10 trials	≥ 80% accuracy
Active State	> 10 µV or depending on the threshold	The EMG signal of the Abductor Pollicis Brevis is filtered, processed,	10 trials	≥ 80% accuracy

	and classified as Active, activating the alarm.

Table 4 Signal Processing Functionality Test

The functional testing results, shown in Table 3.3, indicate that the signal processing module successfully filtered and processed the EMG signals during both resting and Active states, with 10 trials conducted for each condition. The results were deemed acceptable when the classification of resting or non-resting was at least 8 out of 10 (80%) for each set of trials. Additionally, the system should correctly activate the alarm during muscle contraction.

Integrated Massager Module

The functional testing of the integrated massager module focuses on verifying its ability to deliver consistent massage pressure during the resting state. The expected outcome for this test condition is that the integrated massager maintains a consistent pressure of 1.36 kPa for a duration of 2 minutes and 30 seconds. This ensures that the massager operates within the prescribed therapeutic parameters, providing effective support for muscle relaxation and relief.

In the tests, the massager was evaluated over 10 trials, with each trial measuring the consistency of the pressure delivered during the 2.5-minute duration. The pressure was monitored continuously throughout the trials to ensure it remained within the targeted range, with minimal variation. The results were deemed acceptable when the massager's performance met or exceeded an accuracy rate of 80% in consistently delivering the target pressure.

Test Condition	Expected Outcome	Number of Trials	Acceptable Accuracy Rate
Resting State	The Integrated massager delivers a consistent massage pressure of 1.36 kPa for 2.5 minutes	20 trials	≥ 80% accuracy

Table 5 Integrated Massager Functionality Test

The functional testing results, shown in Table 3.4, indicated that the integrated massager successfully maintained a consistent massage pressure of 1.36 kPa during the resting state in 16 out of 20 trials, meeting the acceptable accuracy rate of ≥ 80%. These results confirm that the integrated massager operates within the intended parameters for effective muscle relaxation.

Auto Fit Module

The functional testing of the auto-fit module focuses on verifying the system's ability to apply an optimal pressure of 3.68 kPa to the user's arm, ensuring a comfortable and effective fit. The objective of this testing is to ensure that the pressure exerted by the splint remains within the optimal range, providing adequate support without causing discomfort.

The reference pressure of 3.68 kPa was determined based on the ratio between the measured splint pressures and the optimal massage pressure range (1.36–2.00 kPa) established in prior calibration. By computing the proportional relationship between the splint and massager

pressures, an average ratio of 0.37 was obtained. Using this ratio, the ideal splint pressure was derived as 1.36kPa/0.37=3.68kPa, which served as the target value for the auto-fit module.

During testing, the Em-Brace's built-in pressure sensor continuously recorded pressure data throughout ten trials to verify whether the system could achieve and maintain the target pressure. For each trial, the measured pressure was compared against the expected value of 3.68 kPa to assess the accuracy and stability of the auto-fit module's tightening performance.

The results of the testing were considered acceptable if the splint's pressure readings closely approximated the 3.68 kPa target within a reasonable margin of error in at least seven out of ten trials, yielding an acceptable accuracy rate of ≥ 70 %. This ensured that the auto-fit system consistently applied the correct pressure to the user's arm and could adapt to variations in arm shape and size.

Test Condition	**Expected Outcome**	**Number of Trials**	**Acceptable Accuracy Rate**
Auto-Fit Pressure	The splint applies a pressure of approximately 3.68 kPa to the user's arm based on the derived optimal pressure ratio with the	10 trials	≥ 70% accuracy

massager.

Table 6 Auto-Fit Module Functionality Test

The functional testing results, shown in Table 3.5, indicated that the auto-fit module successfully maintained the target pressure of approximately 3.68 kPa in 7 out of 10 trials, meeting the acceptable accuracy rate of ≥ 70%. These results confirm that the auto-fit module provides consistent and accurate pressure to the user's arm, ensuring optimal comfort and fit for therapeutic support.

Motion Support Module

The functional testing of the motion support module is designed to verify that the wrist splint can adjust its tension in response to muscle contractions, allowing for the necessary wrist movement during daily activities. The system should untighten during muscle contraction, providing flexibility for wrist flexion up to 10 degrees and extension up to 30 degrees. This ensures that the splint supports the wrist during rest or non-contraction states while facilitating proper movement during muscle activity.

To test the motion support module, a goniometer (or an equivalent motion tracking device) is used to measure the wrist's range of motion during both muscle contraction and passive wrist movements. During the trial, when the wrist muscles contract, the splint is expected to loosen its tension to allow for flexion of approximately 10 degrees and extension of about 30

degrees. Muscle contractions are detected using electromyographic (EMG) sensors, and the motion of the wrist is closely monitored to ensure that the splint allows adequate movement without undue resistance.

The expected outcome of the testing is that the splint will enable wrist flexion to 10 degrees and extension to 30 degrees, ensuring sufficient mobility during functional tasks while maintaining support when the muscle is relaxed. The functional testing is conducted over 10 trials, and the splint's performance is evaluated based on its ability to achieve the specified range of motion. The results are considered acceptable if the wrist achieves the specified angles of flexion and extension in at least 8 out of 10 trials.

Test Condition	**Expected Outcome**	**Number of Trials**	**Acceptable Accuracy Rate**
Active State	The splint untightens to allow wrist flexion of 10 degrees and extension of 30 degrees	10 trials	≥ 80% accuracy

Table 7 Motion Support Functionality Test

The functional testing results, shown in Table 3.6, indicated that the motion support module successfully allowed wrist flexion to 10 degrees and extension to 30 degrees in 8 out of 10 trials, meeting the acceptable accuracy rate of ≥ 80%. These results confirm that the motion

support module operates as intended, providing the necessary wrist movement while maintaining optimal support during non-contraction states.

P. System Testing

Signal Acquisition Module and Signal Processing Module

The system testing phase evaluated the integration of the Signal Acquisition and Signal Processing modules to ensure they work together in detecting and processing EMG signals from the Abductor Pollicis Brevis. The primary goal was to confirm that the system reliably differentiates between resting and Active muscle states. The testing focused on verifying that the sensor accurately detects low-amplitude signals in the resting state and responds with proportional increases in signal amplitude during muscle contraction. The system's performance was measured by its ability to process noise-free signals and classify muscle states with high accuracy.

Test Condition	Expected Signal Amplitude	Expected Outcome	Number of Trials	Acceptable Accuracy Rate
Resting State	< 10 µV or depending on the threshold	The EMG signal of the Abductor Pollicis Brevis is detected,	10 trials	≥ 80% accuracy

		filtered, processed, and classified as resting, while the alarm is off.		
Active State	> 10 µV or depending on the threshold	The EMG signal of the Abductor Pollicis Brevis is detected, filtered, processed, and classified as Active, activating the alarm.	10 trials	≥ 80% accuracy

Table 8 Signal Acquisition Module and Signal Processing Module System Testing

Signal Processing Module and Integrated Massager Module

System testing for the Signal Processing and Integrated Massager modules focuses on verifying their integration and ensuring they function together as intended. The primary goal is

to ensure that the processed EMG signals accurately trigger the massager under appropriate conditions, such as when the muscle is Active. In this context, the Signal Processing Module will filter and classify the EMG signals into resting or Active states, while the Integrated Massager Module will respond accordingly by either remaining inactive or delivering the prescribed therapeutic pressure.

During testing, two distinct muscle states are evaluated: resting and Active. In the resting state, the expected outcome is that the Signal Processing Module will correctly classify the EMG signal within the dynamic threshold, prompting the massager to activate and deliver the consistent pressure of 1.36 kPa. In contrast, during the Active state, the Signal Processing Module should identify the signal exceeding the value of the dynamic threshold and prevent the massager from activating, keeping it inactive.

The system's performance is measured through multiple trials to assess the classification accuracy of the muscle state and the massager's response. The goal is for the system to classify the resting state and Active state with at least 80% accuracy, ensuring that the processed EMG signal is correctly interpreted. Similarly, the massager must perform within the acceptable accuracy rate, activating only when necessary and maintaining a consistent pressure of 1.36 kPa during the Active state. The integration of real-time monitoring through tools like the Arduino IDE serial plotter will help confirm that the system operates without significant noise, providing reliable results during testing.

Test Condition	**Expected Signal**	**Expected Outcome**	**Number of Trials**	**Acceptable Accuracy**

	Amplitude			Rate
Resting State	< 10 µV or depending on the threshold	The EMG signal is classified as resting, activating the massager.	20 trials	≥ 80% accuracy
Active State	> 10 µV or depending on the threshold	The EMG signal is classified as Active, activating the alarm.	20 trials	≥ 80% accuracy

Table 9 Signal Processing Module and Integrated Massager Module System Testing

Signal Processing Module and Auto Fit Module

In the system testing for the Signal Processing Module and Auto-Fit Module, it is important to consider that the Auto-Fit module should be applied only when the muscle is at rest. This ensures that the support system adjusts the pressure for comfort and therapeutic benefit exclusively during rest periods, avoiding interference with the Motion Support Module discussed in the succeeding section.

The Signal Processing Module, as previously described, is responsible for filtering and

processing the EMG signals, accurately identifying resting and active muscle states. The muscle's resting state, defined by a signal amplitude within the dynamic threshold, triggers the Auto-Fit module to tighten the splint and achieve the target pressure. Conversely, when muscle activity exceeds the dynamic threshold, indicating contraction, the Auto-Fit module remains inactive to prevent unnecessary tightening during movement.

For testing, the Signal Processing Module was evaluated in both resting and active muscle conditions. The primary objective was to ensure accurate classification of muscle states and proper activation of the Auto-Fit response only when rest was detected. The acceptable accuracy rate for signal classification was set at ≥ 80 %.

The Auto-Fit module, in turn, was tested for its ability to apply the derived target pressure of 3.68 kPa—the optimal splint pressure based on the proportional ratio between the splint's force output and the massage system's therapeutic pressure range. The module was expected to perform tightening only during the resting state and remain inactive during activity. The acceptable accuracy rate for pressure regulation was defined as ≥ 70 % across ten trials.

Test Condition	**Expected Signal Amplitude**	**Expected Outcome**	**Number of Trials**	**Acceptable Accuracy Rate**
Resting State	< 10 µV or depending on the threshold	Signal processed and classified as resting,	10 trials	≥ 80% accuracy

		triggering Auto-Fit to tighten up to 3.68 kPa pressure.		
Active State	> 10 µV or depending on the threshold	Signal processed and classified as Active, Auto-Fit remains inactive.	10 trials	≥ 80% accuracy

Table 10 Signal Processing Module and Auto Fit Module System Testing

The system testing confirmed that the Signal Processing Module accurately differentiated resting and active muscle states, achieving an acceptable classification accuracy. The Auto-Fit module reliably activated only during the resting condition and consistently reached the target pressure of approximately 3.68 kPa in line with the defined operational threshold, validating the integrated performance of both modules in coordinating pressure control with muscle activity.

Signal Processing Module and Motion Support Module

The integration of the Signal Processing and Motion Support modules is crucial for ensuring that the wrist splint not only identifies muscle states accurately but also adjusts its

tension appropriately to accommodate the user's needs. Together, these two modules enable the splint to respond dynamically to muscle activity, providing both support during rest and flexibility during daily activities.

The Signal Processing module classifies muscle states by analyzing the amplitude of the filtered EMG signals. When the muscle is at rest (< 10 µV or depending on the threshold), the system classifies the muscle as in a relaxed state and keeps the splint's tension at a constant level for optimal support as discussed in the previous section. However, when the muscle contracts (> 10 µV or depending on the threshold), the Signal Processing module signals the Motion Support module to loosen the splint, allowing for wrist flexion up to 10 degrees and extension up to 30 degrees. This dynamic response is essential for facilitating functional wrist movements during daily activities while maintaining necessary support when the muscle is not active.

During system testing, both modules work in tandem to ensure proper functionality. The Signal Processing module ensures accurate classification of muscle states (resting or Active), while the Motion Support module ensures that the splint loosens appropriately during contraction, allowing the wrist to move freely within the specified range of motion. This integrated response is tested over 10 trials for each condition (resting and Active), and the results are deemed acceptable when the system achieves ≥80% accuracy.

In practical terms, when the Signal Processing module detects that the muscle is at rest, it maintains the splint's tension to provide support, ensuring comfort. Conversely, when muscle contraction is detected, the system dynamically adjusts the splint tension, enabling the user to perform tasks that require wrist flexibility, such as writing or gripping objects. The combined

testing of these two modules ensures that the wrist splint is both functional and comfortable under various conditions.

Test Condition	Expected Signal Amplitude	Expected Outcome	Number of Trials	Acceptable Accuracy Rate
Resting State	< 10 µV or depending on the threshold	The signal is classified as resting, and the splint remains in a supported state.	10 trials	≥ 80% accuracy
Active State	> 10 µV or depending on the threshold	The signal is classified as Active, and the splint loosens to allow wrist movement (flexion up to 10° and	10 trials	≥ 80% accuracy

extension up to 30°).

Table 11 Signal Processing Module and Motion Support Module System Testing

Q. Beta Testing

The beta testing phase was designed to evaluate the eM-Brace device's effect in alleviating muscle weakness associated with Carpal Tunnel Syndrome (CTS). The testing involved temporarily simulating median nerve compression in healthy participants and measuring grip strength both before and after using the eM-Brace device for massage therapy. This approach ensured the simulation of CTS symptoms in a controlled environment while assessing the device's ability to improve grip strength and reduce discomfort.

The study included 15 female respondents aged 18–25 years from Ateneo de Zamboanga University. These participants were selected based on their frequent keyboard use of at least four hours daily, which is a known risk factor for CTS. Temporary CTS symptoms were replicated through Phalen's Test which involved placing the back of the hands together with fingers pointing downward and holding the position for approximately 60 seconds to create pressure on the median nerve, inducing mild discomfort. The maximum wrist flexion achieved during the test was approximately 90 degrees but may vary from person to person. Moreover, a pain scale evaluation was conducted every 15 to 20 seconds during the test, where participants rated their discomfort on a scale of 0 (no pain) to 10 (severe pain). This allowed for the monitoring of symptom progression and individualized responses to the induced pressure. According to Ms. Frencie

Quintin Z. Purol, PTRP, and established literature [108], [109], [110], while Phalen's Test can cause temporary discomfort or a reduction in grip strength in healthy individuals, it is considered safe. The discomfort typically resolves once the position is relieved, indicating no lasting harm. Additionally, grip strength will also improve shortly after, however there is no basis for how long it takes for grip strength to be restored in healthy individuals and may vary from person to person.

Each participant's baseline grip strength was recorded before symptom induction, and this personalized value served as the benchmark for evaluating the device's effect. Without intervention, grip strength was measured at the 5- and 10-minute marks post-symptom induction to determine natural recovery timeframes. Moreover, grip strength was evaluated using an off-the-shelf Hand Dynamometer. This device measures the maximum isometric grip strength, ensuring consistent and accurate data collection. Participants were seated with their elbows flexed at 90 degrees, forearms in a neutral position, and wrists extended at an angle of 15–30 degrees. This posture minimized compensatory muscle activity and ensured that grip strength measurements reflected the actual performance of the hand and forearm muscles.

Participants	Grip Strength Before Massage (kg)	Grip Strength After Massage (kg)	Improvement in Grip Strength (kg)	Pain Scale Before Massage	Pain Scale During Massage	Pain Scale After Massage
1	< 35.4 ± 5.2 kg	≥ 35.4 ± 5.2 kg	≥ 2.2 kg	0-10	0-10	0-10

2	< 35.4 ± 5.2 kg	≥ 35.4 ± 5.2 kg	≥ 2.2 kg	0-10	0-10	0-10
3	< 35.4 ± 5.2 kg	≥ 35.4 ± 5.2 kg	≥ 2.2 kg	0-10	0-10	0-10
4	< 35.4 ± 5.2 kg	≥ 35.4 ± 5.2 kg	≥ 2.2 kg	0-10	0-10	0-10
5	< 35.4 ± 5.2 kg	≥ 35.4 ± 5.2 kg	≥ 2.2 kg	0-10	0-10	0-10
6	< 35.4 ± 5.2 kg	≥ 35.4 ± 5.2 kg	≥ 2.2 kg	0-10	0-10	0-10
7	< 35.4 ± 5.2 kg	≥ 35.4 ± 5.2 kg	≥ 2.2 kg	0-10	0-10	0-10
8	< 35.4 ± 5.2 kg	≥ 35.4 ± 5.2 kg	≥ 2.2 kg	0-10	0-10	0-10
9	< 35.4 ± 5.2 kg	≥ 35.4 ± 5.2 kg	≥ 2.2 kg	0-10	0-10	0-10
10	< 35.4 ± 5.2 kg	≥ 35.4 ± 5.2 kg	≥ 2.2 kg	0-10	0-10	0-10
11	< 35.4 ± 5.2 kg	≥ 35.4 ± 5.2 kg	≥ 2.2 kg	0-10	0-10	0-10
12	< 35.4 ±	≥ 35.4 ±	≥ 2.2 kg	0-10	0-10	0-10

	5.2 kg	5.2 kg				
13	< 35.4 ± 5.2 kg	≥ 35.4 ± 5.2 kg	≥ 2.2 kg	0-10	0-10	0-10
14	< 35.4 ± 5.2 kg	≥ 35.4 ± 5.2 kg	≥ 2.2 kg	0-10	0-10	0-10
15	< 35.4 ± 5.2 kg	≥ 35.4 ± 5.2 kg	≥ 2.2 kg	0-10	0-10	0-10

Table 12 Beta Testing Table for eM-Brace

Grip strength measurements were taken before and after massage therapy to evaluate the therapeutic effect of the eM-Brace device. Each participant underwent a single session, with grip strength recorded immediately after symptom induction through Phalen's Test and again following a 2-minute and 30-second massage using the device. Although general grip strength norms were initially considered, the evaluation framework was refined using the findings from the literature [137], whose study specifically investigated massage therapy's impact on carpal tunnel syndrome. They reported that a grip strength improvement of 2.2 kg following massage therapy represented a clinically meaningful change. Consequently, this study adopted the 2.2 kg threshold to determine effectiveness, allowing a condition-specific assessment of functional improvement. In parallel, pain levels were documented using a 0–10 numeric rating scale before, during, and after massage. A participant was deemed to have responded positively if their grip strength increased by at least 2.2 kg and pain levels decreased post-intervention. This method enabled a focused evaluation of the eM-Brace device's immediate impact on both grip function

and discomfort reduction, grounded in clinically relevant and condition-specific criteria.

Gantt Chart

The Gantt chart shown in Figure 3.11 provides a detailed timeline for the study, outlining key tasks involved in developing an autonomous wrist splint equipped with an integrated massage system. Each task, listed along the left side, is represented by a horizontal bar, with the length of each bar indicating the duration of that task. The project begins with hardware-focused tasks, such as the "Integration of the Surface EMG (sEMG) electrodes with EMG sensor," the "Integration of the EMG sensor and microcontroller," as well as the “Integration of DC motor and gear system for Myofascial Release” which were done during the last week of October and first week of November. Following this, algorithm development tasks, including the "Signal Acquisition Algorithm" and "Signal Processing Algorithm," were scheduled sequentially, allowing focused attention on each component. Towards the latter part of the timeline, more hardware-based tasks such as "Implementation of Pressure Sensor and Detection Algorithm" and "Integration of Stepper Motor and Control Mechanism" are planned, leading to the project’s anticipated completion in Mid-February.

Table 13 Gantt Chart of the Study

Methods or Task	Weeks of 2025													
	January		February				March				September		October	
	2	3	1	2	3	4	1	2	3	4	3	4	1	2
A. Integration of Surface EMG (sEMG) electrodes with EMG sensor														
B. Calibration of EMG sensor														
C. Integration of EMG sensor and Microcontroller														
D. Signal Acquisition Algorithm														
E. Signal Processing Algorithm														

F. Implementation of Alarm System														
G. Threshold Calibration and Rest Detection Algorithm														
H. Integration of DC Motor and Gear System for Myofascial Release														
I. Utilize Stepper Motor Precision for Myofascial Release														
J. Calibration of Integrated Massager														
K. Integration of Battery Power Supply														
L. Implementation of Pressure Sensor and Detection Algorithm														

M. Implementation of auto-adjusting belt system														
N. Implementation of Tension Adjustment Mechanism														
Functional Testing														
System Testing														
Beta Testing														

CHAPTER IV
RESULTS AND CONCLUSION

Table 14 Summary of Results

Methodology	Summary of Results	Verdict
A. Integration of Surface EMG (sEMG) electrodes with EMG sensor	The sEMG electrodes were successfully integrated with the EMG sensor, which was verified through a continuity test confirming stable electrical connections. Proper electrode placement and adhesive pads ensured minimal motion artifacts and impedance fluctuations, leading to consistent and reliable signal transmission.	Success – The sEMG electrodes were successfully integrated with the EMG sensor, ensuring stable electrical connections and reliable signal acquisition.
B. Calibration of EMG sensor	The EMG sensor calibration confirmed reliable muscle activity detection. Comparison with the Biopac system showed synchronized signals without delays, with the sensor accurately reflecting amplitude changes, validating its effectiveness for muscle signal acquisition.	Success – The EMG sensor was calibrated successfully, demonstrating accuracy, synchronization, and amplitude detection comparable to the BIOPAC system.

C. Integration of EMG sensor and Microcontroller	The EMG sensor was connected to the ESP32 microcontroller, with signal output routed to GPIO 36. Voltage continuity tests confirmed stable power and ground connections. Recorded EMG waveforms showed consistent readings, with minor interference mitigated through grounding and shielding techniques.	Optimized – The EMG sensor was successfully integrated with the ESP32 microcontroller, ensuring stable signal transmission with minimal interference.
D. Signal Acquisition Algorithm	The EMG signal acquisition on the ESP32 converted 12-bit ADC readings into voltage values, capturing relative differences between rest and active states. While the values are a remapped version of true muscle activity, the algorithm reliably sampled and transmitted signals, enabling MATLAB-based processing and RMS segmentation to distinguish resting and active muscle intervals.	Verified – The signal acquisition algorithm successfully retrieved and transmitted EMG signals with accuracy and stability.
E. Signal Processing Algorithm	The real-time implementation of 20–200 Hz bandpass and 50 Hz notch IIR filters on the ESP32 effectively	Optimized – The filtering algorithm enhanced EMG

	replicated the MATLAB calibration results, suppressing baseline drift, high-frequency noise, and 50 Hz interference.	signal clarity and fidelity, ensuring precise detection of muscle activation events.
F. Implementation of Alarm System	The alarm system reliably detected EMG activity beyond the dynamic threshold, activating the LED indicator for real-time feedback. The 12-hour interval mechanism also operated consistently for over 48 hours, maintaining accurate massage scheduling.	Successful – The alarm system reliably detected excessive muscle activity and provided real-time alerts.
G. Threshold Calibration and Rest Detection Algorithm	A calibration-based thresholding algorithm with a 10-second averaging window established user-specific baselines, initialized at 0.0050 to account for residual noise or zero readings.	Accurate – The adaptive threshold and debounce mechanisms ensured reliable muscle state detection by minimizing false triggers and compensating for sensor sensitivity variations.
H. Integration of DC Motor and Gear System for Myofascial Release	The integration of the DC motor and gear system successfully established controlled motion for myofascial	Optimized – The motor-gear system demonstrated proper alignment and sufficient

	release therapy. The rated torque ensured smooth operation, though potential friction effects may require further evaluation. Minor optimizations could enhance long-term efficiency.	torque for continuous motion.
I. Utilize Stepper Motor Precision for Myofascial Release	The direct observational method confirmed that the stepper motor achieved the intended RPM range (18–24 RPM), ensuring controlled and consistent motion for myofascial release therapy. Minimal vibration and stable rotational output further reinforced its suitability for application.	Verified – The stepper motor's rotational speed was experimentally validated and met design expectations.
J. Calibration of Integrated Massager	The therapist confirmed that the applied pressure provided therapeutic relief, but increasing the massage speed might enhance effectiveness. Additionally, the device's weight was deemed acceptable, ensuring user comfort without added strain. Further refinements could focus on optimizing massage intensity for improved therapeutic benefits.	Verified – The calibrated massage pressure (1.36 kPa) was validated by a licensed Physical Therapist and found to be effective, though light.

K. Integration of Battery Power Supply	Two 9V 1100mAh rechargeable batteries were connected in parallel to provide stable and extended power for the wrist splint system. Power tests showed a current draw of 320–500 mA, yielding an estimated battery life of 39–61 hours. The output voltage remained stable at approximately 9.08 V, while the regulated 5.03 V supply ensured consistent performance of the ESP32 and sensors.	Successful – The parallel battery configuration provided stable voltage, efficient power management, and sufficient operational duration for continuous system performance.
L. Implementation of Pressure Sensor and Detection Algorithm	The FSR was calibrated by applying known weights and measuring the resulting voltages, which were converted to resistances and then to forces using a log-log model. The calibration showed consistent, repeatable sensor responses across different positions, enabling the algorithm to accurately convert	Accurate – The FSR reliably measured applied forces, with minor variations corrected through averaging and calibration, enabling precise real-time pressure detection.

	readings into real-time force values for dynamic wrist splint adjustment.	
M. Implementation of auto-adjusting belt system	The predefined three-revolution adjustment cycle provided smooth and controlled strap tightening. Testing confirmed that the motor's precise movements effectively regulated tension, preserving wrist stability without compromising user comfort.	Optimized – The stepper motor-controlled belt system successfully maintained stable and adaptive tensioning, preventing over-tightening while ensuring sufficient support.
N. Implementation of Tension Adjustment Mechanism	The stepper motor, housed in a secure 3D-printed enclosure, enabled smooth and controlled strap adjustments without excessive tightening or slippage. The ESP32-based system regulated movements effectively, maintaining consistent compression and extending the durability of the strap system.	Success – The tension adjustment mechanism demonstrated precise, stable, and controlled strap tightening.
O. Functional Testing	Functional testing confirmed each module met performance targets: Signal Acquisition (≥70%), Signal Processing (≥80%), Integrated	Validated – System proven fully functional and operational with 70–80% accuracy and optimal

	Massager (1.36 kPa, ≥80%), Auto Fit (~3.68 kPa, ≥70%), and Motion Support (10° flexion, 30° extension, ≥80%).	pressure outputs (1.36 kPa, 3.68 kPa).
P. System Testing	System testing verified correct inter-module operation. The integrated modules achieved ≥80% accuracy in EMG capture, classification, and actuator response. The massager delivered 1.36 kPa at rest, the auto-fit module maintained ≈3.68 kPa with ≥70% success, and the motion support module enabled 10° flexion and 30° extension with ≥80% acceptance.	Confirmed – Integrated system proven reliable and fully functional, meeting 70–80% accuracy and pressure specifications (1.36 kPa, 3.68 kPa).
Q. Beta Testing	The device was tested on 15 female participants (18–25 years, ≥ 4 h/day keyboard use). Eleven (73%) achieved ≥ 2.2 kg grip-strength gain, with significant improvement ($t = -6.32$, $p < .001$). Pain scores decreased from 3.27 to 0.33 ($\chi^2 = 17.3$, $p < .001$). Safety and comfort were confirmed through low-voltage operation and user feedback.	Validated – Proven effective and safe, achieving 73% functional improvement and statistically significant pain reduction ($p < .001$).

A. Integration of Surface EMG (sEMG) electrodes with EMG sensor

The integration of the sEMG electrodes with the EMG sensor was successfully verified through a multimeter continuity test, confirming the stability of electrical connections between the electrodes and the sensor's snap connectors as shown in Figure 4.1. The silver/silver chloride (Ag/AgCl) electrodes demonstrated consistent conductivity, ensuring a reliable interface for signal acquisition. The multimeter test indicated negligible resistance across the electrode-sensor junctions, validating the proper attachment of the snap connectors and the integrity of the electrode contacts.

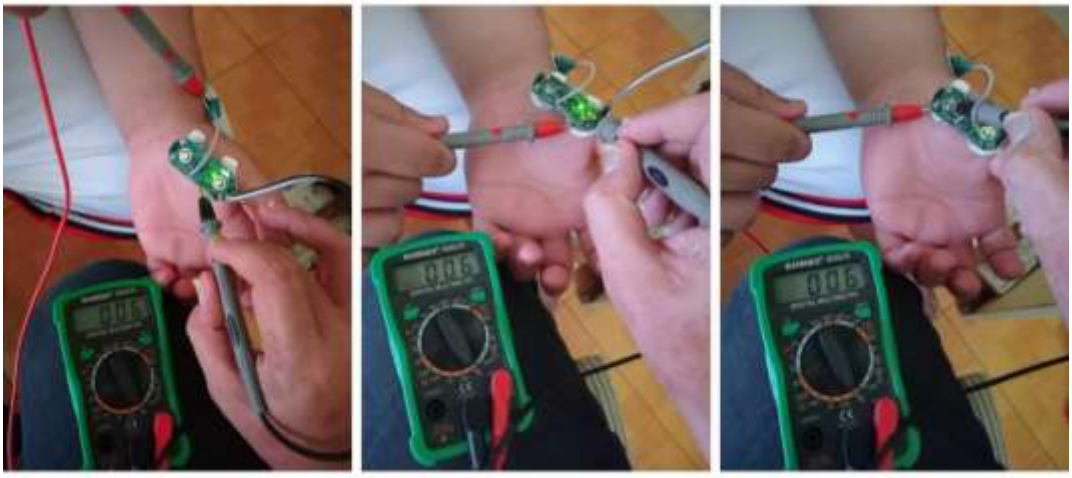

Figure 21 Multimeter Continuity Test of Sensor and Electrodes

To further assess the electrodes' stability, the MID, END, and REF electrodes were positioned on the Abductor Pollicis Brevis muscle, ensuring secure adhesion and proper alignment. Figure 4.2 illustrated the electrode placement and integration setup, showcasing the final configuration used for signal acquisition.

Figure 22 Electrode Placement and Integration with the EMG Sensor

The use of pre-gelled, latex-free adhesive pads provided firm contact with the skin, maintaining consistent connectivity without noticeable detachment or displacement. This stability was essential in minimizing motion artifacts and ensuring uninterrupted signal transmission, particularly during prolonged use or movement. Additionally, no significant impedance fluctuations were observed during testing, confirming that the electrodes effectively isolated the target muscle signals while reducing potential interference from surrounding muscle activity.

B. Calibration of EMG Sensor

The calibration of the EMG sensor was performed using the Biopac system as a reference to validate its ability to detect muscle activity. In the MATLAB analysis, the Biopac signal was first resampled and mapped to simulate the ESP32's 12-bit ADC voltage

range, allowing for a fair comparison under the constraints of the microcontroller. This setup ensured that both signals represented the same muscle source and could be directly compared in terms of amplitude and activation timing.

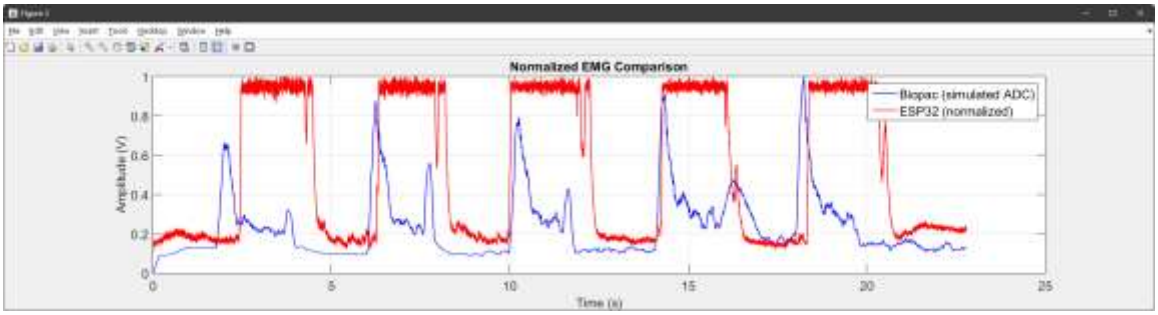

Figure 23 Comparison of Remapped BIOPAC EMG Signal and Raw ESP32 EMG Signal

During testing, the raw ESP32 signal initially appeared highly noisy, resembling a similar figure to a square wave due to interference and baseline fluctuations as shown in Figure 4.3. Then, after applying a 20–200 Hz bandpass filter, a 50 Hz notch filter, rectification, and envelope extraction, the processed ESP32 signal smoothed significantly, closely resembling the Biopac signal in both shape and temporal pattern. The processed ESP32 signal was then normalized alongside the simulated Biopac signal for direct visual comparison. As observed in the normalized plots in the Figure below, both systems captured the temporal patterns of muscle contractions consistently, with the ESP32 reflecting high voltage readings at the same times as the Biopac reference. This confirms that the sensor can reliably detect muscle activation without significant delays.

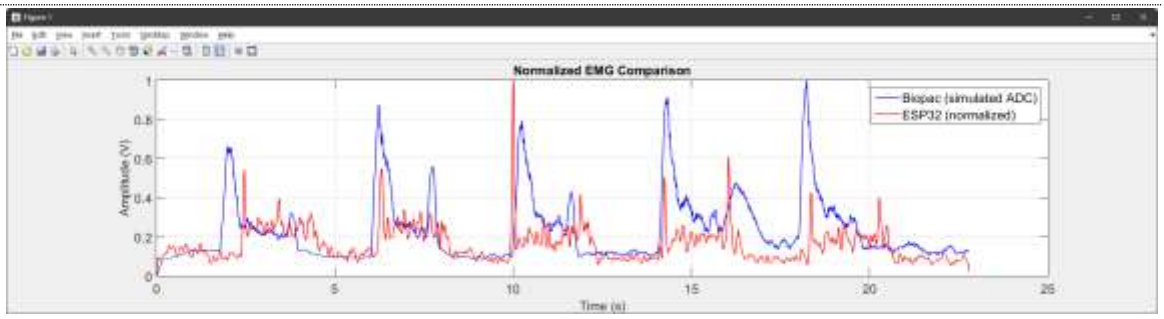

Figure 24 Normalized BIOPAC and ESP32 Signals after applying Filters

Resting EMG levels were also assessed during the first 2 seconds of recording, with the Biopac-mapped signal yielding a resting threshold of approximately 0.7 V in ESP32 units. The ESP32 sensor maintained low values during rest, effectively distinguishing between resting and active muscle states. Additionally, amplitude variations between rest and contraction were clearly observed, aligning with physiological expectations and reinforcing the sensor's accuracy.

Overall, these results demonstrate that the ESP32-based EMG sensor provides a reliable measure of muscle activity comparable to the clinically validated Biopac system. While minor amplitude differences arise due to ADC resolution and filtering, the sensor is well-suited for applications requiring detection of muscle activation patterns, such as triggering massage or dynamic support in a wrist splint system.

C. Integration of EMG sensor and Microcontroller

The integration of the EMG sensor with the ESP32 microcontroller was successfully established, ensuring stable electrical connections and reliable signal transmission. The finalized circuit wiring, as summarized in Table 4.2, outlined the

sensor's connection to the microcontroller, with its signal output routed to GPIO 36 of the analog-to-digital converter (ADC). Proper voltage supply and grounding connections were also implemented to maintain signal integrity and minimize electrical noise.

EMG Sensor Pins	ESP32 Pins	Function
VIN	5V	Power Supply
REF	GND	Ground Reference
RAW	36 (ADC)	Signal Input

Table 15 Actual Connections of Sensor and Microcontroller

Voltage continuity tests were conducted using a multimeter to verify the correctness of electrical connections. The results confirmed that the VIN pin consistently supplied 5V and that the GND reference pin provided a stable ground connection. Figure 4.5 illustrates the continuity test being performed, demonstrating proper pin configurations.

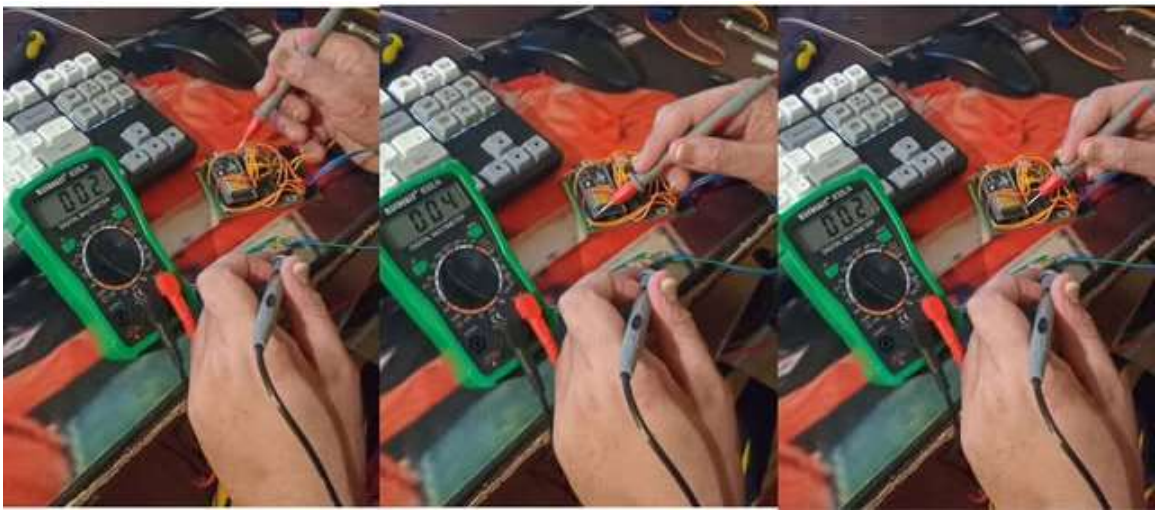

Figure 25 Continuity Tests of EMG Sensor and ESP32 Microcontroller

With these connections, the recorded EMG waveforms exhibited consistent voltage readings with minimal distortions, validating the microcontroller's capability to handle real-time bioelectrical signal acquisition. However, minor fluctuations due to electromagnetic interference were observed in early trials. As such, these were mitigated by optimizing the sensor's power source, implementing proper grounding techniques, and incorporating shielding materials to reduce external noise influences.

D. Signal Acquisition Algorithm

The EMG signal acquisition was implemented on the ESP32 using the Arduino Integrated Development Environment (IDE), with raw voltage values obtained through the line:

$$float\ rawEMG\ =\ (analogRead(36)\ *\ (5.0\ /\ 4095.0));$$

This line converts the 12-bit ADC reading (0–4095) into a voltage range of 0–5 V, effectively translating the bioelectrical activity from the Abductor Pollicis Brevis muscle into meaningful voltage values. However, due to inherent limitations of both the ESP32's ADC resolution and the characteristics of the surface EMG sensor, the recorded signals do not reflect the absolute bioelectrical voltages produced by the muscle. Instead, the values represent a remapped version of the true EMG activity, scaled to fit the ADC's range. Despite this, the relative differences between rest and active states remain preserved, allowing for meaningful signal processing and classification.

The analogRead() function continuously sampled the signal at a controlled rate, while a fixed delay mechanism ensured that data were captured without overwhelming

the microcontroller's processing capacity. Serial output at a baud rate of 115200 allowed real-time monitoring of EMG values, confirming proper signal retrieval. During rest, ADC readings corresponded to stable low voltages (~0.2–0.5 V after conversion), whereas voluntary contractions produced distinctly higher voltages (~3–5 V), demonstrating the algorithm's ability to capture the full dynamic range of muscle activity.

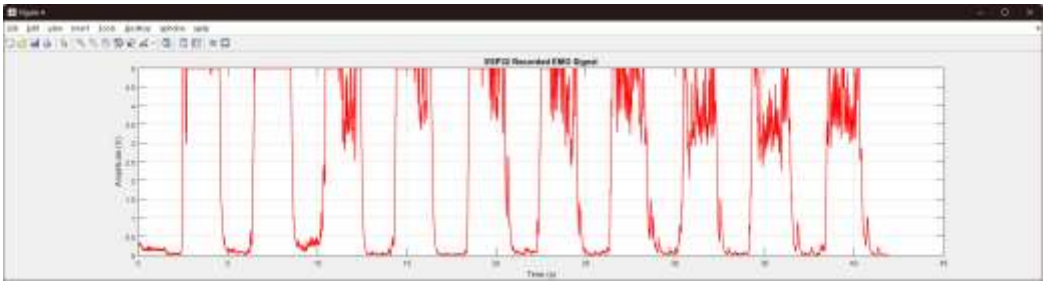

Figure 26 Reconstructed EMG Signal in MATLAB

The acquisition algorithm reliably delivered voltage signals that served as input for subsequent processing in MATLAB, where a 200 ms sliding RMS window and dynamic thresholding were applied to distinguish resting from active muscle states. As detailed in a later discussion, this RMS-based segmentation successfully identified rest and movement intervals across the recorded trials, and statistical analysis further confirmed a significant difference between the two states. The stable and accurate performance of the acquisition algorithm therefore provided a robust foundation for the signal processing, segmentation, and evaluation procedures discussed in the following sections.

E. Signal Processing Algorithm

Following the calibration of the EMG sensor, the filtering strategies established during the MATLAB validation were translated into a real-time implementation on the

ESP32. From the calibration analysis, the 20–200 Hz bandpass and 50 Hz notch filters were converted into equivalent IIR biquadratic filter coefficients for a 600 Hz sampling frequency. These coefficients were embedded into the main system's code using a biquadratic filter structure and recursive processing function as referenced in Appendix C.

The effectiveness of the proposed algorithm was demonstrated through the comparative visualization of the EMG signal before and after filtering, as shown in Figure 4.7. The raw signal exhibited pronounced noise artifacts, including baseline drift and dominant powerline interference at 50 Hz. In contrast, the filtered signal revealed a substantial attenuation of these unwanted components, with baseline stability and high-frequency noise reduction achieved while maintaining the temporal fidelity of the muscle activity waveform.

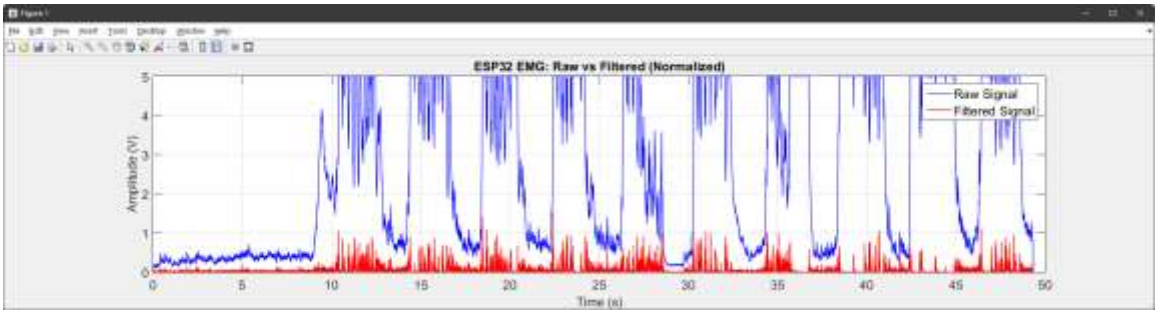

Figure 27 Comparison of Raw EMG Signal and Filtered EMG Signal

To more clearly illustrate this improvement, both the direct voltage-domain comparison and a normalized comparison (Figure 4.8) were examined. In the voltage-domain plot, the filtered signal appears reduced in amplitude because the bandpass and notch filters attenuate non-physiological components such as baseline drift and

powerline interference, which dominate the raw trace. Once these large but irrelevant components are removed, the remaining physiological EMG activity reflects only the true microvolt-level variations of muscle activation, resulting in a lower overall voltage range. By contrast, the normalized plot emphasizes the preserved temporal structure of muscle activation, independent of amplitude scaling, allowing the waveform fidelity of the filtered signal to be assessed without the confounding effect of amplitude reduction.

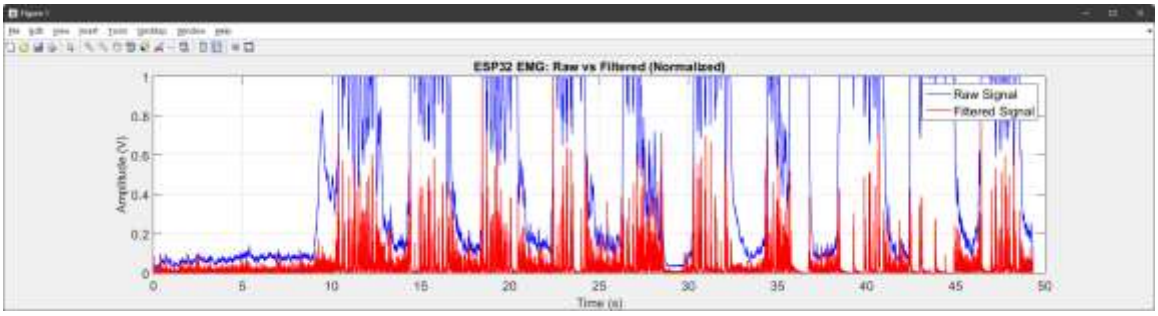

Figure 28 Filtered EMG Signal

As such, this transformation closely mirrored the MATLAB calibration results, confirming that the embedded biquadratic implementation successfully replicated the noise suppression and signal shaping verified during offline analysis. The filtered ESP32 signal thus provided clear envelopes of muscle activation with minimal latency, ensuring accurate onset and offset detection of contractions.

F. Implementation of Alarm System

The alarm system's performance was evaluated based on its ability to respond to EMG signal fluctuations and provide real-time alerts when muscle activity exceeded the dynamic threshold during scheduled massage periods. The system was designed to

activate LED indicator when muscle activity surpassed this limit, ensuring immediate user feedback.

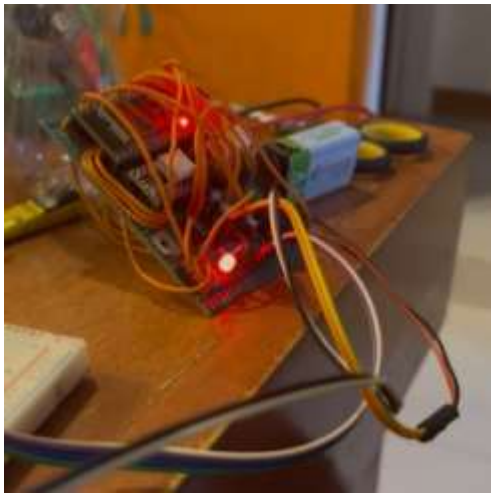

Figure 29 Alarm System with LED

Figure 4.9 shows the alarm system in operation, with the LED illuminated in bright red, confirming the detection of an active muscle state. The LED indicator was consistently triggered while the muscle state remained active, verifying that the alarm system accurately responds to real-time muscle activity. This immediate visual feedback reinforces adherence to scheduled massage therapy by notifying the user when muscle activity exceeds the threshold.

Additionally, the researchers evaluated the functionality of the 12-hour interval massage mechanism. Over a 48-hour testing period, the system consistently activated the massage function at the designated intervals, effectively regulating massage timing. The system's adherence to the schedule aligned with the recommendation of Ms. Frencie Quintin Z. Purol, PTRP.

Furthermore, the alarm feature functioned as intended if the EMG signal did not indicate a resting state at the scheduled time, the LED alert activated, prompting the user to pause and relax before the massage commenced. This ensured massages were delivered under optimal conditions, reducing the risk of overstimulation.

Overall, the test results confirmed the successful implementation of both the 12-hour interval scheduling mechanism and the alarm system.

G. Threshold Calibration and Muscle State Detection

To ensure accurate differentiation between resting and non-resting muscle states, the system incorporated a calibration-based thresholding algorithm which is presented in Appendix C. A 10-second calibration window was used to average incoming EMG values, producing a stable baseline reflective of the user's resting condition. Before calibration, the baseline threshold was initialized to 0.0050 to account for residual background noise typically lingering below this value. In cases where the average resting signal computed during calibration was absolutely 0 due to the low sensitivity of the sensor, the threshold defaulted to 0.0050 to maintain responsiveness to random noise and prevent complete signal inactivity. The dynamic threshold was then set at twice this baseline, introducing a safety margin that enabled the algorithm to distinguish between true voluntary contractions and background electrical noise. A web display was employed throughout the process to display real-time calibration progress, baseline computation, and classification outcomes, thereby serving as an immediate validation tool during testing.

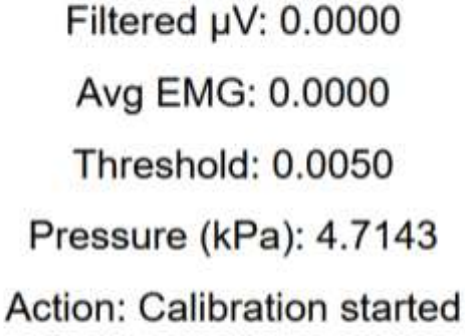

Figure 30 Display showing the 10-second calibration block

During trials, resting EMG signals typically remained within a low-amplitude range, whereas active contractions produced values exceeding the calibrated threshold. When the EMG signal stayed below threshold, the device proceeded with normal operation and initiated the massage system. Figure 4.10 illustrates the 10-second calibration block used to establish this baseline condition. In contrast, sustained elevations beyond the threshold triggered an alarm condition, as shown in Figure 4.11. To minimize false detections from transient spikes or noise artifacts, a debounce mechanism required the signal to remain continuously above threshold for at least five seconds before confirming an alarm, effectively preventing premature massage interruptions while ensuring reliable detection of genuine muscle activation.

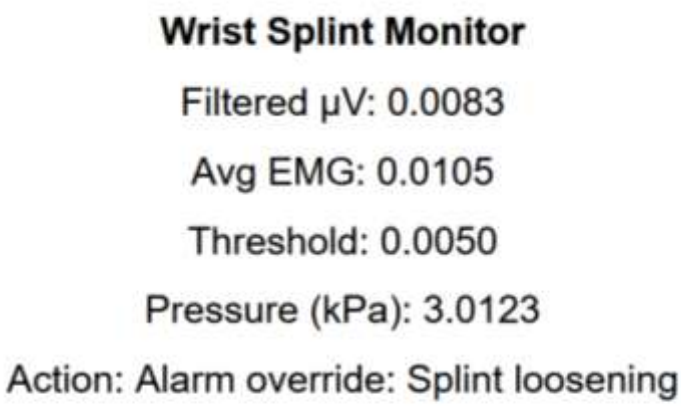

Figure 31 Display indicating the user is not at rest and activating the alarm

The integration of calibration, thresholding, and debounce mechanisms thus provided both adaptability and robustness. By aligning classification with individual baseline activity rather than a fixed cut-off, the system reduced susceptibility to inter-user variability and environmental noise, while preserving a clear and immediate indication of muscle state transitions.

H. Integration of DC Motor and Gear System for Myofascial Release

The integration of the DC motor and gear system was assessed to ensure proper mechanical alignment and expected functionality for delivering myofascial release therapy. The selected motor, rated to provide 290 gf.cm of torque according to its datasheet, was coupled with the gear assembly to generate continuous and controlled motion. Figure 4.12 presents the assembled motor-gear system, illustrating the intended interaction between components. Additionally, the system's design suggests that the

motor's torque should be sufficient to drive the gear mechanism without significant resistance.

Figure 32 Assembled myofascial massager comprising of a motor-gear system

Potential factors affecting long-term performance, such as friction within the gear assembly, may require further evaluation. However, based on the rated torque and mechanical integration, the motor-gear system is expected to provide reliable and continuous motion essential for effective therapy. Minor optimizations, such as improved lubrication or slight design modifications, may be considered to enhance efficiency.

I. Utilize Stepper Motor Precision for Myofascial Release

In this section, the stepper motor's rotational speed was experimentally determined through a direct observational method. As seen in Figure 4.13, a small piece of tape was affixed to the motor shaft to serve as a visual marker, enabling precise counting of revolutions. The motor was activated, and the number of complete rotations

within a 10-second interval was recorded. This measured value was then multiplied by six to obtain the motor's RPM. Testing results indicated that the motor had completed approximately 3 to 4 full revolutions in 10 seconds which makes 18 to 24 revolutions in 60 seconds or revolutions per minute.

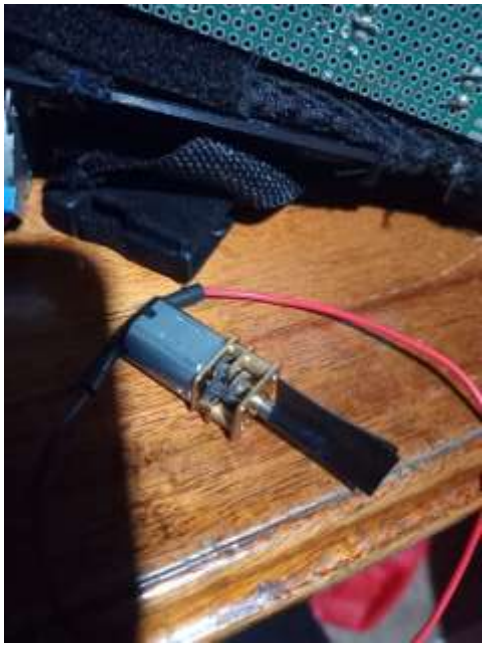

Figure 33 Stepper Motor Direct Observation Testing

This measured RPM aligned with the intended design specification, confirming that the stepper motor, when integrated with the gear system, had achieved the expected speed necessary for myofascial release therapy. The slow and controlled rotation ensured that consistent pressure had been delivered to the targeted areas without abrupt variations that might have caused discomfort. Additionally, observations during testing indicated minimal vibration, which was crucial in preventing unnecessary mechanical stress on the user’s wrist. The stepper motor’s high torque and the gear system’s

reduction ratio had contributed to maintaining a stable rotational output.

J. Calibration of Integrated Massager

During the calibration process, Ma'am Aurora Jasmin Diaz, PTRP tested the integrated massager to evaluate the effectiveness of the pre-set 1.36 kPa massage pressure. As shown in Figure 4.14, the Physical Therapist (PT) wore the device and assessed its performance, noting that while the applied pressure felt light, it was still effective for therapeutic relief. This suggests that the chosen pressure level remains within a functional range, though adjustments could enhance its effectiveness.

Figure 34 Evaluation of Em-Brace by a Licensed Physical Therapist

The PT also observed that the massage speed was relatively slow, suggesting that a higher speed could improve the massage's effectiveness. However, she acknowledged

that the current setting remains effective for providing therapeutic relief to the wrist, indicating that the system functions as intended. Additionally, when asked about the weight of the prototype, the PT stated that it was not heavy, reinforcing that the device does not introduce unnecessary strain during use.

K. Integration of battery power supply

The integration of two 9 V 1100 mAh rechargeable batteries connected in parallel was evaluated to ensure reliable power delivery and sufficient operational longevity for the wrist splint system. Power consumption measurements under varying loads indicated that the system drew approximately 320–500 mA during full operation, resulting in an estimated battery life of 39 to 61 hours. These values correspond closely with theoretical calculations based on the combined capacity of the parallel batteries, confirming efficient power management and minimal energy losses.

The measured output voltage of the parallel-connected batteries remained stable at approximately 9.08 V throughout operation, as shown in Figure 4.15. This voltage stability was verified using a digital multimeter and demonstrated consistent supply performance under different load conditions. The ESP32 microcontroller and associated sensors were powered at a regulated 5.03 V, ensuring that all components received adequate and steady operating voltage. Maintaining a stable voltage is crucial to guarantee uninterrupted system performance, particularly in therapeutic assistive devices such as automated splints, where electrical fluctuations could affect actuation precision and overall functionality.

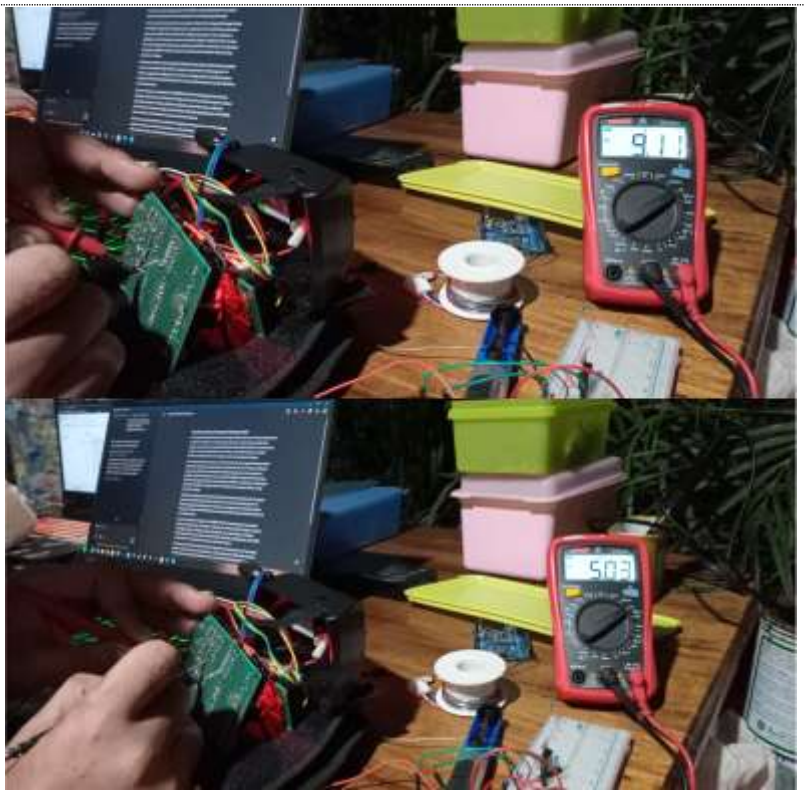

Figure 35 Battery Voltage Continuity Test

These findings align with established power management strategies in wearable medical devices, underscoring the importance of efficient battery utilization and stable voltage regulation for consistent performance. The demonstrated capability of the system to sustain prolonged operation enhances its practicality for real-world therapeutic applications.

L. Implementation of Pressure Sensor and Detection Algorithm

The calibration of the Force Sensing Resistor (FSR) was performed to ensure accurate force measurement and reliable operation of the autonomous wrist splint. The process began by applying known weights to the sensor, ranging from light to heavy loads,

to cover the expected operational range of the device. Figure 4.16 shows the calibration of weights used in the experiment, providing a visual reference for the forces applied.

Figure 36 Pressure Sensor Calibration Setup at 500g, 200g, 100g, and 50g

Voltage readings from the FSR were then obtained using a voltage divider circuit connected to the ESP32 and processed through the Arduino IDE. Each reading consisted of an average of 100 analog samples to minimize noise and fluctuations. These voltages were then converted into FSR resistances using the relationship:

$$R_{FSR} = R_0((\frac{V_{cc}}{V_{FSR}}) - 1)$$

where R0 is the reference resistor, Vcc is the supply voltage, and VFSR is the averaged measured voltage. Initial observations indicated that the resistance readings exhibited minor instabilities, likely due to sensor hysteresis, uneven pressure distribution, and localized surface effects. To address this, each weight was applied at multiple

positions on the FSR's corners and center and the resulting resistances were averaged to obtain a more representative measure of the sensor's response.

The applied weights were converted from mass to force in Newtons by multiplying by the gravitational constant (9.81 m/s²), allowing the calibration to be expressed in terms of force. A log-log model was then selected to relate force to resistance:

$$\log_{10}(Force) = a * \log_{10}(Resistance) + b$$

This model was chosen because FSRs exhibit a nonlinear, approximately inverse power-law relationship between resistance and applied force. Transforming the data into logarithmic space linearizes this relationship, enabling straightforward regression analysis to determine the coefficients a and b. The regression yielded a = -0.217640 and b = 0.168337, with a coefficient of determination R^2 = 0.8568, indicating a strong correlation between resistance and applied force.

Table 4.3 presents the average resistances recorded for each weight, along with the corresponding calculated forces and logarithmic values. This tabular representation allows for a clear comparison between applied loads and sensor output, highlighting the consistency and repeatability of the FSR response. The sensor demonstrated minimal variation across different applied locations, confirming uniform sensitivity and reliable measurement.

mass_kg	R_avg_ohm	Force	logF	logR
0.5	0.001	4.905	0.690639	-3
0.2	5.088	1.962	0.292699	0.706547

0.1	27.5	0.981	-0.00833	1.439333
0.05	80.37	0.4905	-0.30936	1.905094
0.02	1018	0.1962	-0.7073	3.007748

Table 16 Calibration Data of FSR Showing Resistance, Force, and Logarithmic Values

The calibrated resistance-to-force relationship was then integrated into the pressure detection algorithm, which converts incoming FSR readings into real-time force and pressure values. The algorithm successfully captured and processed the measured forces for all tested weights, demonstrating stable functionality and readiness for dynamic wrist splint applications. These results provide confidence that the FSR can reliably detect variations in strap tension, enabling the wrist splint to adjust dynamically in response to user activity and applied force.

M. Implementation of auto-adjusting belt system

The stepper motor in the auto-adjusting belt system was programmed to perform three full revolutions per adjustment cycle to ensure controlled tensioning without over-tightening the belt. This predefined movement was calibrated to provide sufficient strap tension while preventing excessive force that could cause discomfort or mechanical strain on the tightening mechanism.

During testing, as the motor executed its programmed rotations, the belt adjustment remained smooth and consistent, effectively maintaining the intended level of support. The fixed three-revolution setting ensured that the belt did not exceed the allowable range of motion, thus preventing accidental over-tightening, which could

compromise user comfort or restrict wrist movement.

Additionally, the stepper motor's precise stepwise movement minimized abrupt shifts in tension, which is critical for maintaining a gradual and adaptive adjustment process. Observations indicated that the system successfully regulated strap tightness while preserving the stability of the wrist splint, confirming that the predefined motor movement aligned with the design objectives.

N. Implementation of Tension Adjustment Mechanism

The constructed tension adjustment mechanism successfully integrates the stepper motor, 3D-printed housing, and strap system to achieve controlled and reliable belt tightening. As shown in Figure 4.17, the stepper motor is securely mounted within a custom 3D-printed enclosure, ensuring stability during operation. This enclosure effectively prevents unwanted vibrations or misalignment, which could otherwise affect the consistency of the tensioning process. The compact design also maintains the portability and ergonomic fit of the wrist splint, allowing users to wear it comfortably.

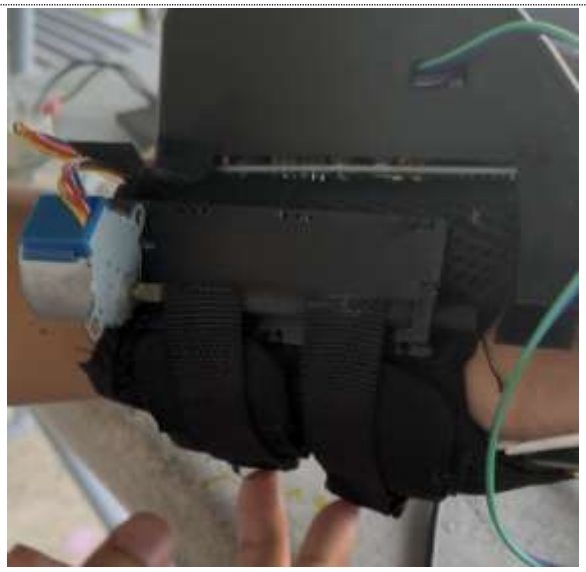

Figure 37 Strap Tension Adjustment Mechanism

During testing, the stepper motor demonstrated smooth and controlled strap adjustments, rotating spools to wind or unwind the belts without sudden tension fluctuations. This mechanism ensured that the applied pressure remained within a comfortable range, preventing excessive tightening while still providing adequate wrist support. The rolling action of the spools further minimized wear on the straps, reducing the risk of material fatigue and extending the system's durability.

Additionally, the ESP32-based control system successfully regulated the motor's movements, maintaining precise adjustments according to pre-programmed limits. The mechanism consistently achieved the intended three full revolutions per cycle, preventing over-tightening while maintaining effective compression. The integration of a structured housing also improved the alignment of the belt system, preventing slippage or uneven pressure distribution.

O. Functional Testing

Signal Acquisition Module

During signal acquisition, raw EMG data from the Abductor Pollicis Brevis muscle was collected from the ESP32 at a sampling frequency of approximately 608.16 Hz. The signal, despite being noisy, exhibited a clear separation between resting and active muscle states, with raw amplitudes around 0.2–0.5 V during rest and 5 V during contraction as visible in the graph shown in Figure 4.18.

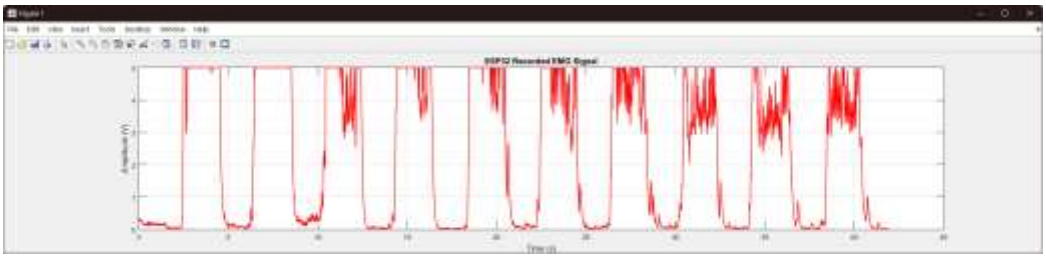

Figure 38 Recorded Raw EMG Signal

To distinguish between periods of rest and muscle activation, the signal was processed using a 200 ms sliding RMS window in MATLAB wherein later, a dynamic thresholding method was applied. The root mean square (RMS) of the signal served as the activity metric, with a computed threshold of 3.3446 used as the decision boundary. Intervals with RMS values below the threshold were classified as rest states, while intervals above the threshold were classified as active muscle contractions.

Trial	Time (s) Intervals	Classification	RMS Value (V)
1	0.04 – 2.57	Rest	0.2027
	2.57 – 4.68	Movement	4.8648

2	4.68 – 6.52	Rest	0.3965
	6.53 – 8.69	Movement	4.9120
3	8.69 – 10.52	Rest	0.5890
	10.52 – 12.58	Movement	4.4679
4	12.58 – 14.47	Rest	0.3363
	14.47 – 16.53	Movement	4.7204
5	16.53 – 18.54	Rest	0.2844
	18.54 – 20.60	Movement	4.7628
6	20.61 – 22.55	Rest	0.5293
	22.55 – 24.25	Movement	4.5797
	24.26 – 24.33	Rest (artifact)	3.1581
	24.34 – 24.63	Movement	4.0832
7	24.63 – 26.54	Rest	0.4075
	26.54 – 28.46	Movement	4.4950
8	28.46 – 30.54	Rest	0.5488
	30.54 – 30.82	Movement	4.1915
	30.82 – 30.97	Rest (artifact)	3.0745
	30.97 – 32.40	Movement	3.8603
9	32.40 – 34.37	Rest	0.4635
	34.37 – 34.85	Movement	4.2575
	34.85 – 35.24	Rest (artifact)	3.1891

	35.24 – 35.89	Movement	3.5140
	35.89 – 35.98	Rest (artifact)	3.2371
	35.99 – 36.51	Movement	4.0845
10	36.51 – 38.61	Rest	0.4662
	38.61 – 40.47	Movement	4.0274
	40.47 – 41.89	Rest	0.4287

Table 17 Segmented intervals of rest and movement based on RMS thresholding.

The segmentation results demonstrate clear alternations between rest and movement phases throughout the 41.89-second recording. During identified rest periods, the signal maintained consistently low RMS values ranging from 0.2027 to 0.5890, reflecting baseline muscle activity and confirming effective detection of inactive states. In contrast, movement intervals were characterized by markedly higher RMS values, typically between 3.86 and 4.91, clearly exceeding the threshold and indicating reliable detection of muscular activation.

However, a few brief anomalies were observed where RMS values within rest-labeled intervals momentarily exceeded 3.0 (e.g., 24.26–24.33 s and 30.82–30.97 s). These short fluctuations may be attributed to motion artifacts, or electrode instability, due to the signal being unfiltered, or transient low-level muscle contractions, rather than sustained activation as shown in the figure below. Nevertheless, the segmentation was able to maintain robustness, consistently distinguishing the longer rest and movement

phases.

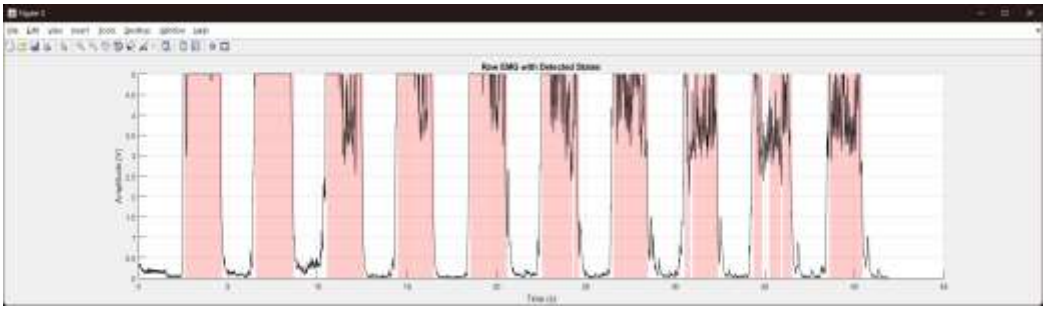

Figure 39 Raw EMG Signal with Movement Detection Overlay

Furthermore, a statistical analysis using a paired-samples t-test confirmed a significant difference between resting and movement states. The mean RMS during rest periods was consistently lower than during movement, resulting in a highly significant t-test result ($t(14) = -6.19$, $p < 0.001$). The effect size, measured by Cohen's d, was -1.6 (95% CI: -2.36 to -0.81), indicating a large and practically meaningful difference between the two states.

Paired Samples T-Test

							95% Confidence Interval	
			Statistic	df	p	Effect Size	Lower	Upper
Rest	Movement	Student's t	-6.19	14.0	<.001	Cohen's d	-1.6	-2.36	-0.811

Note. H_a $\mu_{\text{Measure 1 – Measure 2}} \neq 0$

Table 18 Paired Samples T-test of the Resting and Movement States

The signal acquisition and RMS-based segmentation modules effectively differentiated resting and active muscle activity in the Abductor Pollicis Brevis. The established threshold of 3.3446 V served as a reliable decision boundary, producing consistent alternations between rest and movement intervals across ten trials. RMS averages below this value correctly corresponded to muscle inactivity, while sustained values above it reflected active contractions.

Although minor artifacts momentarily exceeded the threshold, these did not persist long enough to affect classification performance, confirming that the segmentation logic prioritized sustained RMS elevation over short noise spikes. The inclusion of brief “Rest (artifact)” intervals further illustrates that these deviations were transient and properly identified as anomalies rather than misclassifications.

The paired-samples t-test reinforced these findings statistically, showing a significant and large-magnitude difference between rest and movement phases. This quantitative evidence supports the robustness, precision, and validity of the acquisition module in capturing muscle-state transitions. Overall, the results demonstrate that the RMS-thresholding method achieved accurate segmentation, maintained resilience against artifacts, and provided a strong foundation for reliable EMG-based control in the subsequent system modules.

Signal Processing Module

The signal processing module was designed to extract, filter, and classify EMG

signals into Resting and Active states. Filtering was performed, consisting of a 20–200 Hz bandpass filter and a 50 Hz notch filter, which successfully preserved relevant muscle activity while attenuating low-frequency motion artifacts, baseline drift, and high-frequency noise. Figure 4.20 illustrates a representative EMG recording after filtering, while additional results are provided in Appendix F. These results confirm that the preprocessing pipeline effectively produced clean EMG signals suitable for subsequent classification.

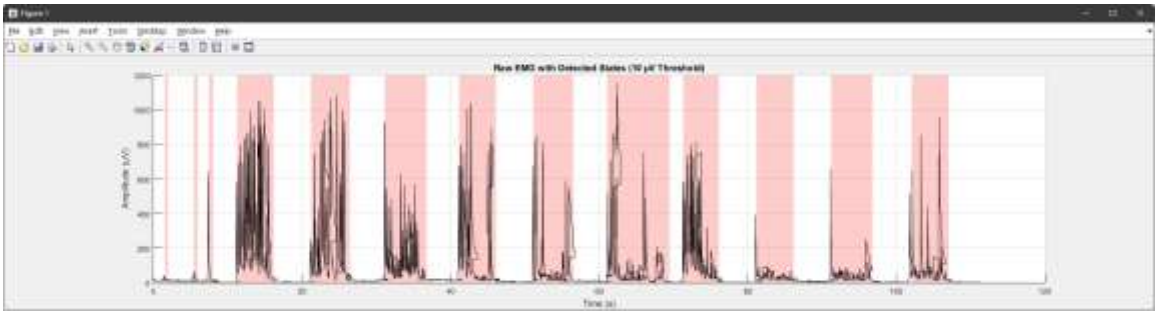

Figure 40 Post Processed EMG Signal Reconstruction

Functional testing was conducted across twenty 5-second trials, giving ten resting and active states each with results summarized in Table 4.6. Calibration yielded a dynamic threshold of 20.00 µV to distinguish resting from active muscle states. The threshold was determined after adjusting the sensor gain to prevent ADC saturation and filter attenuation, ensuring that the EMG signals retained sufficient sensitivity for detecting low-level activity while minimizing noise interference.

Each trial was classified as “Pass” if the average EMG amplitude during the 5-second window correctly aligned with its expected state relative to the 20 µV threshold. Specifically, trials with an RMS reading greater than 20 µV were classified as Active, and

those less than or equal to 10 µV were classified as Resting. A "Fail" result indicated a mismatch between the expected and the classified state.

Although the RMS amplitudes of resting phases were relatively higher than the discussed literature, they remained within physiologically valid levels. The recorded values represented the root mean square (RMS) of muscle potentials over several seconds of sustained activity rather than transient spikes. Hence, even moderate increases above the 20 µV threshold indicated genuine muscle activation, validating the module's ability to distinguish resting and active states with high consistency.

Trial	RMS EMG (µV)	Expected EMG (µV)	Classified State	Pass/Fail
1	11.04	≤ 20.00	Resting	Pass
2	356.61	> 20.00	Active	Pass
3	3.34	≤ 20.00	Resting	Pass
4	263.74	> 20.00	Active	Pass
5	11.50	≤ 20.00	Resting	Pass
6	157.09	> 20.00	Active	Pass
7	17.89	≤ 20.00	Resting	Pass
8	196.46	> 20.00	Active	Pass
9	7.63	≤ 20.00	Resting	Pass
10	112.33	> 20.00	Active	Pass
11	9.75	≤ 20.00	Resting	Pass

12	104.92	> 20.00	Active	Pass
13	14.73	≤ 20.00	Resting	Pass
14	201.24	> 20.00	Active	Pass
15	6.17	≤ 20.00	Resting	Pass
16	38.67	> 20.00	Active	Pass
17	10.95	≤ 20.00	Resting	Pass
18	50.39	> 20.00	Active	Pass
19	6.54	≤ 20.00	Resting	Pass
20	119.20	> 20.00	Active	Pass

Table 19 Average EMG and classification results across trials

Statistical analysis was performed using an Independent Samples T-Test module in Jamovi with the Mann–Whitney U option to account for the zero-inflated, non-normal distribution of EMG values. The null hypothesis (H_0: μ_Resting = μ_Active) was rejected in favor of the alternative (H_a: μ_Resting ≠ μ_Active), indicating a highly significant difference between Resting and Active EMG distributions. The U statistic of 0 reflects the complete separation between groups, as all resting values were zero and all active values were nonzero.

Independent Samples T-Test

		Statistic	p
RMS EMG (µV)	Mann-Whitney U	0.00	< .001

Note. H_a $\mu_{Resting} \neq \mu_{Active}$

Table 20 Independent Samples T-Test of the Classification States

The results demonstrate that the classifier reliably distinguished Resting and Active states across all twenty trials. Resting trials consistently produced RMS EMG amplitudes below the 20 µV threshold, while Active trials exhibited markedly higher values ranging from approximately 38 µV to over 350 µV. This clear separation between resting and active ranges confirms that the threshold was properly calibrated to the recorded muscle activity levels. Despite reduced overall amplitudes due to the adjusted sensor gain, the system preserved a strong binary distinction that enabled accurate functional classification. The classifier's responses aligned with sustained EMG magnitude differences rather than short-term noise or spikes, validating that detected activity corresponded to genuine muscle contractions. Overall, the signal processing pipeline and threshold-based classifier achieved stable, noise-tolerant, and physiologically meaningful performance suitable for integration into the wrist splint's control logic.

Integrated Massager Module

The functional validation of the integrated massager module was conducted to

assess its capacity to sustain a consistent massage pressure of 1.36 kPa for a duration of 2 minutes and 30 seconds during the resting state. This was achieved by placing a pressure sensor between the skin and the massager as shown in Figure 4.20. Performance reliability was evaluated across 20 independent trials, with an established accuracy criterion of ≥ 80% for maintaining the target pressure threshold. Each trial was assessed based on whether the observed average pressure remained within ±0.015 kPa of the target value of 1.36 kPa, which served as the tolerance range for a passing result.

Figure 41 Pressure Sensor and Massager Setup

Empirical findings demonstrated that the massager successfully adhered to the predefined pressure criterion in 16 out of 20 trials, yielding an overall accuracy of 80%, which aligns with the stipulated performance benchmark. This result substantiates the efficacy of the massager module in delivering a controlled and reproducible therapeutic pressure, reinforcing its viability for muscle relaxation applications. The results are

summarized in Table 4.8 below:

Trial	Averaged Observed Pressure (kPa)	Expected Pressure (1.36 kPa)	Difference	Pass/Fail
1	1.367	1.36	0.007	Pass
2	1.355	1.36	-0.005	Pass
3	1.363	1.36	0.003	Pass
4	1.362	1.36	0.002	Pass
5	1.371	1.36	0.011	Pass
6	1.351	1.36	-0.009	Pass
7	1.370	1.36	0.01	Pass
8	1.370	1.36	0.01	Pass
9	1.372	1.36	0.012	Pass
10	1.344	1.36	-0.016	Fail
11	1.372	1.36	0.012	Pass
12	1.340	1.36	-0.02	Fail
13	1.379	1.36	0.019	Fail
14	1.354	1.36	-0.006	Pass
15	1.389	1.36	0.029	Fail
16	1.357	1.36	-0.003	Pass
17	1.363	1.36	0.003	Pass
18	1.373	1.36	0.013	Pass

19	1.392	1.36	0.032	Fail
20	1.364	1.36	0.004	Pass

Table 21 Functionality Testing Results of Integrated Massager Module

A trial was considered Pass if the observed pressure stayed within ±0.015 kPa of the 1.36 kPa target. Any deviation beyond this range was marked Fail. Negative deviations larger than –0.015 kPa indicated insufficient pressure, as shown in trial 10 at –0.016 kPa and trial 12 at –0.020 kPa. Positive deviations greater than +0.015 kPa likewise exceeded the allowable limit, including trial 13 at +0.019 kPa, trial 15 at +0.029 kPa, and trial 19 at +0.032 kPa. The ±0.015 kPa tolerance was also established based on the sensor's measurement resolution and inherent noise level, since fluctuations within this range fall inside normal variability and cannot be interpreted as true shifts in applied pressure. This ensured that only deviations exceeding the sensor's reliable detection threshold were classified as performance drift, allowing a consistent evaluation of the massager's output.

Furthermore, the statistical analysis of the integrated massager module's performance, as processed through Jamovi, provided key insights into its reliability in delivering the target massage pressure of 1.36 kPa. Descriptive statistics from 20 trials indicated a mean observed pressure of 1.37 kPa with a standard deviation of 0.0134, reflecting a tightly clustered dataset with limited variability. The Shapiro-Wilk test yielded a p-value of 0.950, confirming that the data are normally distributed, justifying the use of parametric tests such as the one-sample t-test.

Descriptives

	Averaged Observed Pressure (kPa)	Difference
N	20	20
Mean	1.37	0.00570
Standard deviation	0.0134	0.0134
Minimum	1.34	-0.0200
Maximum	1.39	0.0320
Shapiro-Wilk W	0.981	0.981
Shapiro-Wilk p	0.950	0.950

Table 22 Descriptive Statistics of the Integrated Massager Module

The one-sample t-test compared the observed mean pressure against the expected value of 1.36 kPa and yielded a t-statistic of 1.90 with 19 degrees of freedom. The resulting p-value of 0.072 suggests that the observed difference is not statistically significant at the conventional $\alpha = 0.05$ level, indicating that the massager's average output does not differ meaningfully from the target pressure. Moreover, the effect size (Cohen's $d = 0.426$) reflects a moderate practical effect, suggesting that while the deviation is measurable, it is not substantial enough to compromise functional performance. Collectively, these results affirm that the massager module reliably meets the required therapeutic pressure threshold, albeit with minor, statistically nonsignificant

deviations.

One Sample T-Test

							95% Confidence Interval	
		Statistic	df	p		Effect Size	Lower	Upper
Averaged Observed Pressure (kPa)	Student's t	1.90	19.0	0.072	Cohen's d	0.426	-0.0377	0.897

Note. H_a $\mu \neq 1.36$

Table 23 One Sample T-Test of the Massager's Pressure

In addition to pressure reliability, the massage interval was tested separately to validate the timer function embedded in the system. The device was left powered continuously for 48 hours to assess whether the massager would activate every 12 hours as programmed. Throughout the testing period, the system consistently triggered the massage function four times, once every 12 hours, without failure. This confirms the timing mechanism's reliability and supports the feasibility of semi-daily therapeutic

sessions for long-term user benefit.

However, despite achieving the target pressure range, observed fluctuations in the recorded pressure values suggest a degree of instability inherent to the massager's operational dynamics. Specifically, the circular motion of the massager introduced spatial inconsistencies, limiting the sensor's ability to capture uniform pressure distributions across its surface. As a result, the actual pressure readings, documented in Appendix G, exhibited considerable variability due to the massage head not always covering the entire area of the pressure sensor. This led to intermittent drops and spikes in recorded values, contributing to data inconsistency.

To mitigate this variability and present a more interpretable assessment of the massager's performance, the recorded pressure values were averaged for each trial in Table 4.8. This approach allowed for a more representative measurement of the applied pressure, smoothing out transient fluctuations while maintaining fidelity to the overall massaging effect.

Auto Fit Module

The functional assessment of the auto-fit module aimed to evaluate its ability to apply an optimal tightening pressure that ensures both a secure fit and user comfort. The expected splint pressure was determined to be 3.68 kPa, derived from a literature-based therapeutic pressure of 1.36 kPa for massage, adjusted by an average ratio factor of 0.37 between massage and splint pressure. The objective of this test was to validate whether the module could consistently achieve this target range without over-constriction.

Figure 42 Splint Tightening Ongoing

During testing, the calibrated pressure sensor measured the applied pressure as the splint automatically tightened around the user's wrist, as shown in Figure 4.22. The system underwent 10 trials, each using slightly different wrist circumferences, with an acceptance criterion of achieving the target pressure range in at least 70% of trials.

Trial	Wrist Size (cm)	Measured Pressure (kPa)	Expected Pressure (3.68 kPa)	Pressure Status	Pass/Fail
1	15.1	4.5094	3.68	Pressure threshold	Pass

				reached	
2	16.5	4.3547	3.68	Pressure threshold reached	Pass
3	14.1	4.5997	3.68	Pressure threshold reached	Pass
4	14.0	3.7194	3.68	Pressure threshold reached	Pass
5	15.5	4.9704	3.68	Pressure threshold reached	Pass
6	17.0	5.5481	3.68	Pressure threshold reached	Pass
7	15.0	4.0888	3.68	Pressure threshold reached	Pass
8	15.1	4.1694	3.68	Pressure threshold	Pass

				reached	
9	14.0	3.3343	3.68	Pressure threshold reached	Fail
10	14.3	4.5140	3.68	Pressure threshold reached	Pass

Table 24 Functional Testing Results of the Auto Fit Module

Each trial was individually evaluated based on whether the system successfully reached the predetermined pressure threshold of approximately 3.68 kPa during the automatic tightening sequence. A trial was marked Pass when the measured pressure reached or exceeded 3.68 kPa, confirming that the auto-fit mechanism achieved the required compression level for secure fit and comfort. A trial was marked Fail when the final recorded pressure did not reach the 3.68 kPa threshold, indicating that the tightening process concluded below the target pressure.

The results indicate that the module generally exceeded the theoretical target pressure, with measured values ranging from 3.33 to 5.55 kPa, averaging approximately 4.5 kPa. This represents an average deviation of about 22% above the expected 3.68 kPa, suggesting that the tightening mechanism applies a slightly higher compression than predicted. Nevertheless, the pressure remained within a tolerable range for short-term wrist support applications and did not approach thresholds associated with discomfort or

impaired circulation.

Out of ten trials, nine achieved stable tightening performance, resulting in a 90% success rate, which surpasses the established 70% acceptance criterion. This confirms that the auto-fit module successfully met its functional objective of consistently achieving the target tightening range. The single failed trial (Trial 9) undershot the target by approximately 0.35 kPa, likely due to the sensor initially detecting the target pressure of 3.68 kPa, which triggered the calibration and massage logic that temporarily disables pressure monitoring to prevent interference between modules. During this interval, the user may have slightly shifted their wrist, reducing the contact force on the sensor and causing a lower recorded pressure despite the system having already achieved the intended tightening level.

In contrast, several higher readings were attributed to positional variance during testing. Some users shifted their wrists toward the pressure sensor, momentarily increasing localized compression. This effect was more pronounced in users with larger wrist circumferences, where minor displacements produce proportionally greater localized pressure, accounting for the readings that exceeded the expected range.

To validate this, a one-sample t-test was performed to determine whether the mean measured pressure of the auto-fit module significantly differed from the expected value of 3.68 kPa. Results revealed a statistically significant difference, $t(9) = 3.58$, $p = 0.006$, indicating that the mean measured pressure was higher than the target pressure. The computed effect size (Cohen's $d = 1.13$) denotes a large effect, suggesting that the

deviation from the expected pressure is both statistically and practically meaningful. Furthermore, the 95% confidence interval of [0.31, 1.92] confirms that the true mean pressure likely exceeds the theoretical setpoint by approximately 0.31 to 1.92 kPa.

One Sample T-Test

							95% Confidence Interval	
		Statistic	df	p		Effect Size	Lower	Upper
Measured Pressure (kPa)	Student's t	3.58	9.00	0.006	Cohen's d	1.13	0.307	1.92

Note. H_a $\mu \neq 3.68$

Table 25 One Sample T-Test for The Measured Pressure (kPa)

These findings imply that while the auto-fit module reliably achieved stable tightening performance, the system tended to apply slightly greater compression than

intended. This outcome aligns with observed variations during testing, where minor wrist displacements or positional shifts toward the pressure sensor increased localized readings. Additionally, differences in wrist circumference may have influenced contact distribution, further contributing to elevated values. This relationship is supported by the results of a correlation analysis, which revealed a statistically significant positive association between wrist size and measured pressure ($r = 0.688$, $p = 0.028$) shown in Table 4.13 below.

Correlation Matrix

		Wrist Size (cm)	Measured Pressure (kPa)
Wrist Size (cm)	Pearson's r	—	
	df	—	
	p-value	—	
	95% CI Upper	—	
	95% CI Lower	—	
Measured Pressure (kPa)	Pearson's r	0.688	—
	df	8	—
	p-value	0.028	—

Correlation Matrix

		Wrist Size (cm)	Measured Pressure (kPa)
	95% CI Upper	0.919	—
	95% CI Lower	0.103	—

Table 26 Correlation Matrix Between Wrist Sizes and the Measured Pressure

The strength of this correlation suggests that larger wrist circumferences were consistently linked with higher recorded pressure values, indicating that the auto-fit mechanism responded proportionally to wrist dimensions during tightening. The 95% confidence interval for the correlation coefficient (0.103–0.919) further confirms the reliability of this relationship, although it also reflects some variability likely due to sample size limitations. Overall, these results indicate that the system's pressure output scales with wrist size, maintaining consistent adaptive performance across users while erring slightly on the side of increased compression, thereby ensuring secure yet safe support levels.

Motion Support Module

The functional testing of the Motion Support Module verified its ability to dynamically adjust strap tension in response to muscle contractions, enabling controlled

wrist movement while maintaining support during relaxation. The primary objective was to ensure that the splint facilitated wrist flexion of 10 degrees and extension of 30 degrees during active states, as measured using a goniometer as seen in Figure 4.23. The complete documentation of the results is further summarized in Appendix I.

Figure 43 Flexion and Extension Measurement Using a Goniometer

The results, summarized in Table 4.14, demonstrate that the Motion Support Module consistently allowed controlled wrist movement within clinically acceptable limits. To provide an objective benchmark, the total allowable arc of motion was set at 58° based on literature for partially restrictive splints, reflecting the maximum combined flexion and extension that maintains functional ability without compromising support. Accordingly, the pass/fail criterion was explicitly defined as follows: trials where the

combined wrist motion was less than or equal to 58° were classified as “Pass,” while any trial exceeding 58° was classified as “Fail.” Based on this criterion, nine out of ten trials passed, corresponding to a 90% success rate, while Trial 8 exceeded the allowable arc with a combined motion of 63°, resulting in a failure classification.

Trial No.	Wrist Flexion Achieved (Degrees)	Expected Flexion (Degrees)	Wrist Extension Achieved (Degrees)	Expected Extension (Degrees)	Total Allowable Arc of Motion	Result
1	20	10	36	30	58	Pass
2	10	10	30	30	58	Pass
3	10	10	30	30	58	Pass
4	10	10	30	30	58	Pass
5	10	10	25	30	58	Pass
6	17	10	30	30	58	Pass
7	22	10	25	30	58	Pass
8	23	10	40	30	58	Fail
9	13	10	30	30	58	Pass
10	11	10	30	30	58	Pass

Table 27 Functional Testing Results of the Motion Support Module

To quantitatively evaluate the system’s performance, paired samples t-tests were conducted comparing achieved and expected wrist flexion and extension. The t-test for

wrist flexion yielded a statistically significant difference (t = 2.70, df = 9, p = 0.024), indicating that the achieved flexion was generally higher than expected. This aligns with the observed trials where several participants exceeded the 10° flexion target, yet remained within the 58° total allowable range, validating that the module still maintained functional safety despite the increased flexion.

Conversely, the t-test for wrist extension showed no significant difference (t = 0.421, df = 9, p = 0.683), confirming that the module maintained extension performance close to the expected target of 30° across all trials. The absence of significant deviation in extension further supports the system's consistency in regulating motion within designed specifications.

Paired Samples T-Test

			statistic	df	p
Wrist Flexion Achieved (Degrees)	Expected Flexion (Degrees)	Student's t	2.70	9.00	0.024

Note. H_a $\mu_{\text{Measure 1 - Measure 2}} \neq 0$

Table 28 Paired Samples T-Test of the Achieved and Expected Wrist Flexion

Paired Samples T-Test

				statistic	df	p
Wrist Extension Achieved (Degrees)	Expected (Degrees)	Extension	Student's t	0.421	9.00	0.683

Note. H_a $\mu_{\text{Measure 1 - Measure 2}} \neq 0$

Table 29 Paired Samples T-Test of the Achieved and Expected Wrist Extension

Overall, the findings indicate that the Motion Support Module reliably provides controlled wrist movement during muscle activity while maintaining support during rest. The integration of a clear pass/fail criterion based on the literature-defined allowable motion and the results of statistical analysis confirms that the module operates within clinically acceptable limits. The slightly higher observed flexion, although statistically significant, remains within functional safety margins and does not compromise wrist stability. Hence, the Motion Support Module effectively fulfills its intended function under the tested conditions.

P. System Testing

Signal Acquisition Module and Signal Processing Module

The system testing of the integrated Signal Acquisition and Processing Modules

evaluated their combined performance in capturing, filtering, and classifying EMG signals from the Abductor Pollicis Brevis. The results, summarized in Table 4.17, demonstrate that the modules functioned cohesively to differentiate resting and active muscle states with high consistency and accuracy. During resting trials, the filtered EMG signals exhibited low amplitude levels corresponding to minimal muscle activity, while active trials showed distinctly higher amplitudes following contraction onset. Figure 4.24 illustrates the filtered EMG signal compared to the reconstructed raw signal, confirming that the processed data retained the physiological features necessary for reliable classification.

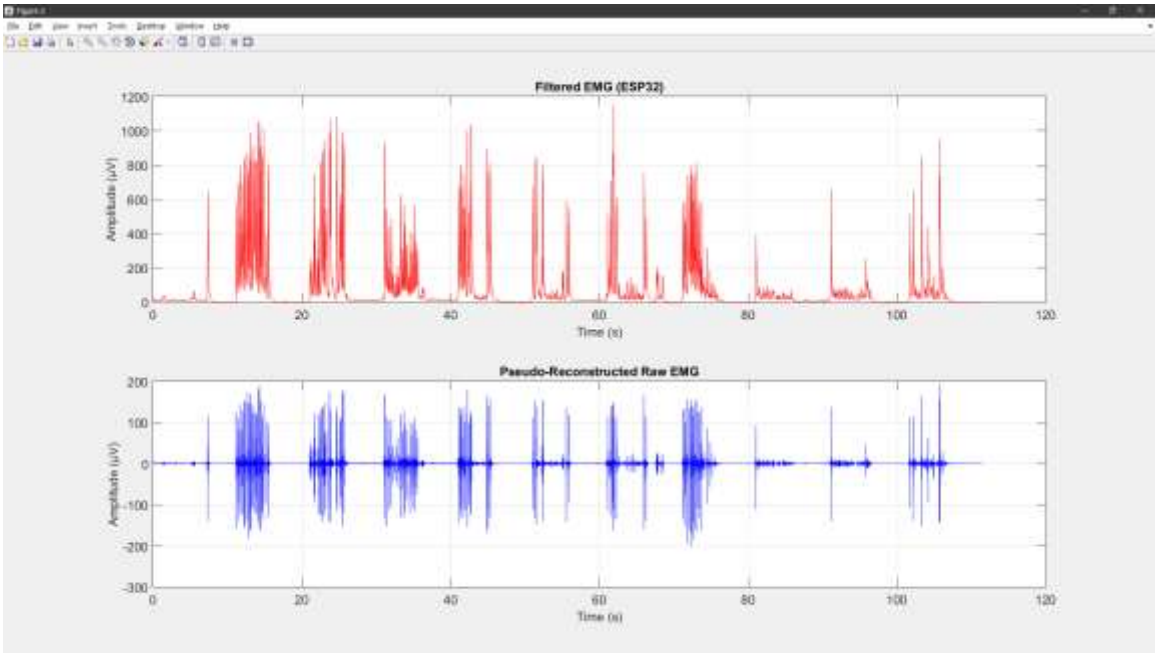

Figure 44 Filtered EMG Signal Compared to the Reconstructed Raw Signal

Each trial was conducted over a fixed time window, during which the average filtered EMG amplitude was compared against a calibrated threshold of 10.00 µV. The

threshold was determined through calibration to optimize detection sensitivity while minimizing false activations due to noise. A trial was classified as “Pass” if the filtered EMG amplitude correctly corresponded to its expected muscle state based on the threshold. Values less than or equal to 10 µV were interpreted as Resting, and values greater than 10 µV were interpreted as Active muscle contraction. A “Fail” result would occur only if the mean filtered amplitude of a trial deviated from its expected classification within the fixed observation window.

As shown in Table 4.17, all twenty trials were correctly classified according to the threshold criterion, achieving a 100% pass rate. Although the Raw EMG values were also tabulated for comparison, it should be noted that these data were pseudo-reconstructed from the filtered EMG and thus may not represent the actual instantaneous EMG activity captured during acquisition. The reconstructed signal served primarily as a visual reference to confirm that the filtering process preserved essential waveform characteristics rather than to quantify true amplitude magnitudes.

While some raw EMG readings appeared near zero during certain active trials, these differences reflected the limitations of reconstruction rather than true signal loss. The filtered EMG maintained clear amplitude distinctions across all trials, signifying that the preprocessing and filtering stages effectively suppressed transient noise and baseline drift while preserving meaningful muscle activity.

The relatively small, filtered voltage values resulted from the low sensor gain used during acquisition, but the differences between resting and active averages remained

physiologically significant. These readings represent the root mean square (RMS)-equivalent averages of sustained contractions rather than instantaneous spikes, ensuring that the measured signals corresponded to true muscle activity instead of transient noise artifacts. The integrated operation of both modules thus confirmed that the system accurately detected and classified EMG signals with high fidelity, effectively distinguishing resting and active states in real time.

Trial	Raw EMG (µV)	Filtered EMG (µV)	Muscle State	Pass/Fail
1	1.48	11.04	Resting	Pass
2	21.39	356.61	Active	Pass
3	2.23	3.34	Resting	Pass
4	27.68	263.74	Active	Pass
5	2.03	11.50	Resting	Pass
6	22.68	157.09	Active	Pass
7	2.18	17.89	Resting	Pass
8	21.38	196.46	Active	Pass
9	1.34	7.63	Resting	Pass
10	10.87	112.33	Active	Pass
11	1.75	9.75	Resting	Pass
12	13.05	104.92	Active	Pass
13	2.88	14.73	Resting	Pass
14	33.95	201.24	Active	Pass

15	1.88	6.17	Resting	Pass
16	9.66	38.67	Active	Pass
17	1.90	10.95	Resting	Pass
18	11.99	50.39	Active	Pass
19	2.07	6.54	Resting	Pass
20	13.50	119.20	Active	Pass

Table 30 System Testing Between Signal Acquisition and Signal Processing Modules

The comparison between the Raw EMG and Filtered EMG signals was statistically examined using the Wilcoxon Signed-Rank Test, selected as a non-parametric alternative to the paired t-test due to the violation of the normality assumption in the filtered signal data. As shown in Table 4.18, the test yielded a Wilcoxon W value of 0.00 with a p-value < .001, indicating a statistically significant difference between the Raw and Filtered EMG signal amplitudes. This finding suggests that the filtering process introduced a measurable alteration in the signal characteristics, likely attributed to the removal of high-frequency noise and baseline drifts inherent in the raw signal.

Wilcoxon Signed-Rank Test

			Statistic	**p**
Raw EMG (μV)	Filtered EMG (μV)	Wilcoxon W	0.00	< .001

Note. H_a $\mu_{\text{Measure 1 - Measure 2}} \neq 0$

Table 31 Comparison of Raw and Filtered EMG Signals Using Wilcoxon Signed-Rank Test

The significant reduction in amplitude variance following filtering indicates that the Signal Processing Module effectively suppressed unwanted noise while preserving physiologically relevant EMG activity. The transformation from raw to filtered signals is consistent with the expected behavior of low-pass or band-pass filtering, which attenuates short-duration fluctuations while maintaining the envelope of muscle activation. In essence, while the amplitude of the filtered signal differs significantly from the unprocessed one, this difference is not a loss of information but a refinement that enhances signal interpretability and classification reliability.

These results confirm that the filtering stage successfully improves signal clarity by stabilizing baseline levels and highlighting meaningful muscle activations. The statistically significant difference between the two signal forms validates that the filtering process achieved its intended function producing smoother, noise-reduced EMG signals suitable for subsequent threshold-based classification. This ensures that the processed data entering the control logic of the system represent physiologically accurate and stable muscle activity patterns rather than transient artifacts or electrical noise.

Signal Processing Module and Integrated Massager Module

During system testing, the Signal Processing Module and Integrated Massager Module consistently identified and responded to varying muscle states, with real-time EMG readings visible through a display interface. This enhancement allowed continuous

monitoring of actual EMG amplitudes and verification of system performance during operation. The setup dynamically adjusted the activation threshold based on each user's baseline activity, ensuring adaptive and accurate detection across different conditions.

Throughout multiple trials, EMG readings were observed in real time as the system alternated between resting and active states. When the EMG amplitude remained below the dynamically computed threshold, the massager activated, performing the myofascial release routine for the set duration. Conversely, when the EMG value exceeded the threshold, indicating muscle contraction, the system immediately halted the massage and triggered the alarm indicator. This consistent behavior confirmed the algorithm's capability to distinguish muscle states accurately while adapting to user-specific signal variations.

Across all 2.5-minute trials, the modules operated synchronously, maintaining precise classification and response timing. The results validated that the Signal Processing Module effectively interpreted real-time EMG data, while the Integrated Massager Module executed corresponding actions with high reliability. The summarized outcomes are presented in Tables 4.19 and 4.20.

The pass/fail criterion for these trials was explicitly defined based on the expected module behavior under each muscle condition. For resting states, a "Pass" was recorded only if the massager successfully activated and the alarm remained inactive, confirming proper relaxation detection. For active states, a "Pass" required the massager to remain inactive while the alarm activated, signifying accurate contraction recognition. Any

deviation from these expected behaviors, such as simultaneous activation or failure to respond, would have constituted a “Fail.” Under this criterion, all trials were classified as “Pass,” demonstrating perfect alignment between expected and actual system performance.

Trial	Test Condition	Massager Activation	Alarm Activation	Result
1	Resting State	Activated	Inactive	Pass
2	Resting State	Activated	Inactive	Pass
3	Resting State	Activated	Inactive	Pass
4	Resting State	Activated	Inactive	Pass
5	Resting State	Activated	Inactive	Pass
6	Resting State	Activated	Inactive	Pass
7	Resting State	Activated	Inactive	Pass
8	Resting State	Activated	Inactive	Pass
9	Resting State	Activated	Inactive	Pass
10	Resting State	Activated	Inactive	Pass
11	Resting State	Activated	Inactive	Pass
12	Resting State	Activated	Inactive	Pass
13	Resting State	Activated	Inactive	Pass
14	Resting State	Activated	Inactive	Pass
15	Resting State	Activated	Inactive	Pass
16	Resting State	Activated	Inactive	Pass

17	Resting State	Activated	Inactive	Pass
18	Resting State	Activated	Inactive	Pass
19	Resting State	Activated	Inactive	Pass
20	Resting State	Activated	Inactive	Pass

Table 32 System Testing Results for Resting State of Signal Processing Module and Integrated Massager Module

Trial	Test Condition	Massager Activation	Alarm Activation	Result
1	Active State	Inactive	Activated	Pass
2	Active State	Inactive	Activated	Pass
3	Active State	Inactive	Activated	Pass
4	Active State	Inactive	Activated	Pass
5	Active State	Inactive	Activated	Pass
6	Active State	Inactive	Activated	Pass
7	Active State	Inactive	Activated	Pass
8	Active State	Inactive	Activated	Pass
9	Active State	Inactive	Activated	Pass
10	Active State	Inactive	Activated	Pass
11	Active State	Inactive	Activated	Pass
12	Active State	Inactive	Activated	Pass
13	Active State	Inactive	Activated	Pass

14	Active State	Inactive	Activated	Pass
15	Active State	Inactive	Activated	Pass
16	Active State	Inactive	Activated	Pass
17	Active State	Inactive	Activated	Pass
18	Active State	Inactive	Activated	Pass
19	Active State	Inactive	Activated	Pass
20	Active State	Inactive	Activated	Pass

Table 33 System Testing Results for Active State of Signal Processing Module and Integrated Massager Module

The results shown in Tables 4.19 and 4.20 demonstrate the system's consistent and accurate response to muscle state transitions across 40 trials. The massager activated exclusively during resting states, while the alarm triggered consistently during active contractions, yielding a 100% pass rate. This behavioral consistency reinforces the validity of the system's logic, which was grounded on EMG amplitude thresholds statistically confirmed via Welch's t-test ($p < 0.001$). Given the non-overlapping confidence intervals and large effect size (Cohen's $d = -5.88$) between resting and active EMG means, the observed system response during testing trials aligns precisely with the defined dynamic threshold. The absence of false positives or negatives in both resting and active states further substantiates the reliability of the Signal Processing Module and the Integrated Massager Module in real-time operation.

Independent Samples T-Test

							95% Confidence Interval	
		Statistic	df	p		Effect Size	Lower	Upper
Muscle States	Welch's t	-13.1	9.39	< .001	Cohen's d	-5.88		

Note. H_a $\mu_{Resting} \neq \mu_{Active}$

Table 34 Independent Samples T-test of the Muscle States

These findings confirm that the integrated system operates with high accuracy and stability under dynamic conditions. The explicit pass/fail criteria based on expected response behavior, together with the statistically significant separation between resting and active EMG signals, establish a robust validation framework. The perfect classification performance, reinforced by quantitative analysis, validates the precision of both the detection algorithm and the control logic. Overall, the Signal Processing Module and Integrated Massager Module function cohesively, ensuring that therapeutic actions are executed only under appropriate muscle states, thereby fulfilling the intended design objective of reliable, adaptive, and user-specific operation.

Signal Processing Module and Auto Fit Module

The system testing for the Signal Processing Module and Auto-Fit Module yielded successful results, confirming the system's reliability in classifying muscle states and regulating splint pressure in accordance with rest or activity conditions. The primary objective of the Signal Processing Module was to distinguish between resting and active muscle states with an acceptable accuracy rate of ≥ 80 %, while the Auto-Fit Module was evaluated based on its ability to apply the derived target pressure of 3.68 kPa during the resting state with a minimum accuracy rate of 70 %.

A trial was classified as "Pass" if the Signal Processing Module accurately identified the muscle state and the Auto-Fit Module responded accordingly, activating and maintaining pressure near the 3.68 kPa target during rest and remaining inactive during active states. Any instance where either misclassification or incorrect pressure regulation occurred was marked as "Fail."

During resting trials, the Auto-Fit Module consistently achieved pressure readings near the expected 3.68 kPa target, demonstrating stable and adaptive tightening performance. Out of ten trials, nine achieved successful regulation, corresponding to a 90 % success rate. The single failed trial (Trial 9) undershot the target by approximately 0.35 kPa, likely due to a minor sensor lag during calibration. It is also possible that the sensor had already registered the target pressure before the user slightly moved their wrist away from the pressure sensor, lowering the detected value. Conversely, higher readings in other trials were likely caused by wrist displacement toward the pressure sensor,

resulting in localized overestimation, especially among users with larger wrist circumferences.

Trial	Muscle State	Wrist Size (cm)	Measured Pressure (kPa)	Expected Pressure (kPa)	Pressure Status	Result
1	Resting	15.1	4.5094	3.68	Pressure threshold reached	Pass
2	Resting	16.5	4.3547	3.68	Pressure threshold reached	Pass
3	Resting	14.1	4.5997	3.68	Pressure threshold reached	Pass
4	Resting	14.0	3.7194	3.68	Pressure threshold reached	Pass
5	Resting	15.5	4.9704	3.68	Pressure threshold reached	Pass
6	Resting	17.0	5.5481	3.68	Pressure	Pass

					threshold reached	
7	Resting	15.0	4.0888	3.68	Pressure threshold reached	Pass
8	Resting	15.1	4.1694	3.68	Pressure threshold reached	Pass
9	Resting	14.0	3.3343	3.68	Pressure threshold reached	Pass
10	Resting	14.3	4.5140	3.68	Pressure threshold reached	Pass

Table 35 System Testing Results for Signal Processing Module and Auto Fit Module

Despite these variations, all recorded pressures remained within acceptable therapeutic limits, indicating that the system maintained effective tightening without compromising comfort. For the active muscle state, the Signal Processing Module correctly inhibited Auto-Fit activation in all cases, confirming that pressure adjustment ceased when muscle activity was detected. These findings validate the integrated performance of the EMG-driven logic and Auto-Fit system, demonstrating functional

coordination between signal classification and adaptive pressure control.

Statistical correlation analysis was also conducted to further verify the relationship between muscle activity and the measured pressure during testing. Using Spearman's rank correlation and Kendall's Tau-b, the results yielded coefficients of $\rho = -0.009$ ($p = 0.981$) and $\tau_\beta = -0.036$ ($p = 0.897$), respectively. Both coefficients are close to zero, with high p-values indicating that the relationship between EMG activity and pressure was statistically insignificant. This lack of correlation confirms that the Auto-Fit Module maintained consistent pressure output regardless of minor fluctuations in EMG signal intensity, effectively tightening only when intended and not during active muscle contractions.

Correlation Matrix

		Measured Pressure (kPa)	EMG
Measured Pressure (kPa)	Spearman's rho	—	
	df	—	
	p-value	—	
	Kendall's Tau B	—	
	p-value	—	

Correlation Matrix

		Measured Pressure (kPa)	EMG
EMG	Spearman's rho	-0.009	—
	df	8	—
	p-value	0.981	—
	Kendall's Tau B	-0.036	—
	p-value	0.897	—

Table 36 Correlation Between Muscle State and Pressure

The absence of significant dependence between EMG readings and pressure measurements supports the system's intended behavior where EMG signal classification and pressure regulation operate as coordinated subsystems under unified control logic. The integrated pass/fail assessment confirms that both modules functioned cohesively and accurately as one system.

Overall, these results demonstrate that the combined Signal Processing and Auto-Fit Modules functioned as designed: the EMG-based classifier accurately differentiated rest and activity phases, and the Auto-Fit mechanism applied stable, therapeutic pressure exclusively during rest. This ensures both functional reliability and user comfort,

validating the system's design objective of achieving adaptive and responsive wrist support through integrated operation.

Signal Processing Module and Motion Support Module

The system testing of the integrated Signal Processing and Motion Support modules evaluated their combined performance in detecting muscle states and dynamically adjusting the splint's tension. The primary objective was to ensure that the Signal Processing module accurately classified muscle states and that the Motion Support module appropriately adjusted the splint's tension to maintain support during muscle rest or allow controlled movement during contraction.

The results, summarized in Table 4.24, indicate that the system successfully classified muscle states and adjusted the splint accordingly across all ten trials, achieving an overall accuracy rate of 100%. The pass criterion was defined as the correct classification of both resting and active states followed by the corresponding and appropriate mechanical response of the Motion Support module. Specifically, maintaining tension during resting states and loosening the splint during active states to permit controlled wrist motion. Any deviation from this coordinated response would have been marked as a failure.

As shown in the table, all ten trials met the pass criterion. During resting states, the splint consistently maintained its set tension, ensuring wrist stability. During active muscle states, the Motion Support module loosened the splint by measured degrees, allowing controlled wrist flexion and extension. The degree of flexion ranged from 10° to

23°, while the degree of extension ranged from 25° to 40°, demonstrating the system's ability to adapt the level of support dynamically in response to EMG-detected activity. The consistent classification and response pairing across trials confirmed the modules' coordinated performance, with the integrated system demonstrating reliability in synchronizing EMG-driven logic and mechanical tension adjustments.

Trial	Classified State	Motion Support Response	Classified State	Motion Support Response	Result
1	Resting	Splint maintained tension	Active	Splint loosened (20° flexion, 36° extension)	Pass
2	Resting	Splint maintained tension	Active	Splint loosened (10° flexion, 30° extension)	Pass
3	Resting	Splint maintained tension	Active	Splint loosened (10° flexion, 30° extension)	Pass
4	Resting	Splint maintained tension	Active	Splint loosened (10° flexion, 30° extension)	Pass
5	Resting	Splint maintained	Active	Splint loosened (10° flexion, 25° extension)	Pass

		tension			
6	Resting	Splint maintained tension	Active	Splint loosened (17° flexion, 30° extension)	Pass
7	Resting	Splint maintained tension	Active	Splint loosened (22° flexion, 25° extension)	Pass
8	Resting	Splint maintained tension	Active	Splint loosened (23° flexion, 40° extension)	Pass
9	Resting	Splint maintained tension	Active	Splint loosened (13° flexion, 30° extension)	Pass
10	Resting	Splint maintained tension	Active	Splint loosened (11° flexion, 30° extension)	Pass

Table 37 System Testing Results for Signal Processing and Motion Support Modules

Furthermore, a Kruskal–Wallis test was performed to statistically assess the effect of muscle state on wrist flexion and extension. The results revealed a significant difference in both wrist flexion ($\chi^2 = 16.5$, $df = 1$, $p < 0.001$) and wrist extension ($\chi^2 = 16.8$, $df = 1$, $p < 0.001$) between resting and active states. Effect size calculations yielded r =

0.866 for flexion and r = 0.886 for extension, both indicating a very strong relationship between muscle state and the resulting wrist movement.

Kruskal-Wallis

	χ^2	df	p	ε^2
Flexion	16.5	1	< .001	0.866
Extension	16.8	1	< .001	0.886

Table 38 Kruskal-Wallis test for flexion and extension

These statistical results quantitatively support the observed functional testing outcomes. The Motion Support module significantly increased wrist mobility during active muscle states while maintaining full stability during rest. The high effect sizes confirm a strong association between EMG-classified muscle activity and corresponding wrist movement, validating that the EMG-driven control logic effectively modulates splint tension. The consistent pass results across trials and the significant statistical findings collectively demonstrate that the integrated system performs with high precision, reliability, and functional relevance in providing adaptive wrist support.

Q. Beta Testing

In this last section, the beta testing aimed to evaluate the effectiveness of the eM-Brace device in alleviating muscle weakness associated with CTS. The study involved 15 female respondents aged 18–25 years from Ateneo de Zamboanga University, all of

whom engaged in keyboard use for at least four continuous hours daily. To simulate CTS symptoms in a controlled environment, Phalen's Test was employed as shown in Figure 4.25, inducing temporary median nerve compression. This method allowed for a measurable assessment of grip strength before and after massage therapy using the eM-Brace device. Additionally, participant safety was a primary consideration throughout the beta testing phase. The eM-Brace device was designed to ensure user safety, eliminating the risk of electrocution through insulated electrical components and low-power operation. The device operates at a safe voltage, adhering to industry standards for wearable medical devices. Furthermore, a failsafe mechanism was integrated, allowing participants to immediately deactivate the device if they experienced significant discomfort. This emergency stop feature ensured that users maintained full control over the intervention, preventing any potential adverse effects.

Figure 45 Phalen's Test

Grip strength measurements were then taken using a Hand Dynamometer before and after the massage therapy session as presented in Appendix M. Initial grip strength

was recorded immediately after Phalen's Test to establish the induced weakness, followed by a 2-minute and 30-seconds massage session using the eM-Brace device s outlined in Appendix N. Grip strength was measured again post-massage to determine the immediate effects of the intervention.

To justify the pass/fail criteria, a grip strength (GS) improvement of at least 2.2 kg was considered clinically meaningful, based on prior studies: a systematic review [138] reported the minimum clinically important difference (MCID) in healthy individuals as 2.44–2.69 kg, while a study on massage therapy for CTS [137] identified improvements ≥2.2 kg as associated with symptomatic relief.

Each participant's pass/fail determination was directly tied to measurable changes in grip strength. By comparing pre- and post-massage GS values (see Table 4.26), participants who demonstrated a GS increase of 2.2 kg or more were considered to have experienced a physiologically meaningful improvement, while those below this threshold were considered non-responders for the purpose of the beta test. For example, Participant 1 improved from 15.90 kg to 18.90 kg (Δ = 3.00 kg, Pass), Participant 3 improved from 10.10 kg to 12.00 kg (Δ = 1.90 kg, Fail), and Participant 8 showed no change (Δ = 0.00 kg, Fail). Using this method, 11 out of 15 participants (73%) achieved a clinically meaningful GS improvement and were classified as pass, whereas 4 participants did not reach the threshold and were classified as fail.

Participants	Grip Strength	Grip Strength	Improvement in Grip	Pain Scale	Pain Scale	Pain Scale	Result

	Before Massage (kg)	After Massage (kg)	Strength (kg)	Before Massage	During Massage	After Massage	
1	15.90	18.90	3.00	5	0	0	Pass
2	5.00	8.80	3.80	4	2	0	Pass
3	10.10	12.00	1.90	8	0	0	Fail
4	14.40	15.60	1.20	2	0	0	Fail
5	15.00	19.90	4.90	2	3	3	Pass
6	27.80	32.40	4.60	0	0	0	Pass
7	6.30	10.70	4.40	3	0	0	Pass
8	15.20	15.20	0.00	1	0	0	Fail
9	14.20	19.30	5.10	6	3	0	Pass
10	29.50	33.70	4.20	2	0	1	Pass
11	30.10	39.10	9.00	5	1	1	Pass
12	5.50	5.80	0.30	5	0	0	Fail
13	19.40	23.30	3.90	5	0	0	Pass
14	20.80	26.80	6.00	1	0	0	Pass
15	12.20	16.00	3.80	0	0	0	Pass

Table 39 Beta Testing Results for eM-Brace

Furthermore, participants who passed the beta test demonstrated a clear improvement in grip strength after using the eM-Brace device, suggesting that the device had a positive effect on recovery from induced CTS symptoms. However, the level of

improvement varied among participants. Specifically, three participants exhibited grip strength gains exceeding 5 kg, with an average improvement of 6.7 kg. These individuals reported daily pain levels of 0, 3, and 6. During the beta test, they recorded an average pain level of 1.66 before performing the Phalen's test and 4.00 afterward. The increase in their pain scores following the Phalen's test highlights its effectiveness in provoking symptoms consistent with early-stage CTS.

Despite these improvements, correlation analyses revealed that grip strength improvement was largely independent from pain scores either before massage (Pearson's $r = -0.019$, $p = 0.946$) or after massage (Spearman's $\rho = 0.461$, $p = 0.084$). This lack of association may reflect inter-individual differences in pain perception and tolerance, as participants with similar median nerve compression could report widely varying pain levels. These findings suggest that the device's effects on muscular function occur independently of participants' subjective pain perception. Expert evaluation from Ms. Frencie Quintin Z. Purol, PTRP, confirmed that positive Phalen's test results indicate CTS, implying that individuals with pronounced symptom response may experience greater functional benefit from the eM-Brace device.

Correlation Matrix

		Improvement in Grip Strength (kg)	Pain Scale Before Massage	Pain Scale After Massage
Improvement in Grip Strength (kg)	Pearson's r	—		
	df	—		
	p-value	—		
	Spearman's rho	—		
	df	—		
	p-value	—		
Pain Scale Before Massage	Pearson's r	-0.019	—	
	df	13	—	
	p-value	0.946	—	
	Spearman's rho	-0.043	—	
	df	13	—	

Correlation Matrix

		Improvement in Grip Strength (kg)	Pain Scale Before Massage	Pain Scale After Massage
	p-value	0.880	—	
Pain Scale After Massage	Pearson's r	0.351	-0.123	—
	df	13	13	—
	p-value	0.200	0.663	—
	Spearman's rho	0.461	-0.034	—
	df	13	13	—
	p-value	0.084	0.905	—

Note. * p < .05, ** p < .01, *** p < .001

Table 40 Correlation Matrix between Improvement in Grip Strength and Pain Scales

Meanwhile, another eight participants, who reported daily pain levels of 0 to 6, average pain level of 0.625 before the Phalen's test, and average pain level of 2.625 after, showed grip strength improvements between 3 and 5 kg with an average of 4.075 kg. Their lower pain levels suggest they were still within the normal range and not yet at high risk for CTS, which explains why their improvement was less noticeable compared to the

first group. This contrast between the first and second groups indicates that participants with higher baseline pain scores after the Phalen's test tended to exhibit greater improvements in grip strength following use of the eM-Brace device, suggesting that individuals showing early CTS symptoms may experience more benefit from the massage therapy intervention. Participants with lower baseline pain levels showed smaller gains, possibly because they had not yet developed substantial nerve compression, and thus the therapeutic effects of the device were less pronounced.

In addition, the researchers found that EMG readings obtained through the BIOPAC software showed a significant decrease in EMG amplitude immediately after conducting Phalen's Test. As explained in a study [138], Phalen's Test increases intracarpal pressure by forcing the wrist into flexion, leading to compression of the median nerve. This compression disrupts motor unit recruitment and reduces neuromuscular efficiency, resulting in a drop in EMG amplitude [138]. Based on this physiological mechanism, the researchers examined EMG amplitude data immediately following Phalen's Test in a participant who passed the test (defined as demonstrating at least a 2.2 kg increase in grip strength after massage intervention). The results, recorded using Biopac software, revealed that the participant exhibited a noticeable decrease in EMG amplitude immediately after Phalen's Test.

This distinction further supports the idea that Phalen's Test effectively provokes symptoms in individuals with suspected carpal tunnel syndrome (CTS) [138], while those without CTS or with minimal nerve involvement do not exhibit the same physiological

response. It also helps explain why participants who failed the beta test showed less improvement in grip strength after massage, likely because their symptoms were not primarily due to median nerve compression, and thus massage provided limited benefit [138].

Furthermore, the study noted that EMG readings typically took at least three minutes to return to baseline after performing Phalen's Test, indicating a sustained neuromuscular response to nerve compression. In contrast, when a massage intervention was applied immediately after the test, EMG amplitude recovered within just one minute. This suggests that massage may facilitate quicker reduction of nerve compression, enabling faster neuromuscular recovery [138].

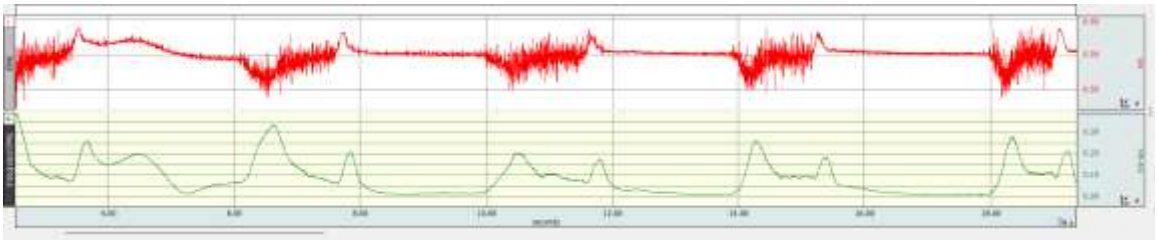

Figure 46 Baseline EMG Amplitude Before Performing Phalen's Test

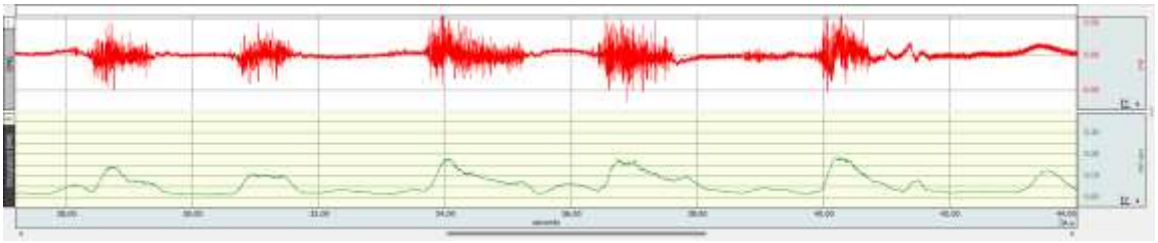

Figure 47 EMG Amplitude Before Massage Intervention Post-Phalen's Test

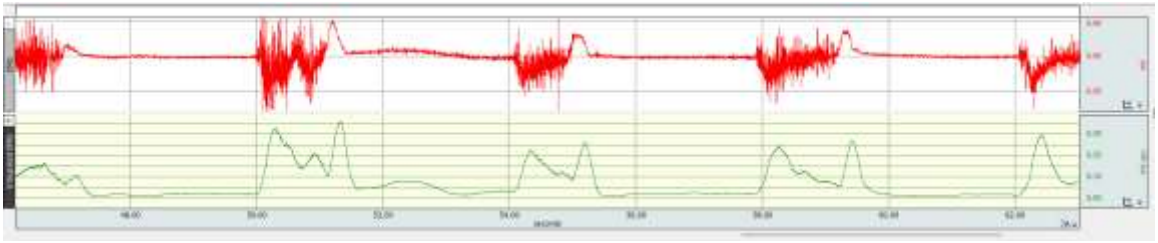

Figure 48 EMG Amplitude After Massage Intervention Post-Phalen's Test

Statistical analysis further confirmed these observations, as a repeated measures ANOVA revealed a significant main effect of condition on EMG activity, $F(2, 16) = 6.05$, $p = 0.011$, indicating that EMG values differed significantly across the three time points: before the Phalen's test, before massage, and after massage. Post hoc comparisons showed a significant decrease in EMG activity before the massage (mean difference = 0.0363, $p = 0.023$), confirming that the Phalen's test induced measurable muscular weakness. EMG activity then significantly increased after the massage compared to the post-Phalen's condition (mean difference = –0.1090, $p = 0.039$), suggesting that the massage effectively helped alleviate the Phalen's test–induced weakness and supporting the earlier conclusion that massage therapy facilitated functional recovery.

Repeated Measures ANOVA

Within Subjects Effects

	Sum of Squares	df	Mean Square	F	p
Condition	0.0555	2	0.02775	6.05	0.011
Residual	0.0733	16	0.00458		

Note. Type 3 Sums of Squares

Between Subjects Effects

	Sum of Squares	df	Mean Square	F	p
Residual	0.0211	8	0.00263		

Note. Type 3 Sums of Squares

Table 41 Repeated Measures ANOVA for the Beta Testing

Post Hoc Comparisons - Condition

Comparison							
Condition		Condition	Mean Difference	SE	df	t	p_{tukey}
Before Phalen's	-	Before Massage	0.0363	0.0107	8.00	3.39	0.023
	-	After Massage	-0.0727	0.0405	8.00	-1.80	0.231
Before Massage	-	After Massage	-0.1090	0.0361	8.00	-3.02	0.039

Table 42 Post Hoc Comparison of EMG Signals Pre-Phalen's and Pre-/Post-Massage

Additionally, participants who failed the beta test, defined by grip strength improvements of less than 2.2 kg (averaging 0.85 kg), showed variable baseline pain levels, ranging from 1 to 8, with minimal or no pain recorded during and after the massage session. Their grip strength improvements were limited, from 0.3 to 1.9 kg. These results suggest that some participants exhibited high baseline discomfort without corresponding functional gains, while others had low pain and minimal muscle weakness. Overall, the eM-Brace device had limited impact for this group, as their muscle weakness was either insufficiently pronounced or not strongly linked to CTS-like symptoms.

The non-parametric repeated measures analysis using the Friedman test revealed a significant effect of the massage intervention on pain levels ($\chi^2(2) = 17.3$, $p < .001$). Descriptive statistics indicate that participants' average pain decreased from 3.27 before massage to 0.60 during, and 0.33 after the session. These results suggest that the eM-Brace device effectively alleviates wrist discomfort associated with CTS, providing immediate symptomatic relief during and after the massage.

Friedman

χ^2	df	p
17.3	2	< .001

Descriptives

	Mean	Median
Pain Scale Before Massage	3.267	3
Pain Scale During Massage	0.600	0
Pain Scale After Massage	0.333	0

Table 43 Friedman Test and Descriptive Statistics for Pain Scores

In addition, a paired samples t-test showed a significant increase in grip strength after using the eM-Brace device ($t(14) = –6.32$, $p < .001$). This indicates that, on average, participants were able to exert more force with their hands following the massage session, suggesting that the device effectively reduces temporary muscle weakness associated with CTS and can enhance hand function even after a single use.

Paired Samples T-Test

							95% Confidence Interval	
		Statistic	df	p	Effect Size	Lower		Upper
Grip Strength Before	Grip Strength After Massage (kg)	Student's t	-6.32	14.0	< .001	Cohen's d	-1.63	-2.40	-0.836

Note. H_a $\mu_{\text{Measure 1 – Measure 2}} \neq 0$

Table 44 Paired Samples T-Test of Grip Strength Before and After Massage

The eM-Brace's auto-fit module was also tested to evaluate its effectiveness in providing a secure and comfortable fit. Participants were instructed to wear the device, and all users reported a snug yet non-restrictive fit, with no need for manual adjustments after initial placement. The device automatically conformed to the wrist, maintaining consistent support without excessive pressure or discomfort. This confirms that the auto-fit feature enhances usability by eliminating the need for manual resizing, addressing a

common limitation of traditional wrist splints. Additionally, during the massage session, the device maintained a pressure of at least 3.68 kPa on the wrist, ensuring adequate support. After the session, it automatically loosened, preventing unnecessary compression and allowing for natural relaxation of the wrist.

This design is based on Ms. Purol's (Appendix B) suggestion that while wrist splints are commonly used to immobilize the hand in the treatment of Carpal Tunnel Syndrome (CTS), they do not necessarily have to completely immobilize the wrist. Instead, the splints can be designed to allow for specific degrees of movement, particularly during work tasks or daily activities. For instance, a splint may restrict motion by limiting wrist flexion to around 10 degrees and extension to about 30 degrees, rather than preventing all movement [41]. This approach provides support while still permitting some motion within a controlled range, which can be beneficial for individuals who need to use their hands during the day, without exacerbating the symptoms of CTS. This type of motion restriction helps manage the condition effectively while maintaining some functional mobility.

Finally, the eM-Brace device, weighing just 280 grams, is notably lightweight compared to similar wrist massagers like the COZYMA R-R-ran-560 (845 grams), ATEX Rilagyo Air Massager (500 grams), JIEJUNJIE Wrist Massager (349 grams), and the CINCOM Hand Massager (680 grams). This was further confirmed by participants in the beta testing, and Ma'am Aurora Jasmin Diaz, PTRP during a visit to ZCMC, who stated that the eM-Brace is not heavy to carry, making it a convenient option for extended use. A comparison is further summarized in the Table 4.32 below:

Device	Weight	Remarks
eM-Brace	280 grams	Lightweight, confirmed by beta testing participants.
COZYMA R-R-ran-560	845 grams	Heavier, features air pressure massage and heat therapy.
ATEX Rilagyo Air Massager	500 grams	Medium weight, offers air massage for wrists and ankles.
JIEJUNJIE Wrist Massager	349 grams	Close in weight, designed for wrist massage with airbag and heat.
CINCOM Hand Massager	680 grams	Heavier, provides deep muscle massage for hands and wrists.

Table 45 Wrist Massager Weight Comparison

Overall, with a 73% passing rate, the findings suggest that the eM-Brace device effectively improves grip strength and alleviates muscle weakness in CTS. Beyond that, it provides support without restricting movement and features an adaptive fit, unlike existing wrist splints. This underscores the significance of eM-Brace as an innovative solution for CTS-related muscle weakness, offering both comfort and effectiveness in managing symptoms.

CHAPTER V
CONCLUSIONS AND RECOMMENDATIONS

This study successfully designed, developed, and evaluated the eM-Brace, an autonomous wrist splint equipped with an integrated massage system aimed at alleviating muscle weakness associated with Carpal Tunnel Syndrome (CTS). Beta testing results demonstrated a significant improvement in grip strength recovery and a reduction in discomfort linked to median nerve compression. Compared to natural recovery processes, the integration of EMG-based activation for myofascial release therapy facilitated a more rapid alleviation of symptoms, validating the device's effectiveness as a therapeutic intervention for CTS management.

The implementation of surface electromyography (sEMG) sensors enabled real-time monitoring of muscle activity, ensuring that the massage system was activated only when the muscle was in a resting state. This feature enhanced the therapeutic efficacy of the intervention while preventing unintended stimulation. Furthermore, the auto-fit module dynamically adjusted the splint's tension in response to muscle activity, ensuring optimal wrist support across various movements. The combination of these features underscores the potential of the eM-Brace as a cutting-edge solution for mitigating the progression of CTS symptoms.

Additionally, the study confirmed that the massage system, calibrated to deliver a standardized pressure of 1.36 kPa, effectively provided therapeutic relief without inducing discomfort. Safety assessments verified the device's adherence to wearable medical device standards, incorporating insulated electrical components and an

emergency stop mechanism to ensure user safety. Collectively, these findings support the feasibility of eM-Brace for real-world applications in CTS symptom management and rehabilitation.

Although the eM-Brace demonstrated effectiveness in alleviating CTS-related muscle weakness and discomfort, several technical limitations were identified during system testing. The Wi-Fi display exhibited noticeable latency, which may depend on internet speed and affect the responsiveness of real-time monitoring. The EMG sensor, while capable of distinguishing relative voltage variations, did not capture absolute muscle activity data since it operated based on a reference voltage rather than true physiological baselines. Furthermore, the sampling frequency exhibited minor drift over time, potentially affecting the accuracy of digital filter coefficients and introducing signal processing inconsistencies. The amplification stage also presented a limitation, as the current gain setting may be insufficient for users with weaker EMG signals, leading to unreliable detection. Finally, calibration errors were observed when users moved during setup, which caused the EMG threshold to be set too high—making it difficult for the system to halt massage or loosen the splint when necessary.

To address these limitations and further enhance the system's functionality, the following recommendations are proposed for future development:

Improved Wireless Display Protocols: Implementing local communication protocols such as Bluetooth Low Energy (BLE) or ESP-NOW can reduce latency and dependence on internet speed, ensuring more reliable and responsive data visualization.

Enhanced EMG Signal Calibration: Future versions should incorporate absolute referencing or baseline correction to more accurately reflect physiological EMG signals. This adjustment would improve signal reliability and make readings more representative of true muscle activity.

Stable Sampling Frequency Control: Incorporating a hardware-based timer or phase-locked loop (PLL) can minimize sampling drift, ensuring filter coefficients remain accurate throughout continuous operation.

Adjustable Amplification Settings: Introducing configurable gain parameters would allow the system to adapt to varying EMG signal strengths across different users, improving the consistency of muscle state detection.

Refined Calibration Procedure: A guided calibration process with motion detection can prevent users from moving during setup, thereby avoiding artificially elevated thresholds and ensuring accurate activation of massage and support modules.

By addressing these technical concerns, future iterations of the eM-Brace can achieve greater precision, reliability, and adaptability. Further research may also explore extending its application to other musculoskeletal disorders, expanding its relevance beyond CTS management.

REFERENCES

[1] M. Soubeyrand, R. Melhem, M. Protais, M. Artuso, and M. Crézé, "Anatomy of the median nerve and its clinical applications," *Hand Surg. Rehabil.*, vol. 39, no. 1, pp. 2–18, Feb. 2020, doi: 10.1016/j.hansur.2019.10.197.

[2] A. Genova *et al.*, "Carpal Tunnel Syndrome: A Review of Literature," *Cureus*, vol. 12, Mar. 2020, doi: 10.7759/cureus.7333.

[3] J. O. Sevy, R. E. Sina, and M. Varacallo, "Carpal Tunnel Syndrome," in *StatPearls*, Treasure Island (FL): StatPearls Publishing, 2024. Accessed: Sep. 07, 2024. [Online]. Available: http://www.ncbi.nlm.nih.gov/books/NBK448179/

[4] E. Al Shahrani, A. Al Shahrani, and N. Al-Maflehi, "Personal factors associated with carpal tunnel syndrome (CTS): a case-control study," *BMC Musculoskelet. Disord.*, vol. 22, no. 1, p. 1050, Dec. 2021, doi: 10.1186/s12891-021-04941-y.

[5] M. S. Aboonq, "Pathophysiology of carpal tunnel syndrome," *Neurosciences*, vol. 20, no. 1, p. 4, Jan. 2015.

[6] A. B. Schmid, "Pathophysiology of the Carpal Tunnel Syndrome," *physioscience*, vol. 11, pp. 2–10, Feb. 2015, doi: 10.1055/s-0034-1398907.

[7] Aziz Nusrat, "Diagnosis of carpal tunnel syndrome in perspective of clinical features, neurophysiological studies and high resolution ultrasound," in *World Journal of Advanced Research and Reviews*, Jun. 2020, pp. 086–096. doi: 10.30574/wjarr.2020.6.3.0182.

[8] K. Holzapfel, T. Ghosh, S. Krischak, and M. Naumann, "Nerve Echogenicity: Changes in High-Resolution Nerve Ultrasound in Carpal Tunnel Syndrome after Surgery,"

Ultrasound Med. Biol., vol. 48, no. 2, pp. 223–227, Feb. 2022, doi: 10.1016/j.ultrasmedbio.2021.10.005.

[9] J. Wipperman and K. Goerl, "Carpal Tunnel Syndrome: Diagnosis and Management," *Am. Fam. Physician*, vol. 94, no. 12, pp. 993–999, Dec. 2016.

[10] P. Roomizadeh *et al.*, "Ultrasonographic Assessment of Carpal Tunnel Syndrome Severity: A Systematic Review and Meta-Analysis," *Am. J. Phys. Med. Rehabil.*, vol. 98, no. 5, p. 373, May 2019, doi: 10.1097/PHM.0000000000001104.

[11] C. Phongamwong, N. Soponprapakorn, and W. Kumnerddee, "Determination of Electrophysiologically Moderate and Severe Carpal Tunnel Syndrome: Ultrasonographic Measurement of Median Nerve at the Wrist," *Ann. Rehabil. Med.*, vol. 41, no. 4, p. 604, 2017, doi: 10.5535/arm.2017.41.4.604.

[12] A. E. Lincoln, J. S. Vernick, S. Ogaitis, G. S. Smith, C. S. Mitchell, and J. Agnew, "Interventions for the primary prevention of work-related carpal tunnel syndrome," in *Database of Abstracts of Reviews of Effects (DARE): Quality-assessed Reviews [Internet]*, Centre for Reviews and Dissemination (UK), 2000. Accessed: Sep. 11, 2024. [Online]. Available: https://www.ncbi.nlm.nih.gov/books/NBK68251/

[13] H. M. A. Raihan *et al.*, "Orthotic Treatment Overview of Carpal Tunnel Syndrome," in *Peripheral Nerve Disorders and Treatment*, IntechOpen, 2020. doi: 10.5772/intechopen.85101.

[14] M. A. Gatheridge, E. A. Sholty, A. Inman, M. Pattillo, F. Mindrup, and D. L. Sanderson, "Splinting in Carpal Tunnel Syndrome: The Optimal Duration," *Mil. Med.*, vol. 185,

no. 11–12, pp. e2049–e2054, Nov. 2020, doi: 10.1093/milmed/usaa222.

[15] K. Shem, J. Wong, and B. Dirlikov, “Effective self-stretching of carpal ligament for the treatment of carpal tunnel syndrome: A double-blinded randomized controlled study,” *J. Hand Ther.*, vol. 33, no. 3, pp. 272–280, Jul. 2020, doi: 10.1016/j.jht.2019.12.002.

[16] F. Georgiew, J. Florek, S. Janowiec, and P. Florek, “The use of orthoses in the treatment of carpal tunnel syndrome. A review of the literature from the last 10 years,” *Rheumatology*, vol. 60, no. 6, pp. 408–412, Dec. 2022, doi: 10.5114/reum.2022.123681.

[17] A. de Sire *et al.*, “Efficacy of kinesio taping on hand functioning in patients with mild carpal tunnel syndrome. A double-blind randomized controlled trial,” *J. Hand Ther.*, vol. 35, no. 4, pp. 605–612, Oct. 2022, doi: 10.1016/j.jht.2021.04.011.

[18] “CarpalRx: A Certified Massager for Carpal Tunnel Syndrome.” Accessed: Sep. 12, 2024. [Online]. Available: https://www.carpalrx.com/massager-for-carpal-tunnel

[19] B. M. Sucher, “Myofascial release of carpal tunnel syndrome,” *J. Osteopath. Med.*, vol. 93, no. 1, pp. 92–92, Jan. 1993, doi: 10.7556/jaoa.1993.93.1.92.

[20] R. Elliott and B. Burkett, “Massage therapy as an effective treatment for carpal tunnel syndrome,” *J. Bodyw. Mov. Ther.*, vol. 17, no. 3, pp. 332–338, Jul. 2013, doi: 10.1016/j.jbmt.2012.12.003.

[21] “Carpal tunnel syndrome: Learn More – Wrist splints and hand exercises,” in *InformedHealth.org [Internet]*, Institute for Quality and Efficiency in Health Care

(IQWiG), 2021. Accessed: Sep. 12, 2024. [Online]. Available: https://www.ncbi.nlm.nih.gov/books/NBK279596/

[22] Y. Hamaue *et al.*, "Effects of Vibration Therapy on Immobilization-Induced Hypersensitivity in Rats," *Phys. Ther.*, vol. 95, no. 7, pp. 1015–1026, Jul. 2015, doi: 10.2522/ptj.20140137.

[23] K. T. Palmer, E. C. Harris, and D. Coggon, "Carpal tunnel syndrome and its relation to occupation: a systematic literature review," *Occup. Med.*, vol. 57, no. 1, pp. 57–66, Jan. 2007, doi: 10.1093/occmed/kql125.

[24] T. Nilsson, J. Wahlström, and L. Burström, "Hand-arm vibration and the risk of vascular and neurological diseases—A systematic review and meta-analysis," *PLOS ONE*, vol. 12, no. 7, p. e0180795, Jul. 2017, doi: 10.1371/journal.pone.0180795.

[25] Y. Usui, J. E. Zerwekh, H. Vanharanta, R. B. Ashman, and V. Mooney, "Different effects of mechanical vibration on bone ingrowth into porous hydroxyapatite and fracture healing in a rabbit model," *J. Orthop. Res.*, vol. 7, no. 4, pp. 559–567, Jul. 1989, doi: 10.1002/jor.1100070414.

[26] D. B. DC, "The Best Hand Massager for Carpal Tunnel, Arthritis, and Neuropathy," Recovatech. Accessed: Nov. 22, 2024. [Online]. Available: https://recovatech.com/best-hand-massager/

[27] M. James, "The 5 Best Heated Hand Massagers for Arthritis & Carpal Tunnel," InfraRed Light Therapy. Accessed: Nov. 22, 2024. [Online]. Available: https://www.infrared-light-therapy.com/heated-hand-massagers/

[28] J. R. Gravlee and D. J. V. Durme, “Braces and Splints for Musculoskeletal Conditions,” *Am. Fam. Physician*, vol. 75, no. 3, pp. 342–348, Feb. 2007.

[29] J. D. Carlson and C. A. Trombly, “The Effect of Wrist Immobilization on Performance of the Jebsen Hand Function Test,” *Am. J. Occup. Ther.*, vol. 37, no. 3, pp. 167–175, Mar. 1983, doi: 10.5014/ajot.37.3.167.

[30] M. M. Veehof, E. Taal, M. J. Willems, and M. A. F. J. van de Laar, “Determinants of the use of wrist working splints in rheumatoid arthritis,” *Arthritis Care Res.*, vol. 59, no. 4, pp. 531–536, 2008, doi: 10.1002/art.23531.

[31] C.-N. Hsu, Y.-S. Yang, J.-J. Hsu, Y.-C. Tsai, P.-H. Lin, and C.-L. Lee, “The Effect of Static Wrist Position on Median Nerve over Six Hours,” *Rehabil. Pract. Sci.*, vol. 42, no. 1, pp. 51–61, Dec. 2014, doi: 10.6315/2014.42(1)06.

[32] P. Loh and S. Muraki, “Effect of Wrist Deviation on Median Nerve Cross-Sectional Area at Proximal Carpal Tunnel Level,” *Iran. J. Public Health*, Nov. 2014, Accessed: Nov. 22, 2024. [Online]. Available: https://www.semanticscholar.org/paper/Effect-of-Wrist-Deviation-on-Median-Nerve-Area-at-Loh-Muraki/fa2e6bc955c072db650b0ec8fad4251f36674bcd

[33] T. L. Marquardt, J. N. Gabra, and Z.-M. Li, “Morphological and positional changes of the carpal arch and median nerve during wrist compression,” *Clin. Biomech. Bristol Avon*, vol. 30, no. 3, pp. 248–253, Mar. 2015, doi: 10.1016/j.clinbiomech.2015.01.007.

[34] J. M. Abzug, B. S. Schwartz, and A. J. Johnson, “Assessment of Splints Applied for

Pediatric Fractures in an Emergency Department/Urgent Care Environment," *J. Pediatr. Orthop.*, vol. 39, no. 2, p. 76, Feb. 2019, doi: 10.1097/BPO.0000000000000932.

[35] K. T. Conry, D. S. Weinberg, J. H. Wilber, and R. W. Liu, "Assessment of Splinting Quality: A Prospective Study Comparing Different Practitioners," *Iowa Orthop. J.*, vol. 41, no. 1, pp. 155–161, 2021.

[36] K. Valdes, N. Naughton, and S. Michlovitz, "Therapist supervised clinic-based therapy versus instruction in a home program following distal radius fracture: a systematic review," *J. Hand Ther. Off. J. Am. Soc. Hand Ther.*, vol. 27, no. 3, pp. 165–173; quiz 174, 2014, doi: 10.1016/j.jht.2013.12.010.

[37] M. P. Gaspar, J. Lou, P. M. Kane, S. M. Jacoby, A. L. Osterman, and R. W. Culp, "Complications Following Partial and Total Wrist Arthroplasty: A Single-Center Retrospective Review," *J. Hand Surg.*, vol. 41, no. 1, pp. 47-53.e4, Jan. 2016, doi: 10.1016/j.jhsa.2015.10.021.

[38] Z. Kirac Unal, E. Umay, and E. Unlu Akyuz, "Splinting in carpal tunnel syndrome—should we use it during the daytime?," *Egypt. Rheumatol. Rehabil.*, vol. 50, no. 1, p. 46, Sep. 2023, doi: 10.1186/s43166-023-00214-9.

[39] W. C. Walker, M. Metzler, D. X. Cifu, and Z. Swartz, "Neutral wrist splinting in carpal tunnel syndrome: A comparison of night-only versus full-time wear instructions," *Arch. Phys. Med. Rehabil.*, vol. 81, no. 4, pp. 424–429, Apr. 2000, doi: 10.1053/mr.2000.3856.

[40] Z. Jan, M. Abas, I. Khan, M. I. Qazi, and Q. M. U. Jan, "Design and analysis of wrist hand orthosis for carpal tunnel syndrome using additive manufacturing," *J. Eng. Res.*, Dec. 2023, doi: 10.1016/j.jer.2023.12.001.

[41] "Phalen's Test," Physiopedia. Accessed: Nov. 22, 2024. [Online]. Available: https://www.physio-pedia.com/Phalen%E2%80%99s_Test

[42] "Splints and Braces: Understanding the Difference." Accessed: Nov. 20, 2024. [Online]. Available: https://www.alimed.com/splints-and-braces-understanding-the-difference-blog/

[43] "Wrist Splint vs. Wrist Brace: Key Differences." Accessed: Nov. 20, 2024. [Online]. Available: https://www.hansaplastindia.com/articles/relief-and-care/wrist-splint-vs-wrist-brace-which-one-do-you-need

[44] "(PDF) Dynamometer Measurements of Hand-Grip Strength Predict Multiple Outcomes," *ResearchGate*, Oct. 2024, doi: 10.2466/PMS.93.5.323-328.

[45] L. Torborg, "Mayo Clinic Q and A: Myofascial release therapy for pain," Mayo Clinic News Network. Accessed: Nov. 19, 2024. [Online]. Available: https://newsnetwork.mayoclinic.org/discussion/mayo-clinic-q-and-a-myofascial-release-therapy-for-pain/

[46] D. E. Mouzakis, G. Rachiotis, S. Zaoutsos, A. Eleftheriou, and K. N. Malizos, "Finite element simulation of the mechanical impact of computer work on the carpal tunnel syndrome," *J. Biomech.*, vol. 47, no. 12, pp. 2989–2994, Sep. 2014, doi: 10.1016/j.jbiomech.2014.07.004.

[47] K. Yim Nam and K. Hong, “Effects of Pressurization on Finger’s Blood Velocity of Tendon and Muscle Areasin Forearm of 20’s male,” *Fash. Text. Res. J.*, vol. 21, no. 4, pp. 488–496, Aug. 2019, doi: 10.5805/SFTI.2019.21.4.488.

[48] D. Simovic and D. H. Weinberg, “Carpal Tunnel Syndrome,” *Arch. Neurol.*, vol. 57, no. 5, pp. 754–755, May 2000, doi: 10.1001/archneur.57.5.754.

[49] M. T. Boskovski and J. G. Thomson, “Acroparesthesia and Carpal Tunnel Syndrome: A Historical Perspective,” *J. Hand Surg.*, vol. 39, no. 9, pp. 1813-1821.e1, Sep. 2014, doi: 10.1016/j.jhsa.2014.05.024.

[50] C. G. Barnes and H. L. Currey, “Carpal tunnel syndrome in rheumatoid arthritis. A clinical and electrodiagnostic survey.,” *Ann. Rheum. Dis.*, vol. 26, no. 3, pp. 226–233, May 1967, doi: 10.1136/ard.26.3.226.

[51] J. K. WILSON and T. L. SEVIER, “A review of treatment for carpal tunnel syndrome,” *Disabil. Rehabil.*, vol. 25, no. 3, pp. 113–119, Jan. 2003, doi: 10.1080/0963828021000007978.

[52] H. Carlson, A. Colbert, J. Frydl, E. Arnall, M. Elliot, and N. Carlson, “Current options for nonsurgical management of carpal tunnel syndrome,” *Int. J. Clin. Rheumatol.*, vol. 5, no. 1, p. 129, Feb. 2010, doi: 10.2217/IJR.09.63.

[53] A. A. M. Gerritsen, M. C. T. F. M. de Krom, M. A. Struijs, R. J. P. M. Scholten, H. C. W. de Vet, and L. M. Bouter, “Conservative treatment options for carpal tunnel syndrome: a systematic review of randomised controlled trials,” *J. Neurol.*, vol. 249, no. 3, pp. 272–280, Mar. 2002, doi: 10.1007/s004150200004.

[54] N. L. Ashworth, J. D. P. Bland, K. M. Chapman, G. Tardif, L. Albarqouni, and A. Nagendran, "Local corticosteroid injection versus placebo for carpal tunnel syndrome - Ashworth, NL - 2023 | Cochrane Library", Accessed: Oct. 21, 2024. [Online]. Available: https://www.cochranelibrary.com/cdsr/doi/10.1002/14651858.CD015148/full

[55] B. M. Huisstede, M. S. Randsdorp, J. van den Brink, T. P. C. Franke, B. W. Koes, and P. Hoogvliet, "Effectiveness of Oral Pain Medication and Corticosteroid Injections for Carpal Tunnel Syndrome: A Systematic Review," *Arch. Phys. Med. Rehabil.*, vol. 99, no. 8, pp. 1609-1622.e10, Aug. 2018, doi: 10.1016/j.apmr.2018.03.003.

[56] P. Y. W. Chan, A. Santana, T. Alter, M. Shiffer, S. Kalahasti, and B. M. Katt, "Long-term Efficacy of Corticosteroid Injection for Carpal Tunnel Syndrome: A Systematic Review," *Hand N. Y. N*, p. 15589447231222320, Jan. 2024, doi: 10.1177/15589447231222320.

[57] E. E. Fess, "A History of splinting: To understand the present, view the past," *J. Hand Ther.*, vol. 15, no. 2, pp. 97–132, Apr. 2002, doi: 10.1053/hanthe.2002.v15.0150091.

[58] B. Golriz *et al.*, "Comparison of the efficacy of a neutral wrist splint and a wrist splint incorporating a lumbrical unit for the treatment of patients with carpal tunnel syndrome," *Prosthet. Orthot. Int.*, vol. 40, no. 5, pp. 617–623, Oct. 2016, doi: 10.1177/0309364615592695.

[59] M. S. Nadar, N. Alotaibi, and F. Manee, "Efficacy of splinting the wrist and metacarpophalangeal joints for the treatment of Carpal tunnel syndrome: an

assessor-blinded randomised controlled trial," *BMJ Open*, vol. 13, no. 11, p. e076961, Nov. 2023, doi: 10.1136/bmjopen-2023-076961.

[60] G. T. Bulut, N. S. Caglar, E. Aytekin, L. Ozgonenel, S. Tutun, and S. E. Demir, "Comparison of static wrist splint with static wrist and metacarpophalangeal splint in carpal tunnel syndrome," *J. Back Musculoskelet. Rehabil.*, vol. 28, no. 4, pp. 761–767, Jan. 2015, doi: 10.3233/BMR-140580.

[61] B. Farahmand, E. Pourhosaingholi, and A. Bagheri, "Investigating the effects of volar wrist cock-up splint and dorsal lock wrist hand orthosis in reducing signs of carpal tunnel syndrome," *Med. J. Islam. Repub. Iran*, vol. 35, p. 53, Apr. 2021, doi: 10.47176/mjiri.35.53.

[62] B. Povlsen, M. Bashir, and F. Wong, "Long-term result and patient reported outcome of wrist splint treatment for Carpal Tunnel Syndrome," *J. Plast. Surg. Hand Surg.*, vol. 48, no. 3, pp. 175–178, Jun. 2014, doi: 10.3109/2000656X.2013.837392.

[63] M. Hernández-Secorún *et al.*, "Effectiveness of Conservative Treatment According to Severity and Systemic Disease in Carpal Tunnel Syndrome: A Systematic Review," *Int. J. Environ. Res. Public. Health*, vol. 18, no. 5, Art. no. 5, Jan. 2021, doi: 10.3390/ijerph18052365.

[64] M. Zhou *et al.*, "The design and manufacturing of a Patient-Specific wrist splint for rehabilitation of rheumatoid arthritis," *Mater. Des.*, vol. 238, p. 112704, Feb. 2024, doi: 10.1016/j.matdes.2024.112704.

[65] A. Moraska, C. Chandler, A. Edmiston-Schaetzel, G. Franklin, E. L. Calenda, and B.

Enebo, “Comparison of a Targeted and General Massage Protocol on Strength, Function, and Symptoms Associated with Carpal Tunnel Syndrome: A Randomized Pilot Study,” *J. Altern. Complement. Med.*, vol. 14, no. 3, pp. 259–267, Apr. 2008, doi: 10.1089/acm.2007.0647.

[66] E. Madenci, O. Altindag, I. Koca, M. Yilmaz, and A. Gur, “Reliability and efficacy of the new massage technique on the treatment in the patients with carpal tunnel syndrome,” *Rheumatol. Int.*, vol. 32, no. 10, pp. 3171–3179, Oct. 2012, doi: 10.1007/s00296-011-2149-7.

[67] H. Syed, S. I. Ahmed, A. Arif, M. Zia, N. N. Shahbaz, and M. Kashif, “Effects of Soft Tissue Massage Along with Mobilization Technique on Intensity of Symptoms and Functional Status of Carpal Tunnel Syndrome: A Randomized Controlled Trial : Effects of Soft Tissue Massage,” *Pak. J. Health Sci.*, pp. 125–131, Nov. 2023, doi: 10.54393/pjhs.v4i11.1144.

[68] R. E. Hamoda *et al.*, “Effect of myofascial release on electrophysiological and clinical measures of pregnant women with carpal tunnel syndrome,” *Physiother. Q.*, vol. 27, no. 1, pp. 18–24, Mar. 2019, doi: 10.5114/pq.2019.83057.

[69] B. Sadu, U. Wicaksono, and D. Proyogo, “Providing Neurodynamic Mobilization Exercises is Better than Myofascial Release in Improving Complaints in Construction Workers with Carpal Tunnel Syndrome in Cahaya Dinar Housing,” *J. EduHealth*, vol. 13, no. 02, Art. no. 02, Nov. 2022.

[70] R. G. Graham, D. A. Hudson, M. Solomons, and M. Singer, “A Prospective Study to

Assess the Outcome of Steroid Injections and Wrist Splinting for the Treatment of Carpal Tunnel Syndrome," *Plast. Reconstr. Surg.*, vol. 113, no. 2, p. 550, Feb. 2004, doi: 10.1097/01.PRS.0000101055.76543.C7.

[71] W. C. Walker, M. Metzler, D. X. Cifu, and Z. Swartz, "Neutral wrist splinting in carpal tunnel syndrome: A comparison of night-only versus full-time wear instructions," *Arch. Phys. Med. Rehabil.*, vol. 81, no. 4, pp. 424–429, Apr. 2000, doi: 10.1053/mr.2000.3856.

[72] L. Šošić, V. Bojnec, D. Lonzarić, and B. Jesenšek Papež, "An advanced stage of carpal tunnel syndrome - is night-time splinting still effective?," *Int. J. Occup. Med. Environ. Health*, vol. 33, no. 6, pp. 771–780, Oct. 2020, doi: 10.13075/ijomeh.1896.01611.

[73] G. Halac *et al.*, "Splinting is effective for night-only symptomatic carpal tunnel syndrome patients," *J. Phys. Ther. Sci.*, vol. 27, no. 4, p. 993, Apr. 2015, doi: 10.1589/jpts.27.993.

[74] B. Hall, H. C. Lee, H. Fitzgerald, B. Byrne, A. Barton, and A. H. Lee, "Investigating the effectiveness of full-time wrist splinting and education in the treatment of carpal tunnel syndrome: a randomized controlled trial," *Am. J. Occup. Ther. Off. Publ. Am. Occup. Ther. Assoc.*, vol. 67, no. 4, pp. 448–459, 2013, doi: 10.5014/ajot.2013.006031.

[75] R. Weiss, "Student Section: Splinting for Carpal Tunnel Syndrome," *Can. J. Occup. Ther.*, vol. 44, no. 3, pp. 144–144, Sep. 1977, doi: 10.1177/000841747704400312.

[76] M. J. Page, N. Massy-Westropp, D. O'Connor, and V. Pitt, "Splinting for carpal tunnel

syndrome," *Cochrane Database Syst. Rev.*, vol. 2012, no. 7, p. CD010003, Jul. 2012, doi: 10.1002/14651858.CD010003.

[77] S. Nobuta, K. Sato, T. Nakagawa, M. Hatori, and E. Itoi, "Effects of Wrist Splinting for Carpal Tunnel Syndrome and Motor Nerve Conduction Measurements," *Ups. J. Med. Sci.*, Jan. 2008, doi: 10.3109/2000-1967-228.

[78] P. Storey, D. Armstrong, H. Dear, M. Bradley, and F. Burke, "Pilot randomised controlled trial comparing C-Trac splints with Beta Wrist Braces for the management of carpal tunnel syndrome," *Hand Ther.*, vol. 18, no. 2, pp. 35–41, Jun. 2013, doi: 10.1177/1758998313488476.

[79] F. S. Georgiew, J. Florek, S. Janowiec, and P. Florek, "The use of orthoses in the treatment of carpal tunnel syndrome. A review of the literature from the last 10 years," *Reumatologia*, vol. 60, no. 6, pp. 408–412, Dec. 2022, doi: 10.5114/reum.2022.123681.

[80] T. Wolny and P. Linek, "Long-term patient observation after conservative treatment of carpal tunnel syndrome: a summary of two randomised controlled trials," *PeerJ*, vol. 7, p. e8012, Nov. 2019, doi: 10.7717/peerj.8012.

[81] S. A. Zaheer and Z. Ahmed, "Neurodynamic Techniques in the Treatment of Mild-to-Moderate Carpal Tunnel Syndrome: A Systematic Review and Meta-Analysis," *J. Clin. Med.*, vol. 12, no. 15, Art. no. 15, Jan. 2023, doi: 10.3390/jcm12154888.

[82] M. T. Altinok, O. Baysal, H. M. Karakas, and A. K. Firat, "Sonographic Evaluation of the Carpal Tunnel After Provocative Exercises," *J. Ultrasound Med.*, vol. 23, no. 10,

pp. 1301–1306, Oct. 2004, doi: 10.7863/jum.2004.23.10.1301.

[83] I.-N. Lo, P.-C. Hsu, Y.-C. Huang, C.-K. Yeh, Y.-C. Yang, and J.-C. Wang, "Dynamic Ultrasound Assessment of Median Nerve Mobility Changes Following Corticosteroid Injection and Carpal Tunnel Release in Patients With Carpal Tunnel Syndrome," *Front. Neurol.*, vol. 12, Aug. 2021, doi: 10.3389/fneur.2021.710511.

[84] M. Zhu, W. Adams, and P. Polygerinos, "Carpal Tunnel Syndrome Soft Relief Device for Typing Applications," in *2017 Design of Medical Devices Conference*, Minneapolis, Minnesota, USA: American Society of Mechanical Engineers, Apr. 2017, p. V001T03A003. doi: 10.1115/DMD2017-3374.

[85] H. Porrata, A. Porrata, and J. Sosner, "New Carpal Ligament Traction Device for the Treatment of Carpal Tunnel Syndrome Unresponsive to Conservative Therapy," *J. Hand Ther.*, vol. 20, no. 1, pp. 20–28, Jan. 2007, doi: 10.1197/j.jht.2006.10.001.

[86] A. Alhialy, W. H. Alkhaled, T. G. Al-Sultan, Z. H. Al-Sawaff, and F. Kandimerli, "Design of an orthopedic smart splint using nickel-titanium shape memory alloy," *Indones. J. Electr. Eng. Comput. Sci.*, vol. 29, no. 3, Art. no. 3, Mar. 2023, doi: 10.11591/ijeecs.v29.i3.pp1300-1309.

[87] S. Rattanaphan and P. Srichandr, "Mechanical Model of Traditional Thai Massage for Integrated Healthcare," *J. Healthc. Eng.*, vol. 6, no. 2, p. 305201, 2015, doi: 10.1260/2040-2295.6.2.193.

[88] P. A. FEMANO and M. F. Zanakis, "Method and device to alleviate carpal tunnel syndrome and dysfunctions of other soft tissues," US20120253244A1, Oct. 04, 2012

Accessed: Sep. 06, 2024. [Online]. Available: https://patents.google.com/patent/US20120253244/en

[89] S. Liu *et al.*, "A Compact Soft Robotic Wrist Brace With Origami Actuators," *Front. Robot. AI*, vol. 8, Mar. 2021, doi: 10.3389/frobt.2021.614623.

[90] T. L. Marquardt, P. J. Evans, W. H. Seitz Jr., and Z.-M. Li, "Carpal arch and median nerve changes during radioulnar wrist compression in carpal tunnel syndrome patients," *J. Orthop. Res.*, vol. 34, no. 7, pp. 1234–1240, 2016, doi: 10.1002/jor.23126.

[91] Y. Yao *et al.*, "Changes of median nerve conduction, cross-sectional area and mobility by radioulnar wrist compression intervention in patients with carpal tunnel syndrome," *J. Orthop. Transl.*, vol. 18, pp. 13–19, Feb. 2019, doi: 10.1016/j.jot.2019.01.002.

[92] Z.-M. Li *et al.*, "A preliminary study of radioulnar wrist compression in improving patient-reported outcomes of carpal tunnel syndrome," *BMC Musculoskelet. Disord.*, vol. 23, no. 1, p. 971, Nov. 2022, doi: 10.1186/s12891-022-05943-0.

[93] A. Barsalou, E. Crooks, L. Phan, and B. St. George, "Design of a Rapid Fabrication Custom-Fit CROW Orthosis," Dec. 2022, Accessed: Sep. 16, 2024. [Online]. Available: http://hdl.handle.net/1993/37681

[94] W. Shin, D. Nam, U. Heo, J. Kim, and B. Ahn, "Wearability improvement of untethered pneumatic ankle foot orthosis", Accessed: Sep. 16, 2024. [Online]. Available:

https://www.authorea.com/doi/full/10.22541/au.165521441.14229223?commit=6d727f8636a9e193c7975bf5460c21fdfdd1bf90

[95] C. A. Myers, W. Allen, P. J. Laz, J. Lawler-Schwatz, and B. P. Conrad, "Motorized self-lacing technology reduces foot-shoe motion in basketball shoes during dynamic cutting tasks," *Footwear Sci.*, vol. 11, no. sup1, pp. S189–S191, Jun. 2019, doi: 10.1080/19424280.2019.1606326.

[96] J. Guo *et al.*, "Massage Alleviates Delayed Onset Muscle Soreness after Strenuous Exercise: A Systematic Review and Meta-Analysis," *Front. Physiol.*, vol. 8, p. 747, Sep. 2017, doi: 10.3389/fphys.2017.00747.

[97] P. Dębski, E. Białas, and R. Gnat, "The Parameters of Foam Rolling, Self-Myofascial Release Treatment: A Review of the Literature," *Biomed. Hum. Kinet.*, vol. 11, no. 1, pp. 36–46, Feb. 2019, doi: 10.2478/bhk-2019-0005.

[98] K. A. Spurgin *et al.*, "A Calibrated Method of Massage Therapy Decreases Systolic Blood Pressure Concomitant With Changes in Heart Rate Variability in Male Rats," *J. Manipulative Physiol. Ther.*, vol. 40, no. 2, pp. 77–88, Feb. 2017, doi: 10.1016/j.jmpt.2016.10.010.

[99] U. Chatchawan, N. Srimuang, and J. Yamauchi, "Determination of light pressing pressure for improving foot skin blood flow in type 2 diabetic patients," *J. Bodyw. Mov. Ther.*, vol. 33, pp. 14–19, Jan. 2023, doi: 10.1016/j.jbmt.2022.09.015.

[100] J. Goldberg, S. J. Sullivan, and D. E. Seaborne, "The Effect of Two Intensities of Massage on H-Reflex Amplitude," *Phys. Ther.*, vol. 72, no. 6, pp. 449–457, Jun. 1992,

doi: 10.1093/ptj/72.6.449.

[101] P. Chaves, D. Simões, M. Paço, F. Pinho, J. A. Duarte, and F. Ribeiro, "Pressure Applied during Deep Friction Massage: Characterization and Relationship with Time of Onset of Analgesia," *Appl. Sci.*, vol. 10, no. 8, p. 2705, Apr. 2020, doi: 10.3390/app10082705.

[102] P. J. Keir, J. M. Bach, M. Hudes, and D. M. Rempel, "Guidelines for Wrist Posture Based on Carpal Tunnel Pressure Thresholds," *Hum. Factors*, vol. 49, no. 1, pp. 88–99, Feb. 2007, doi: 10.1518/001872007779598127.

[103] L. Roberts, "Effects of Patterns of Pressure Application on Resting Electromyography During Massage," *Int. J. Ther. Massage Bodyw.*, vol. 4, no. 1, pp. 4–11, Mar. 2011.

[104] "Long-Term Use of a Static Hand-Wrist Orthosis in Chronic Stroke Patients: A Pilot Study - Andringa - 2013 - Stroke Research and Treatment - Wiley Online Library." Accessed: Nov. 07, 2024. [Online]. Available: https://onlinelibrary.wiley.com/doi/10.1155/2013/546093

[105] T. Nakamura, "Wrist Biomechanics," *J. Wrist Surg.*, vol. 6, no. 2, p. 87, May 2017, doi: 10.1055/s-0037-1602128.

[106] R. G. Volz, M. Lieb, and J. Benjamin, "Biomechanics of the Wrist:," *Clin. Orthop.*, vol. 149, no. NA;, p. 112???117, Jun. 1980, doi: 10.1097/00003086-198006000-00013.

[107] "Anatomy, Biomechanics, and Loads of the Wrist Joint." Accessed: Nov. 07, 2024.

[Online]. Available: https://www.mdpi.com/2075-1729/12/2/188

[108] "Phalen's Maneuver for Diagnosing Carpal Tunnel Syndrome," Healthline. Accessed: Nov. 24, 2024. [Online]. Available: https://www.healthline.com/health/phalens-maneuver

[109] J. Brüske, M. Bednarski, H. Grzelec, and A. Żyluk, "The usefulness of the Phalen test and the Hoffmann-Tinel sign in the diagnosis of carpal tunnel syndrome.," *Acta Orthop. Belg.*, Apr. 2002, Accessed: Nov. 24, 2024. [Online]. Available: https://www.semanticscholar.org/paper/The-usefulness-of-the-Phalen-test-and-the-sign-in-Br%C3%BCske-Bednarski/ffe04748097573e428afe26e24922d864ce893bf

[110] R. M. Szabo, R. R. Slater, T. B. Farver, D. B. Stanton, and W. K. Sharman, "The Value of Diagnostic Testing in Carpal Tunnel Syndrome," *J. Hand Surg.*, vol. 24, no. 4, pp. 704–714, Jan. 1999, doi: 10.1053/jhsu.1999.0704.

[111] T. Than, A. San, and T. Myint, "Biokinetic study of the wrist joint," *Int. J. Collab. Res. Intern. Med. Public Health*, May 2012, Accessed: Nov. 30, 2024. [Online]. Available: https://www.semanticscholar.org/paper/Biokinetic-study-of-the-wrist-joint-Than-San/2d6d8abd66a6704a3995a388fa70ae17d801a503

[112] T. S. Kim *et al.*, "A Study on the Measurement of Wrist Motion Range Using the iPhone 4 Gyroscope Application," *Ann. Plast. Surg.*, vol. 73, no. 2, p. 215, Aug. 2014, doi: 10.1097/SAP.0b013e31826eabfe.

[113] M. S. Hallbeck, "Flexion and extension forces generated by wrist-dedicated

muscles over the range of motion," *Appl. Ergon.*, vol. 25, no. 6, pp. 379–385, Dec. 1994, doi: 10.1016/0003-6870(94)90057-4.

[114] M. Cadogan, "Phalen sign," Life in the Fast Lane • LITFL. Accessed: Nov. 30, 2024. [Online]. Available: https://litfl.com/phalen-sign/

[115] M. R. Emad, S. H. Najafi, and M. H. Sepehrian, "The effect of provocative tests on electrodiagnosis criteria in clinical carpal tunnel syndrome," *J. Electromyogr. Kinesiol.*, vol. 19, no. 6, pp. 1061–1063, Dec. 2009, doi: 10.1016/j.jelekin.2008.11.015.

[116] A. Tetro, B. Evanoff, S. Hollstien, and R. Gelberman, "ASSESSMENT OF WRIST FLEXION AND NERVE COMPRESSION," 1998. Accessed: Nov. 30, 2024. [Online]. Available: https://www.semanticscholar.org/paper/ASSESSMENT-OF-WRIST-FLEXION-AND-NERVE-COMPRESSION-Tetro-Evanoff/04319633867a7a76b2d17e3387ed7b9ba83a52d1

[117] S. H. Kuschner, E. Ebramzadeh, D. Johnson, W. W. Brien, and R. Sherman, "TINEL'S SIGN AND PHALEN'S TEST IN CARPAL TUNNEL SYNDROME," *Orthopedics*, vol. 15, no. 11, pp. 1297–1302, Nov. 1992, doi: 10.3928/0147-7447-19921101-08.

[118] J. C. MacDermid, T. Turgeon, R. S. Richards, M. Beadle, and J. H. Roth, "Patient Rating of Wrist Pain and Disability: A Reliable and Valid Measurement Tool," *J. Orthop. Trauma*, vol. 12, no. 8, p. 577, Nov. 1998.

[119] P. Voche, T. Dubert, C. Laffargue, and A. Gosp-Server, "[Patient-rated wrist questionnaire: preliminary report on a proposed French version of a North American

questionnaire designed to assess wrist pain and function].," *Rev. Chir. Orthop. Reparatrice Appar. Mot.*, 2003, Accessed: Nov. 30, 2024. [Online]. Available: https://www.semanticscholar.org/paper/%5BPatient-rated-wrist-questionnaire%3A-preliminary-on-Voche-Dubert/e4a03ef73336a0fdc0423c0b78f2c7288c2b78bd

[120] O. Ozturk, "Validity and Reliability of the Turkish 'Patient-Rated Wrist Evaluation' Questionnaire," *ACTA Orthop. Traumatol. Turc.*, 2015, doi: 10.3944/AOTT.2015.14.0208.

[121] N. D. Weiss, L. Gordon, T. Bloom, Y. So, and D. M. Rempel, "Position of the wrist associated with the lowest carpal-tunnel pressure: implications for splint design.," *JBJS*, vol. 77, no. 11, p. 1695, Nov. 1995.

[122] D. Maya Limbu, B. H. Poudel, D. Thakur, and R. Maskey, "Peripheral Nerve Disorders P-PN001. Electromyography (EMG) of abductor pollicis brevis (ABP) muscles in diabetes mellitus type 2," *Clin. Neurophysiol.*, vol. 132, no. 8, p. e107, Aug. 2021, doi: 10.1016/j.clinph.2021.02.255.

[123] C. A. De Meulenmeester, P. R. Bourque, and R. C. Grondin, "The abductor pollicis brevis R1 response: normative data and physiological behavior," *Electromyogr. Clin. Neurophysiol.*, vol. 38, no. 4, pp. 253–256, Jun. 1998.

[124] C. M. Stinear and W. D. Byblow, "Role of Intracortical Inhibition in Selective Hand Muscle Activation," *J. Neurophysiol.*, vol. 89, no. 4, pp. 2014–2020, Apr. 2003, doi: 10.1152/jn.00925.2002.

[125] E. van Oudenaarde and R. A. Oostendorp, “Functional relationship between the abductor pollicis longus and abductor pollicis brevis muscles: an EMG analysis,” *J. Anat.*, vol. 186, no. Pt 3, p. 509, Jun. 1995.

[126] K. Dawson-Amoah and M. Varacallo, “Anatomy, Shoulder and Upper Limb, Hand Intrinsic Muscles,” in *StatPearls*, Treasure Island (FL): StatPearls Publishing, 2024. Accessed: Oct. 09, 2024. [Online]. Available: http://www.ncbi.nlm.nih.gov/books/NBK539810/

[127] N. Deak, A. C. Black, and B. Bordoni, “Anatomy, Shoulder and Upper Limb, Wrist Flexor Retinaculum,” in *StatPearls [Internet]*, StatPearls Publishing, 2023. Accessed: Oct. 09, 2024. [Online]. Available: https://www.ncbi.nlm.nih.gov/books/NBK545198/

[128] M. P. McHugh, K. F. Orishimo, I. J. Kremenic, J. Adelman, and S. J. Nicholas, “Electromyographic Evidence of Excessive Achilles Tendon Elongation During Isometric Contractions After Achilles Tendon Repair,” *Orthop. J. Sports Med.*, vol. 7, no. 11, p. 2325967119883357, Nov. 2019, doi: 10.1177/2325967119883357.

[129] R. Martinek *et al.*, “Advanced Bioelectrical Signal Processing Methods: Past, Present, and Future Approach—Part III: Other Biosignals,” *Sensors*, vol. 21, no. 18, Art. no. 18, Jan. 2021, doi: 10.3390/s21186064.

[130] F. Di Nardo, T. Basili, S. Meletani, and D. Scaradozzi, “Wavelet-Based Assessment of the Muscle-Activation Frequency Range by EMG Analysis,” *IEEE Access*, vol. 10, pp. 9793–9805, 2022, doi: 10.1109/ACCESS.2022.3141162.

[131] B. Chen *et al.*, "A Real-Time EMG-Based Fixed-Bandwidth Frequency-Domain Embedded System for Robotic Hand," *Front. Neurorobotics*, vol. 16, Jun. 2022, doi: 10.3389/fnbot.2022.880073.

[132] Y. P. Shah, "Applications of Fourier Series and Fourier Transformation," *Cognition*, vol. 2, no. 1, Art. no. 1, Oct. 2019, doi: 10.3126/cognition.v2i1.55605.

[133] H. Guan, H. Song, Y. Yang, and J. Zhang, "The Fourier Transform and its application in solving the equation," *J. Phys. Conf. Ser.*, vol. 2012, no. 1, p. 012056, Sep. 2021, doi: 10.1088/1742-6596/2012/1/012056.

[134] G. Zhou and Q. Zhao, "A short proof on the Plancherel formula," *J. Phys. Conf. Ser.*, vol. 2012, no. 1, p. 012080, Sep. 2021, doi: 10.1088/1742-6596/2012/1/012080.

[135] T. O. Salim, A. A. K. Abu Hany, and M. S. El-Khatib, "On Katugampola Fourier Transform," *J. Math.*, vol. 2019, pp. 1–6, Oct. 2019, doi: 10.1155/2019/5942139.

[136] "Notch filter of 50/60 Hz." Accessed: Nov. 09, 2024. [Online]. Available: https://elemyo.com/support/start_info/bandstop

[137] T. Field *et al.*, "Carpal tunnel syndrome symptoms are lessened following massage therapy," *J. Bodyw. Mov. Ther.*, vol. 8, no. 1, pp. 9–14, Jan. 2004, doi: 10.1016/S1360-8592(03)00064-0.

[138] N. B. Rosario and O. De Jesus, "Electrodiagnostic Evaluation of Carpal Tunnel Syndrome," in *StatPearls*, Treasure Island (FL): StatPearls Publishing, 2025. Accessed: Apr. 26, 2025. [Online]. Available: http://www.ncbi.nlm.nih.gov/books/NBK562235/

APPENDIX A

INTERVIEW TRANSCRIPT WITH MS. FRENCIE QUINTIN Z. PUROL, PTRP, THROUGH ZOOM

Chezter: first concern ko po is how can we detect any signs of CTS? using emg kasi mostly nakikita ko is nerve conduction studies. pero we hoping to use only emg lang sana. tapos yung pinagkaiba po ng muscle weakness and muscle fatigue. kasi if we will record yung CTS using emg baka pwede namin sya kunin yung amplitude ng muscle fatigue if that is possible. and then once namin ma detect yun sya yung signs of CTS, mag ask po kame what type of massages pwede?

Ms. Frencie: basically yung cts kasi is kung nerve conduction test gagawin natin, emg i think considered na ata sya as nerve conduction test eh kasi tinitignan yan gaano kabilis yung firing ng nerve once like activated yung muscle. if hindi kayo gagamit ng nerve conduction test what we usually do sa clinic and i think doctors often use this as well may mga special test kame ginagawa which is non invasive there is certain period lang na iprovoke lang tapos pag mag show symptoms like tingling, numbness, weakness dun sa area ng innervation ng median nerve, positive na sya for CTS.

Chezter: pwede din ba sya wala na yung provovation?

Ms. Frencie: if wala yung provocation mahirap sya eh. usually if hindi naman sya iproprovoke then wala naman signs ng symptoms lalabas, walang tingling walang numbness, makikita mo lang may swelling, pero hindi naman lahat ng swelling nasa wrist cts agad.

Chezter: ok po maam

Ms. Frencie: ganun sya, i dont know if ganun parin ngayon yung mga nerve conduction test mag emg parin ganon i think kaya for severe cases or may other associated condition yun kailangan. pero kapag early stages pa naman mild to moderate symptoms more on special tests lang ginagawa.

Chezter: so if mag gamit kame ng emg maam ano po yung mareerecord namin dun

Ms. Frencie: makikita nyo yun kung gaano kabilis eh, as far as i can remember if its less than 3.0mg yung bilis ng nerve conduction, positive na yun for cts. pero dipende yan i don't know if different ba yan per device or may bagong studies na or nag update na about sa bilis ng firing ng nerve.

and iaadd kolang rin i think more on andyan na yung nerve conduction tests may atrophy na ng muscle may prominent na ng muscle wasting mga ganon. i think dun pa nag coconduct ng nerve conduction tests pero yun nga yung sa sinabi ko is mild to moderate cases pa man more on on special tests lang sya. like median nerve compression test, palance, reverse palance mga ganon.

Chezter: so yung next po is muscle fatigue and muscle weakness

Ms. Frencie: ang muscle weakness kasi if masasabi mo muscle weakness lang there's what we call manual muscle testing to test ano yung strength ng muscle like example, you have your wrist flexors in cases with cts so mag aaply ka ng resistance, you will not let the patient move before exercises before doing anything. so even if you are not doing anything if makita mo hindi complete ang rom nya kung nakikita mo hirap sya nanginginig sya yun could be muscle weakness lang yun, however ang muscle fatigue kasi if muscle fatigue, one, it could be na galing na syang exercise pagod na yung muscle na exert na yung effort yun it could be muscle fatigue or kaya may prior activities or different exercises or even we just hold something for prolonged periods of time tapos pag Nakita mong panginginig could be muscle fatigue lang yun. or meron talaga something happening sa central nervous system. like may spasticity increase yung muscle tone tapos pag pinagalaw mo Kahit short periods of time nakikita mo may fatigue agad. pag muscle weakness Kahit wala ginagawa, hirap gumawa ang patient ng movement, rule out mo yung central nervous system affectation, muscle weakness lang sya. it could happen then for cts na severe cases na masakit ng yung muscle. yun muscle weakness yun sya.

Chezter: so if lets say may diagnose na yung patient with cts, pwede ba namin makuha yung level of muscle weakness sa apb

Ms. Frencie: hindi mo makukuha ang muscle weakness but you can get the level of muscle strength.

Chezter: pwede yan sya using emg parin maam?

Ms. Frencie: using emg, ang emg parang may certain amount of stimulus yan ilalagay, and dun mag rerespond ang muscle diba. if muscle strength i dont think so. more on integrity parin ng nerve ang itetest nyan eh kasi ang nerve ang ististimulate nya eh hindi yung muscle mismo. so istimulate ang nerve kung may contraction then induct ang nerve.

Chezter: yung muscle fatigue, common din ba sya sa cts patients? in general lang yan sya

Ms. Frencie: pag cts kasi more on peripheral muscle condition, peripheral nerve disease. ang muscle fatigue commonly makikita mo pag central application. pwede mo masabi na easily fatigue yung muscle once pinagalaw mo pero and root cause nya parin is muscle weakness.

Chezter: kasi yung sa paper po namin we wanted to ano sana deliver a automated massage sa wrist ng patient kapag may na detect nna yung emg namin but we dont know what will the emg detect.

Ms. Frencie: basically ang emg mag dedetect sya ng integrity ng median nerve mo, sa case ng cts

Chezter: so saan sya banda place maam sa median nerve mismo sa taas?

Ms. Frencie: ano to sya eh conducted by doctors to sya pero directly above the muscle tapos may monitor yan tapos mag seset ng stimulus kung nag contruct yung muscle then induct yung median nerve mo, yung inervation sa certain muscle for example, if your going to use you apb, directly above sya sa thinner muscles mo

Chezter: so focusing dun sa moderate cases, pwede po yun massage dun? massage techniques

Ms. Frencie: MFR or myofascial release, pwede sya. tapos mag fofocus ka sa flexor retinaculum and then pwede ka mag apply ng deep friction or what we call active release. pag active release, mag lalagay ka ng direct pressure sa base ng apb, then you'll actively let the patient abduct the thumb. it will release on its own. so with your case if your planning ng ganon, mag apply ka ng direct pressure yung tolerable lang sa patient and then let the patient do abduction.

Chezter: paano po yung abduction?

Ms. Frencie: abduction ng thumb, moving away from the first palance

Chezter: pero massage apply namin sa flexor retinaculum?

Ms. Frencie: yes sa flexor retinaculum but not directly above sa median nerve. and median nerve mo medyo nasa gitna sya ng ano eh second palance yung middle finger mo and your pointing finger andun yun banda ang median nerve eh, if mag aaply ka ng pressure dun then you'll be visiting more symptoms. pero move ka a little away dito ka banda sa frist palance sa base nyan dun ka mag aaply ng pressure and let the patient do abduction, induction ng thumb then mag release yan on its own. as long as while doing the movement andun yung pressure.

Chezter: so yung pressure is depende po sa patient?

Ms. Frencie: hinde, hindi sya depende sa patient, yung amount of pressure yes pero kung saan mo ilalagay ang pressure based sya ng thumb and ng first palance.

Chezter: tapos yung plan namin is to deliver the massage mechanically. mag gawa kame ng device for massaging. pwede ba namin ma mimic yung myofascial release.

Ms. Frencie: there are different kinds of myofascial release, yung usually ginagamit dyan is yung deep friction massage. yun na yun yung circles along the fibers ng fasha, or yung sinabi ko kanina yung active release. if yung deep friction massage yung goal nyo, along your flexor retinaculum. hindi naman yun one place lang ang application ng massage

Chezter: tapos how about yung duration ng massage?

Ms. Frencie: limit ka lang to 2-3 mins, usually dyan yung pinaka beneficial yung massage na iaaply.

Chezter: so yung emg sensor maam, kasi siguro gagamitin nalng namin sya to take a signal kapag at rest na siguro yung patient at rest yung muscle nya. san namin pwede iplace yung electrodes?

Ms. Frencie: (shows pic) bale sa may thinner muscle ito sya, kasi usually naman kapag cts yung thinner muscles mo naman yun unang...

(skip demonstration)

Chezter: yung pressure ng massage namin, ma measure po namin yan sya?

Ms. Frencie: yan ang hinde, hinde nyo sya ma memeasure but siguro you can add that to your device like may certain amout like level 1, level 2, level 3. ganun na yun magagawa nyo para hindi na man too painful para sa patient. kasi tight yun fascia nyan eh masakit yan. so theres a certain amount subjective kasi rin ang pain tolerance nyan so nasa sainyo na yan pwede niyo ma adjust ang pressure

Ms. Mudznalyn: yung sa massage ilang mins dapat yung interval ng first massage sa second massage

Ms. Frencie: usually ang ginagwa namen ano sya like per session naman namin nakikita yung patient what we usually recommend is if at home sya hindi naman sya pwede as often as possible kasi mag sosore ang muscles pati ang area. what i usually recommend is isa sa umaga, isa sa gabi or kaya if may nafefeel na nag tighten olet, stretch then apply massage. same talga for everyone. as long it would last 2-3 mins. or what others would do Kahit hindi umabot ng 2-3 mins kasi example very painful for some if makita na medyo umminit yung area may color changes na, may release na yan nangyayare

APPENDIX B

2ND INTERVIEW TRANSCRIPT WITH MS. FRENCIE QUINTIN Z. PUROL, PTRP, THROUGH ZOOM

Vin: so yung first question po naming maam is how can we justify the need for splints to be worn during the day or for extended periods of time?

Ms Frencie: teka tatanungin muna kita ano yung purpose ng splint para sainyo

Vin: for us maam its to support naman din po yung activites since target audience naming is yung mga gumagamit ng keyboard, I guess its to help them with their activites ganun maam

Ms Frencie: one purpose naman din ng splint is to limit mobility kasi there are motions that would aggravate, magkakaroon ng tension then magkakaroon ng tension towards your median nerve, example flexion ng wrist, extension ng wrist, so its also to provide feedback, tacktile feedback sa patient. kasi kapag may splint ka limited yung motion, although may motion pero limited motion, hindi sya like extreme range of motion, so pwedeng its to remind the patient na hangang dito lang yung pwde kasi, it could cause na ma aggravate yung CTS ng patient. also it would position the hand in an optimal position na theres still motion without aggravating the symptoms.

Vin: nagka problem din po kame maam na point out ng panelist namin kasi diba ang wrist splint is to suppose to restrict ng movement, pero yung goal po sana namin maam is to provide a dynamic support system to give them more movement maam, so nagkamali po kame on that part maam or is there a way to counteract that arguement maam.

Ms Frencie: yun like what I've said, the main purpose ng splint is immobilization to restrict movement kasi diba ive explained kanina, hindi mo ma fleflex ng Mabuti, yung wrist mo hindi mo ma extend ng todo. if you say dynamic support, anong inclusion dun sa naiisip nyo, what kind of support are you giVing?

Vin: yung idea kasi namin maam since may mga na research kame na uncomfy daw yung wrist splint kasi mag cause daw sya ng skin irritation then inisip namin if uncomfy sa patient yung wrist splint mag loosen sya konti to the point na may konting breathability lang, and then if okay na sya mag tighten na sya ulit. kumbaga parang auto adjusting strap.

Ms Frencie: for me if ganyan yung support na sinasabi nyo, kasi yung splint ginagamit for cts is maintained na neutral yung wrist eh, at 0 degrees RON, kasi dun pinaka relaxed lahat ng tendons passing through the (inaudible) spaces sa wrist. especially those sa area kung saan dadaan yung median nerve. if your saying dynamic support, tapos yung patient nyo yung working sa computer doing a desk job, I dont think na tama yung term na dynamic support. kasi restriction talaga sya eh ng movement para neutral lang talga yung wrist. ano

pang better term, I think you can like switch it to like tactile feedback or like proprioceptive feedback. familiar ka about that?

Vin: not po maam

Ms Frencie: when you say proprioception kase its the joint awareness ano yung position ng wrist nyo. I think mas fit sya in using wrist splint, explain ko muna yung proprioception, its like joint awareness eh so even if your not looking at your wrist lets say for example, even if not looking at your wrist alam mo na, neutral ba sya or naka bend ba sya, or ano bang position nya. your body is aware of it. so providing proprioceptive feedback magiging aware eventually yung mga patients Ninyo na eto yung neutral positioning ng wrist and they would be aware of it. ng tactile feedback or proprioceptive feedback. kasi kapag dynamic support, hindi naman sya mag lilift, wala naman sya other activites, purely desk work lang yung focus nyo. so I think mas okay na yung ganun.

Vin: thank you po maam, so yung next question namin is what can an emg offer better than a dynamometer. yung inexplain kasi ni sir since yung system namin mag detect sya if at rest yung patient mag stastart na yung massage namin and then inargue nya na if miotion yung hinahanap namin why not dynamometer nalng. so yung hinahanap namin is whats better sa emg or sa dynamometer.

Ms Frencie: I would agree on that kasi yung sa first na kinausap nyo ako emg is really for strength eh. if you want to measure the strength then you'll have something to measure the strength more than the manual muscle test. if deep friction massage kase it would provide ng relief ng symptoms kame mag rerelease ang flexor retinaculum pero relief lang ng symptoms, symptoms yung tingling, ung numbness, yung pins and needles, dun lang sya nagkakaroon ng relief. but if your aming na bumalik yung strength to normal, its a little gray area dun eh, kasi for example do you work out ba?

Vin: not frequent maam but time to time maam

Ms Frencie: if magiging basis mo lang is like for example ano ba sport mo?

Vin: basketball maam

ms. frencie: example if you are shooting on your own hinde mo mameasure yung capacity mo if you are not playing with other people same lang din dito na if you want to have results sa ganito increase ng strength, you won't develop that strength it you don't exercise it. since EMG gamit Ninyo so mas maganda pag dynamometer, kasi hindi rin enough kapag friction

massage tapos you would test the strength, present yung tingling medyo subjective yun eh. magiging subjective kayo dun. parang hindi sya ganun ka strong. if wala kayong dynamometer, if mahirapan kayo sa dynamometer what we usually do yung bp calf, bp inflate mo sya ng 20mmhg and then let the patient grip sa bp calf then tignan nyo kung saan papunta yung arrow sa valve. you repeat it 3 times. you can still get the strength sa ganung test. pero yes I would agree with sa panel nyo. if grip strength yung hanap nyo. then better use something mag grip din sya.

Vin: yung next question po namin maam is how can we assess the accuracy of our device

Ms Frencie: accuracy ng device. isang test lang ba kailangan nyo? or pwde syang multiple

Vin: dipende po samin maam pero I think pwde na man multiple

Ms Frencie: if subjective, you can check for pain scale, ang usual dyan is from 0-10, what are you feeling right now, 10 being the most painful 0 being walang pain, let them describe tapos let them rate it. you can do both subjective and objective. you can also ask them if radiating ba, are you feeling better may relief ba. yan usually pag subjective. pag ojective naman, yun grip strength trought dynamometer. you can try pinch grip. may dynamometer na designed for pinch.

Vin: so next question namin maam is how can we measure the pressure sa massage as is there a standard for it?

Ms Frencie: wala, magiging subjective kayo nyan, kase iba iba yung pain tolerance yan, if your going to base it sa isa it could be different sa iba.

Vin: so yung last question maam is how can we measure comfort.

Ms Frencie: subjective parin talga sya, you can verbally ask the patient. since doing deskjob ang magiging subject nyo. I think you can ask with their daily activities. others would have problem holding a glass, others would have problem with anything involVing a grip. you can ask them, may changes ba sa daily activities. pwde din ano feedback na din yun sainyo kung okay na sainyo. yun na din nagiging reason bat sila napupunta sa mga doctor. so you can add that, Kahit hindi nyo na include sa research nyo alam noy sa sarili alam nyo na may relief na ganito may comfort na.

Vin: thank you po maam yun lang po question namin so far.

Ms Frencie: ikaw mudz may question ka?

Ms Mudsnalyn: yung dun lang sya pressure plan kasi nila is 1 pressure lang kasi medyo mahirap gawin given the time frame. if ever nga mag stick sila sa 1 pressure meron kang ma recommend na specific pressure for a specific age group for example like 25-30 may specified pressure ka for that age group?

Ms Frencie: hindi naman to speficied if lalake or babae to diba?

Ms Mudsnalyn: we can specify further din if that helps pag determine ng pressure?

Ms Frencie: I would suggest na kasi common kasi sya sa mga babae so go for female, after pregnancy or during pregnancy kayo na bahala dun if include nyo yan or emit. so if ganun I think go for peak light lang, like its the lightest. paano nyo ba imemeasure?

Ms Mudsnalyn: yun nga eh paano ba usually minemeasure ang pressure na inaapply nyo?

Ms Frencie: kasi manual lang talga kame through thumb

Ms Mudsnalyn: kase pag for example moderate pressure may specific value like walang ganun?

Ms Frencie: wala, wala talga kasi the strength would differ from one pt to another. I dont know if tama ba or if phg or masyadong magibat din if kilo or if pounds eh.

Ms Mudsnalyn: anong ma suggest mong way na pwdeng grounds na anong pressure for 1 person pwde na for lahat

Ms Frencie: I suggest sinong may pinaka mababang pain tolerance dun mo itry, then hanapin mo kung saan nya ma tolerate, even without any condition. and then form there kasi Kahit hangang even with lightest pressure mag kakaroon na yan ng changes. maging tolerable sya.

Ms Mudsnalyn: so ganung nalng mag base nalng sa isang tao talga go for the lightest, tapos specify to females I dont think possible yung sa pregnant women

Ms Mudsnalyn: yung purpose ng wrist splint is to imobalize talga? may nabasa kasi din akong wrist brace tapos yun daw yung semi lang tama ba? kase yung goal nila si not immobilization kame nga moderate pa lang nga naman. kase hindi pa naman complete immobilization. nagging target kase nila is kaya parin ng dynamic movement magamit parin sya during the day. hindi ata dynamic movement ang term magiging, limit lang yung motion like may movement parin pero to do like soguro yung like bare minimum lang.

Ms Frencie: like motion restriction like ganun?

Ms Mudsnalyn: parang hindi lang complete immobilization. kapag wrist splint ba ganun? like full complete immobilization ba ang goal?

Ms Frencie: oo kasi some splint yan may bakal sa may interior area ng wrist, so hindi nya talga magagalaw ng Mabuti. mag stay in neutral position lang talga yan.

Ms Mudsnalyn: kapag may cts naman na moderate need ba talga immobilize ang kamay talaga?

Ms Frencie: if gagamitin sya during work then it should allow some movement. pero splints kasi ginagamit for cts kasi is for sleeping eh. immobilizer talga. think mas ok yung term na restrict motion or limitation ng motion kesa sa dynamic, like you could still allow motion pero kailangan nyo talga ilimit

Ms Mudsnalyn: pero ok lang gagamitin nya may cts sya pero gagamitin nya ang kamay in the morning para may support lang?

Ms Frencie: I think pwde naman kase yun din yung nagging complaint ng mga patiente gumagamit sila ng splint like ugh ayaw ko muna gumamit ng splint kasi hindi sila makagalaw. if im correct 10 degrees flexion and 30 degrees extension ang allowed

Ms Mudsnalyn: bale within this range pwde nya magalaw. so yun nalng yung goal nila is to restrict movement within that allowable range.

APPENDIX C
SOFTWARE REQUIREMENTS

The provided code controls an autonomous wrist splint with integrated massage, managing signal acquisition, filtering, motor control, massage activation, and safety monitoring. It continuously reads sensor inputs, processes the signals to determine the user's muscle state, dynamically adjusts the splint's tension, activates the massage system when appropriate, and triggers alarms to ensure safe operation during therapy.

The process begins with continuous reading of the EMG signal from pin 36 using analogRead(36), which is then filtered through two band-pass biquad filters and a notch filter to isolate the relevant muscle activity frequencies and remove power line interference. The filtering is implemented with the process() function, which applies the standard second-order IIR biquad algorithm using internal state variables z1 and z2 to maintain memory of previous inputs and outputs. The output is converted to an absolute value for decision-making:

```
// --- filter structure + function ---
struct Biquad {
  float b0, b1, b2, a1, a2;
  float z1, z2;
};

inline float process(Biquad &f, float x) {
  float y = f.b0 * x + f.z1;
  f.z1 = f.b1 * x - f.a1 * y + f.z2;
  f.z2 = f.b2 * x - f.a2 * y;
  return y;
}

// --- Bandpass biquad coefficients (Fs = 600 Hz) ---
inline Biquad bp1 = { 0.3913, 0.7827, 0.3913, 0.5768, 0.2619,  0, 0 };
inline Biquad bp2 = { 1.0000, -2.0000, 1.0000, -1.7050, 0.7477,  0, 0 };

// --- Notch biquad coefficients (Fs = 600 Hz) ---
inline Biquad notch = { 0.9896, -1.7142, 0.9896, -1.7142, 0.9793,  0, 0 };
```

The filtered EMG is further smoothed with an exponentially moving average to reduce short-term fluctuations and provide a stable input for controlling both the splint and massage system:

```
  // --- Moving Averages ---
  EMAEMG = 0.05 * filteredEMG+ (1 - 0.05) * EMAEMG;
```

Simultaneously, the pressure sensor on pin 34 is read, calibrated, and converted to kilopascals. The reading is passed through a moving average function to smooth transient spikes and ensure reliable values for safe motor operation:

```
  float pressure_kPa = addToMovingAverage(pressureMovingAvg,
filteredPressure);

// --- Moving Average ---
const int AVG_SAMPLES = 300;
inline int avgIndex = 0;

inline float addToMovingAverage(float avgArray[], float newValue) {
  avgArray[avgIndex] = newValue;
  avgIndex = (avgIndex + 1) % AVG_SAMPLES;

  float sum = 0;
  for (int i = 0; i < AVG_SAMPLES; i++) {
    sum += avgArray[i];
  }

  return sum / AVG_SAMPLES;
}
```

The splint control logic, implemented in manageSplint(), evaluates the EMG and pressure readings to determine whether to tighten, loosen, or hold the splint. Tightening occurs when the muscle is at rest and pressure is below the upper limit, loosening occurs if muscle activity exceeds the dynamic threshold or during an alarm override, and holding occurs if pressure exceeds a safety threshold. State transitions are debounced to prevent rapid oscillations, and motor movement is handled non-blocking using the AccelStepper library:

```
    if (proposedState == LOOSENING) {
      myStepper.moveTo(-1);
      splintStatus = "Splint Loosening";
    } else if (proposedState == TIGHTENING) {
      myStepper.moveTo(2750);
      splintStatus = "Splint Tightening";
    }
```

The massage system, managed by manageMassager(), first performs calibration

to determine a baseline EMG and sets the dynamic threshold:

```
if (calibrating) {
  calibSum += emgValue;
  calibCount++;
  if (currentMillis - calibStart >= 10000) {
    float baseline = calibSum / calibCount;
    dynamicThreshold = max(baseline * 2.0, 0.005);
    calibrating = false;
    startTime = currentMillis;
    isRunning = true;
    lastMassageTime = currentMillis;

    splintStatus = "calibration complete";
    Serial.print("Calibration complete. Baseline = ");
    Serial.print(baseline, 4);
    Serial.print(" µV, Threshold = ");
    Serial.println(dynamicThreshold, 4);
    Serial.println("Massager activated");
  }
}
```

Once calibrated, the massager activates for a set duration using PWM control:

```
// --- Massage control ---
if (isRunning) {
  if (currentMillis - startTime >= MASSAGE_DURATION) {
    isRunning = false;
    lastMassageTime = currentMillis;
    analogWrite(MOTOR_PIN, 0);
    splintStatus = "Massage Ended";
  } else {
    analogWrite(MOTOR_PIN, 150);
    splintStatus = "Massage Active";
  }
} else {
  analogWrite(MOTOR_PIN, 0);
}
```

During massage, EMG readings are monitored. If the muscle activity exceeds the threshold for more than a debounce period, the alarm is triggered, and the massage

stops:

```
  // --- Alarm interupt ---
  if (isRunning) {
    if (emgValue > dynamicThreshold) {
      if (aboveThresholdStart == 0) {
        aboveThresholdStart = currentMillis;
      } else if (currentMillis - aboveThresholdStart >= 2750) { // 3s
debounce
        isAlarming = true;
        isRunning = false;
        alarmStartTime = currentMillis;
        aboveThresholdStart = 0;
        analogWrite(MOTOR_PIN, 0);
        alarmFromMassage = true;
        splintStatus = "Alarm triggered during massage";

      }
    } else {
      aboveThresholdStart = 0;
    }
  }
```

The alarm system, managed by manageAlarm(), uses non-blocking timers to toggle the LED while forcing the splint to loosen for safety. Post-alarm, the system waits for rest confirmation, may perform calibration, or resumes normal tightening to maintain therapeutic operation:

Additionally, a web server provides real-time monitoring by sending JSON with EMG, pressure, dynamic threshold, and splint status to a front-end interface updated every 200 milliseconds:

```
// --- Web server ---
server.on("/", [](){ server.send(200,"text/html", htmlPage()); });
server.on("/data", [](){
String json = "{";
json += "\"filtered\":" + String(filteredEMG, 4) + ",";
json += "\"avg\":" + String(emgreading, 4) + ",";
json += "\"threshold\":" + String(dynamicThreshold, 4) + ",";
json += "\"fsr\":" + String(fsrreading, 4);
json += ",\"status\":\"" + splintStatus + "\"";
json += "}";
server.send(200,"application/json",json);
});
```

The system operates as a continuous loop: EMG and pressure signals are acquired, filtered, and smoothed, fed into control logic that adjusts the splint, manages massage therapy, and triggers alarms if unsafe conditions are detected, while the web interface provides live feedback. This integration ensures both operational safety and effective therapy delivery.

APPENDIX D
HARDWARE REQUIREMENTS

The assembly of the therapeutic wrist splint device involved careful integration of electronic, mechanical, and ergonomic components to achieve optimal functionality, and reliability.

The heart of the device is the ESP32 38-pin microcontroller, mounted securely onto a universal PCB for ease of wiring and efficient circuit management. This microcontroller was strategically positioned to facilitate connections with peripheral sensors and actuators while providing easy access for maintenance and troubleshooting.

The wrist splint serves as the primary wearable platform of the therapeutic system, designed for direct use by patients. It provides structural support and immobilization of the wrist joint, promoting proper hand positioning and alleviating strain associated with Carpal Tunnel Syndrome (CTS). Essential electronic and mechanical components—including the EMG MyoWare sensor, massage motor assembly, pressure sensor, and strap adjustment mechanism—are securely integrated onto the splint. Components were thoughtfully arranged to maintain a balance between functionality and

wearer comfort, minimizing obstruction to normal hand movements while ensuring optimal therapeutic performance. The strategic placement and secure attachment of these components allow seamless and comfortable long-term use by patients.

To effectively detect muscle activity indicative of Carpal Tunnel Syndrome (CTS), an EMG MyoWare sensor was utilized. The sensor was strategically placed over the Abductor Pollicis Brevis muscle, an optimal site known for its diagnostic relevance in CTS. For improved user convenience and ease of application, the sensor was designed to be detachable, simplifying the process of donning and removing the wrist splint. This design ensured secure, consistent skin contact, significantly enhancing the accuracy and reliability of muscle-state detection necessary for timely activation of therapeutic mechanisms.

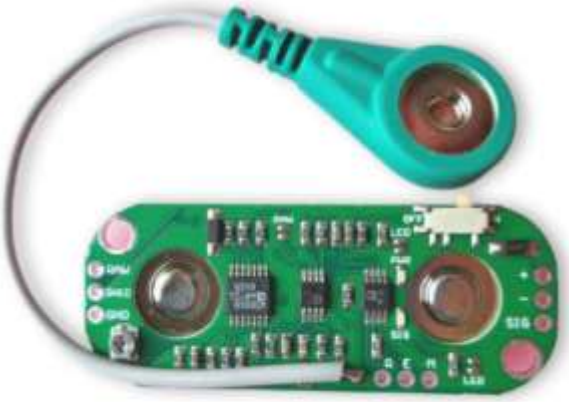

Power distribution was carefully managed through the integration of two 9 V 1100 mAh rechargeable batteries connected in parallel, ensuring a stable and reliable 9 V supply for the entire system. This voltage directly powered the main actuating components and served as the primary source for all essential subsystems. To provide safe and consistent power for sensitive electronics such as the ESP32 microcontroller and the EMG and pressure sensors, the 9 V supply was regulated down to a stable 5 V output using a 7805 MOSFET voltage regulator. The regulator was supported by two 10 µF capacitors to reduce voltage ripple and maintain steady performance across varying load conditions, ensuring consistent operation of all control and sensing circuits.

The device's massage functionality was implemented using a compact N20 gear motor, driven by an IRF744N motor driver. This motor was selected for its compact form factor, efficient torque output, and smooth operational characteristics, crucial for delivering consistent and controlled therapeutic massage motions. Its precise performance ensures gentle yet effective pressure, ideal for relieving discomfort associated with Carpal Tunnel Syndrome (CTS).

To effectively translate motor rotation into therapeutic massage motion, a custom-designed 3D-printed gear system was developed. The gear assembly precisely

converted the rotational output of the N20 motor into the desired linear and oscillating massage motion, optimizing contact pressure and coverage on the targeted wrist area. The use of 3D printing allowed rapid prototyping and iterative design improvements, resulting in an ergonomically shaped gear design tailored specifically to user comfort and therapeutic effectiveness.

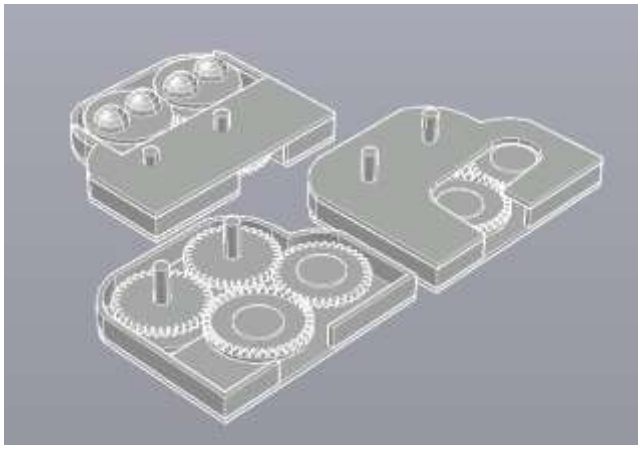

The automated strap adjustment system featured a 28BYJ-48 stepper motor, managed by a ULN2003 motor driver. This setup facilitated precise incremental adjustments of strap tension. Integrated feedback from a strategically placed pressure sensor allowed the system to autonomously adjust and maintain optimal therapeutic pressure, balancing effective wrist support and user comfort.

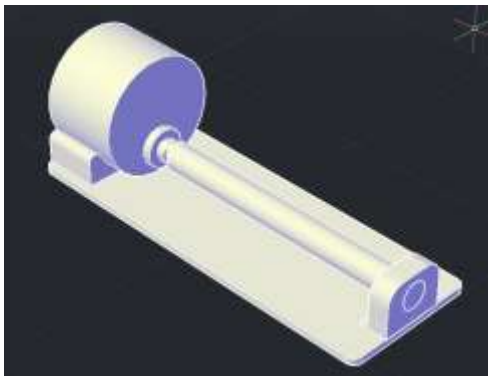

A compact, high-accuracy pressure sensor was integrated into the wrist splint to continuously monitor and manage strap tension. Strategically positioned on top of the forearm, this sensor provided real-time feedback on applied pressure, enabling automatic and precise adjustments of strap tightness. By maintaining consistent therapeutic compression, the sensor significantly improved comfort and effectiveness during prolonged device use.

User accessibility and feedback mechanisms were enhanced through the inclusion of a clearly positioned on/off switch, and an LED indicator for visual status updates, improving user interaction and safety.

To house all components, a custom 3D-printed casing was developed. This casing was designed to hold the wrist splint firmly, accommodating electronic components securely, protecting them from external factors, and maintaining user interaction. The use of straps ensured a snug fit.

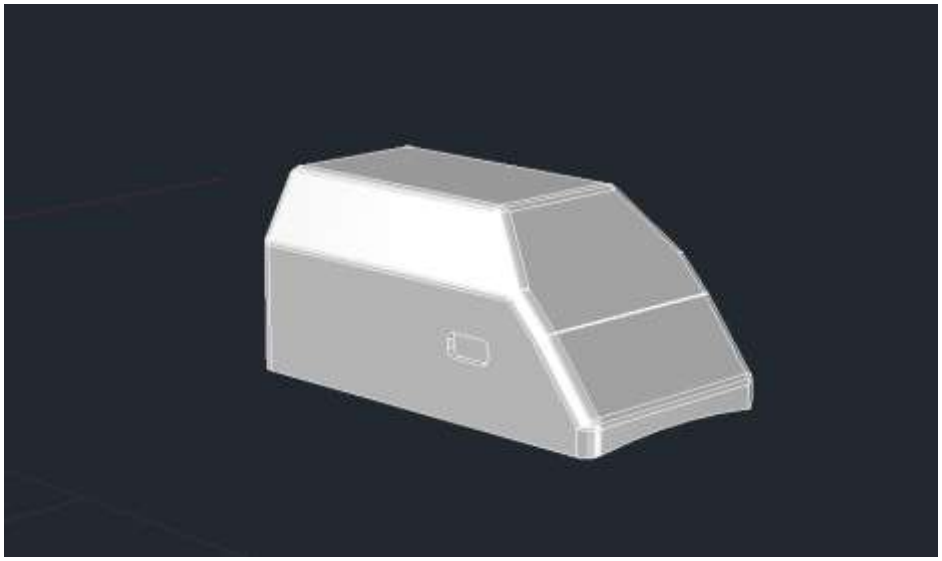

This systematic assembly process resulted in a compact, reliable, and user-friendly therapeutic device. The careful placement and robust integration of components effectively met the design objectives, ensuring the device provided both therapeutic relief and continuous support. Future assembly improvements may focus on optimizing internal wiring layouts, further enhancing modularity for simplified maintenance, and exploring lighter, stronger materials to improve user comfort and durability.

APPENDIX E

SIGNAL ACQUISITION RESULTS

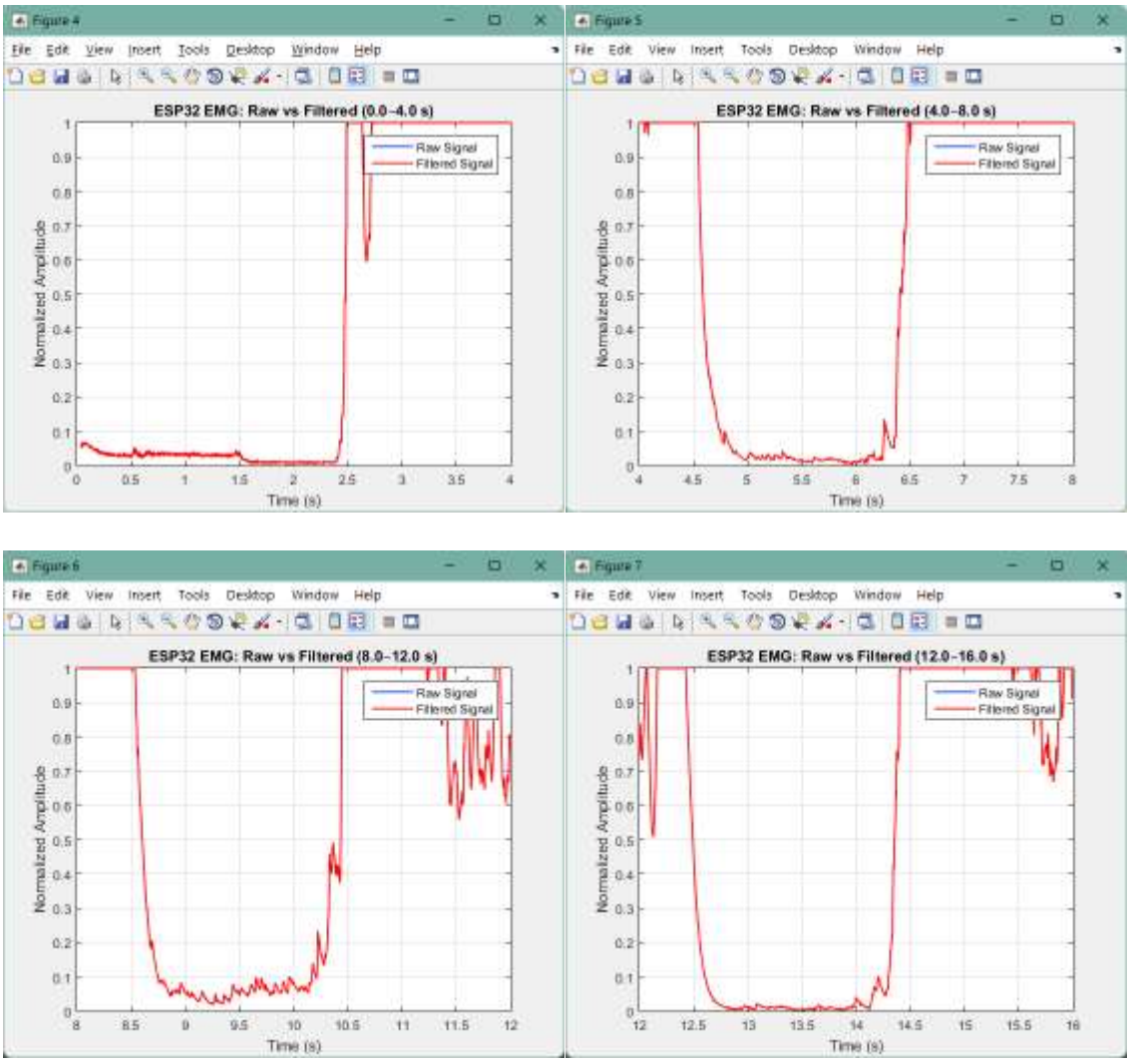

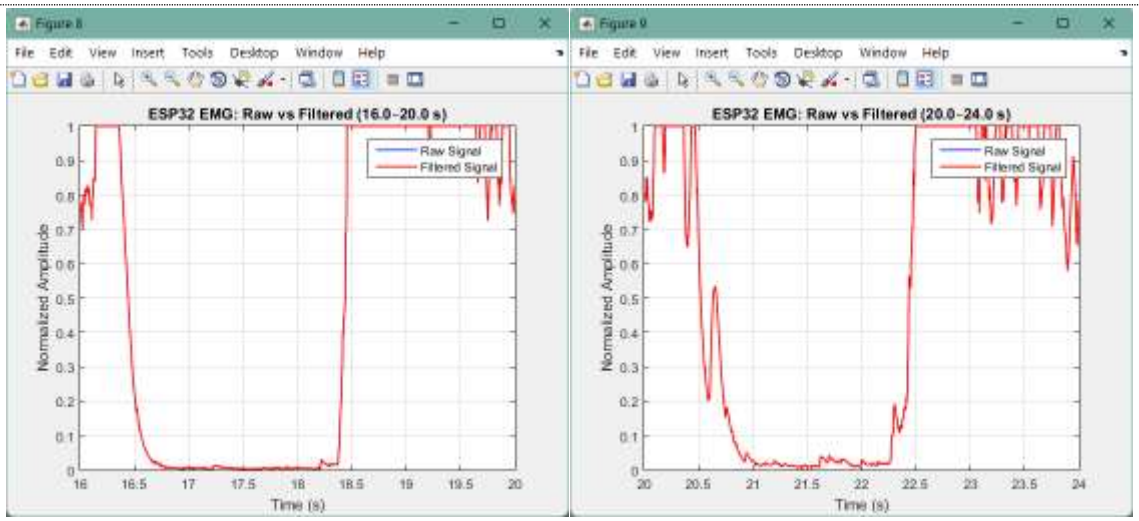
Figure 8
File Edit View Insert Tools Desktop Window Help
ESP32 EMG: Raw vs Filtered (16.0–20.0 s)
Raw Signal
Filtered Signal
Normalized Amplitude
Time (s)
Figure 9
File Edit View Insert Tools Desktop Window Help
ESP32 EMG: Raw vs Filtered (20.0–24.0 s)
Raw Signal
Filtered Signal
Normalized Amplitude
Time (s)

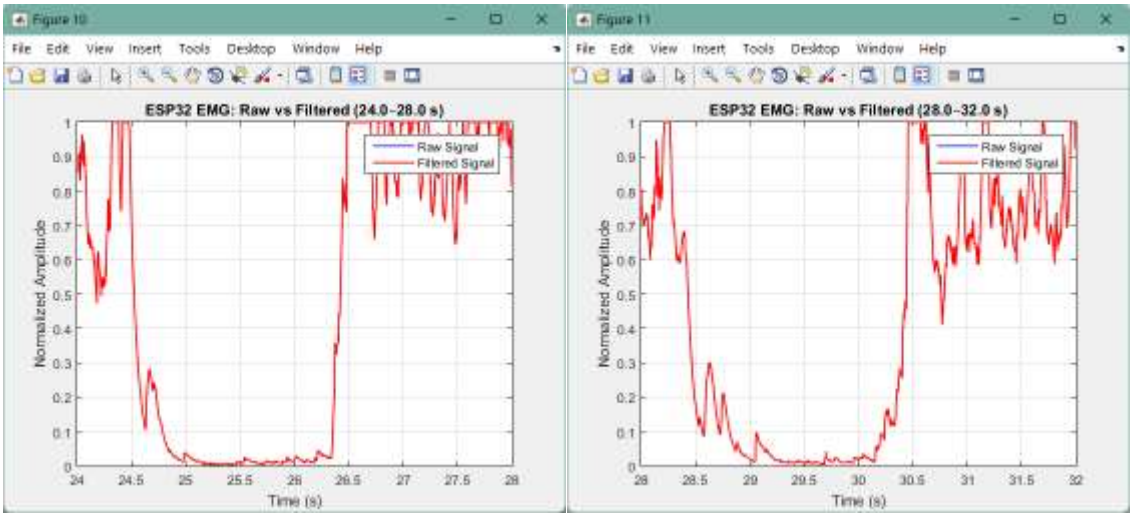
Figure 10
File Edit View Insert Tools Desktop Window Help
ESP32 EMG: Raw vs Filtered (24.0–28.0 s)
Raw Signal
Filtered Signal
Normalized Amplitude
Time (s)
Figure 11
File Edit View Insert Tools Desktop Window Help
ESP32 EMG: Raw vs Filtered (28.0–32.0 s)
Raw Signal
Filtered Signal
Normalized Amplitude
Time (s)

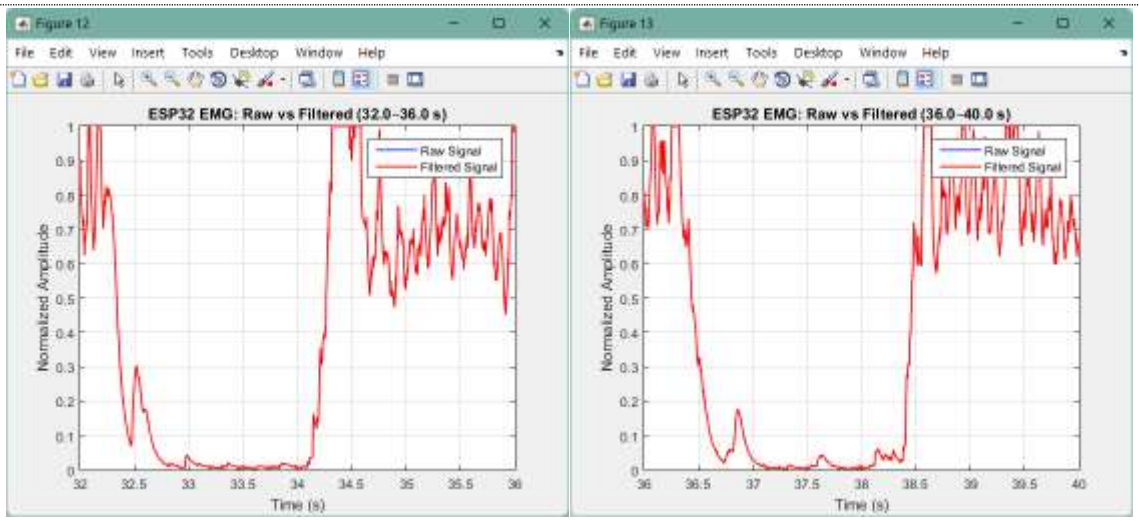
Figure 12
File Edit View Insert Tools Desktop Window Help
ESP32 EMG: Raw vs Filtered (32.0–36.0 s)
Raw Signal
Filtered Signal
Normalized Amplitude
Time (s)
Figure 13
File Edit View Insert Tools Desktop Window Help
ESP32 EMG: Raw vs Filtered (36.0–40.0 s)
Raw Signal
Filtered Signal
Normalized Amplitude
Time (s)

APPENDIX F

SIGNAL PROCESSING RESULTS

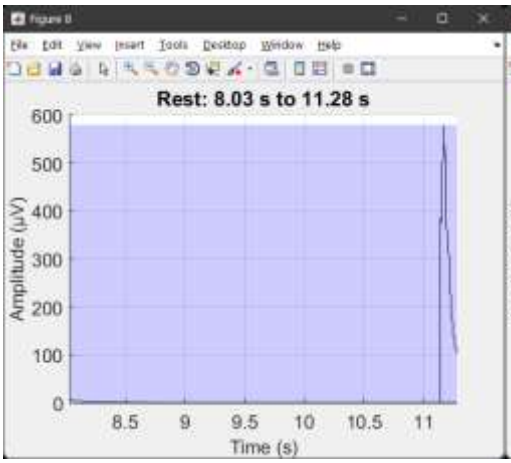

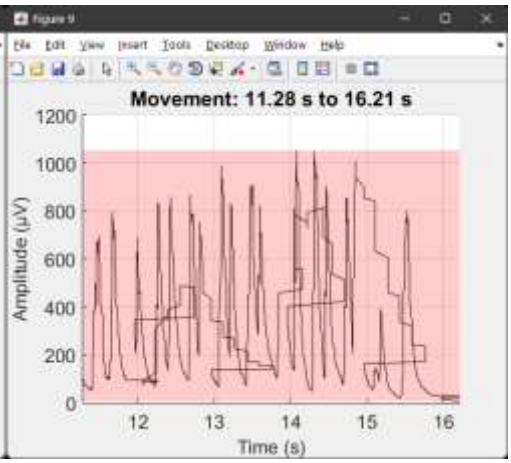

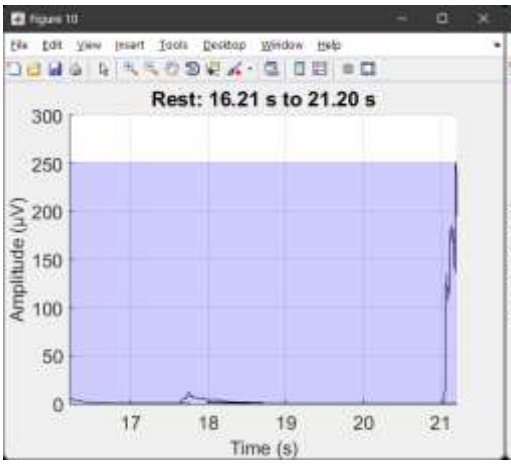

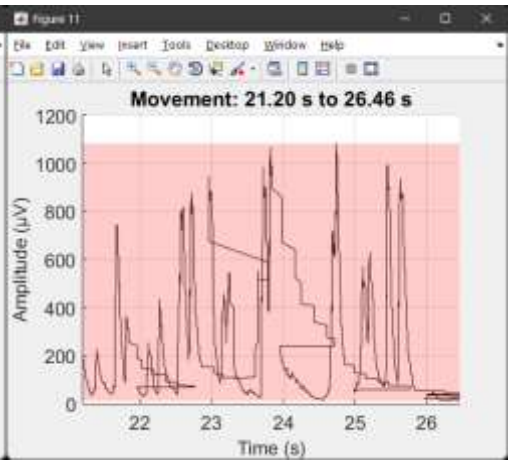

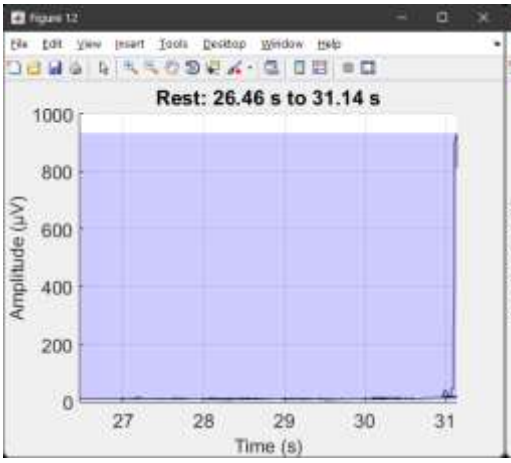

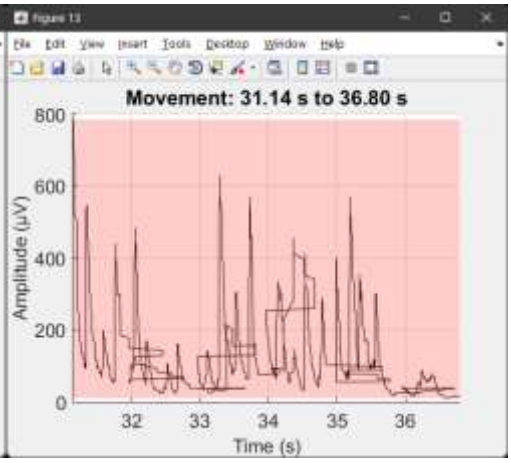

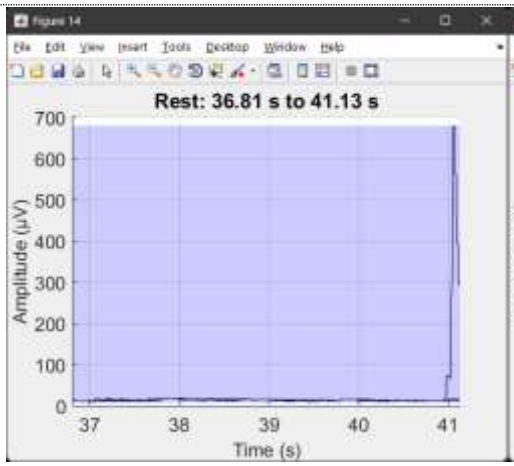
Rest: 36.81 s to 41.13 s
Amplitude (μV)
Time (s)

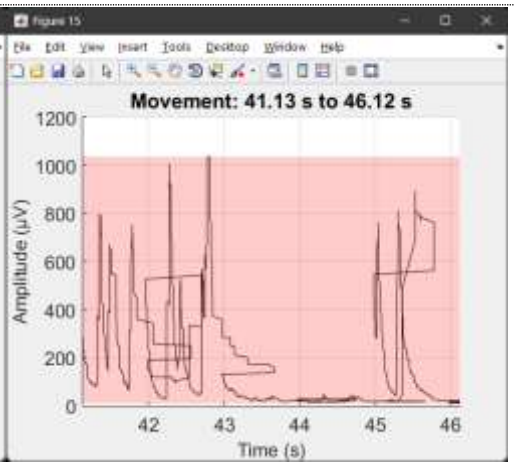
Movement: 41.13 s to 46.12 s
Amplitude (μV)
Time (s)

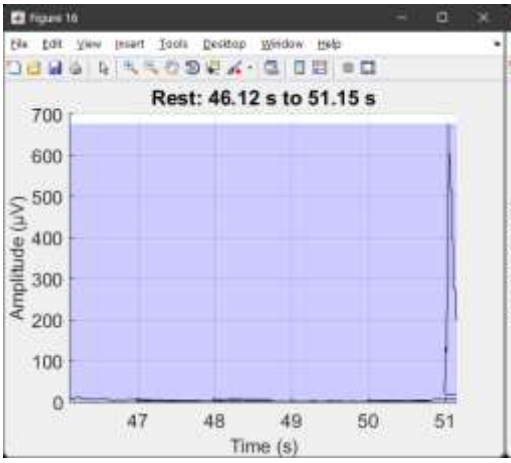
Rest: 46.12 s to 51.15 s
Amplitude (μV)
Time (s)

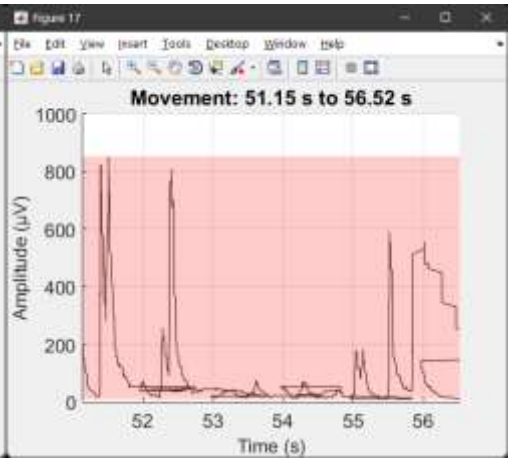
Movement: 51.15 s to 56.52 s
Amplitude (μV)
Time (s)

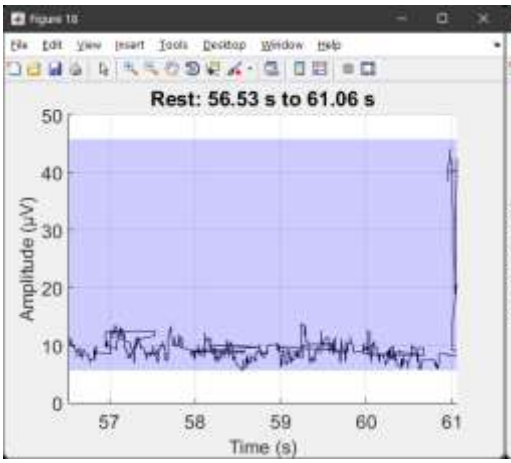
Rest: 56.53 s to 61.06 s
Amplitude (μV)
Time (s)

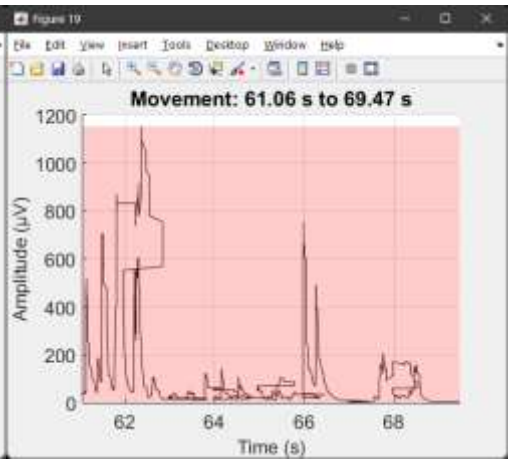
Movement: 61.06 s to 69.47 s
Amplitude (μV)
Time (s)

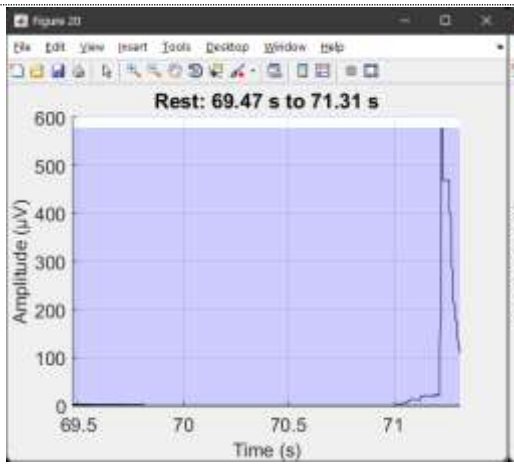
Rest: 69.47 s to 71.31 s
Amplitude (μV)
Time (s)

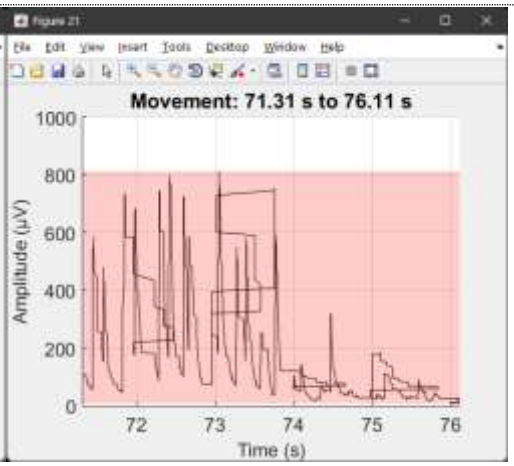
Movement: 71.31 s to 76.11 s
Amplitude (μV)
Time (s)

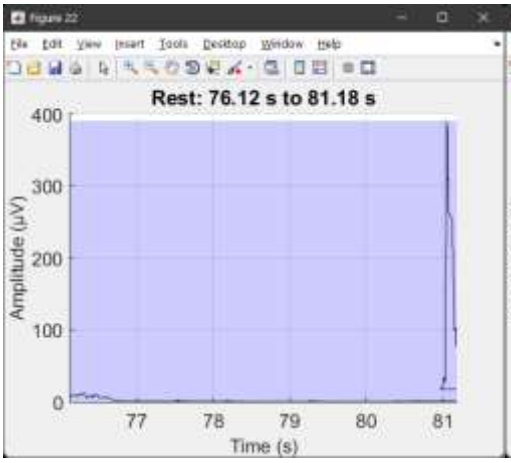
Rest: 76.12 s to 81.18 s
Amplitude (μV)
Time (s)

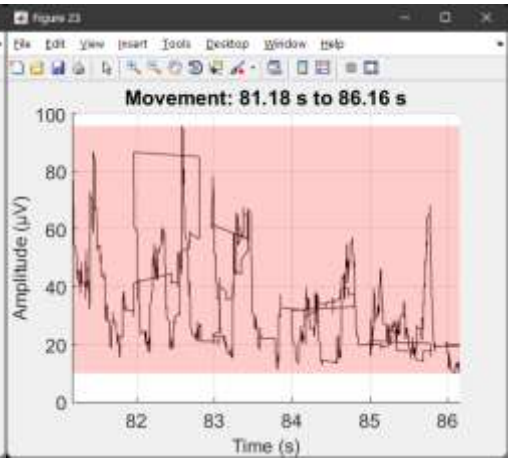
Movement: 81.18 s to 86.16 s
Amplitude (μV)
Time (s)

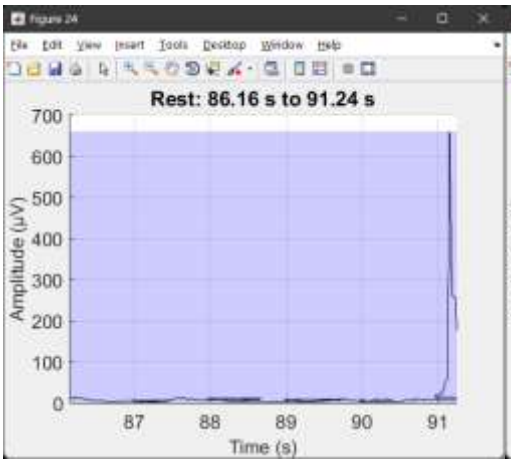
Rest: 86.16 s to 91.24 s
Amplitude (μV)
Time (s)

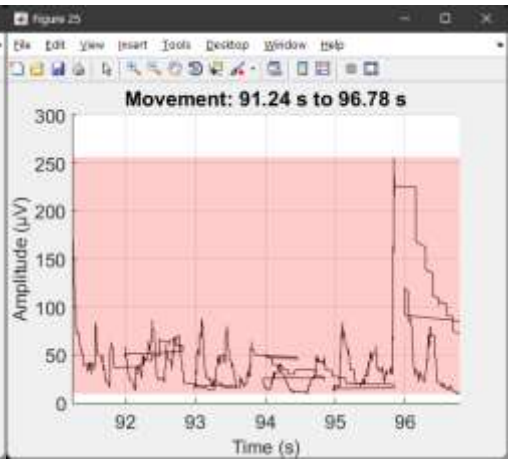
Movement: 91.24 s to 96.78 s
Amplitude (μV)
Time (s)

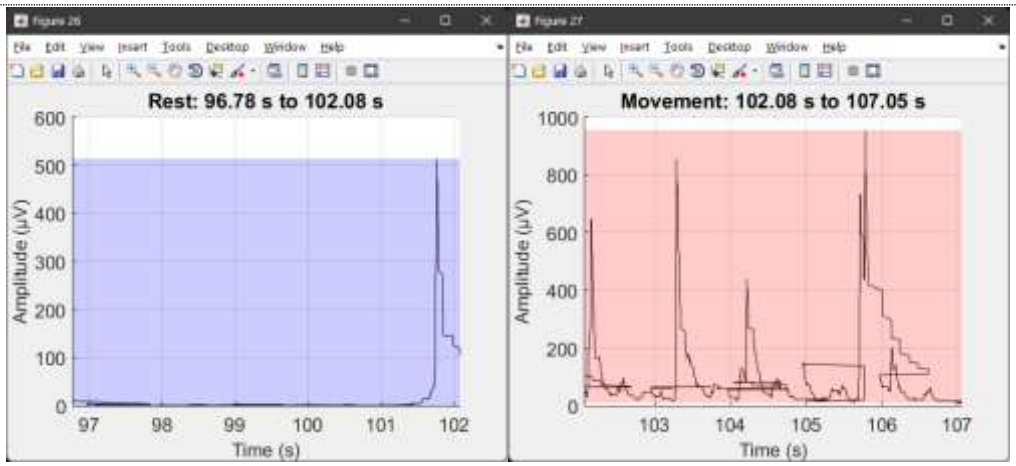
Rest: 96.78 s to 102.08 s
Amplitude (μV)
Time (s)
Movement: 102.08 s to 107.05 s
Amplitude (μV)
Time (s)

APPENDIX G

INTEGRATED MASSAGER RESULTS

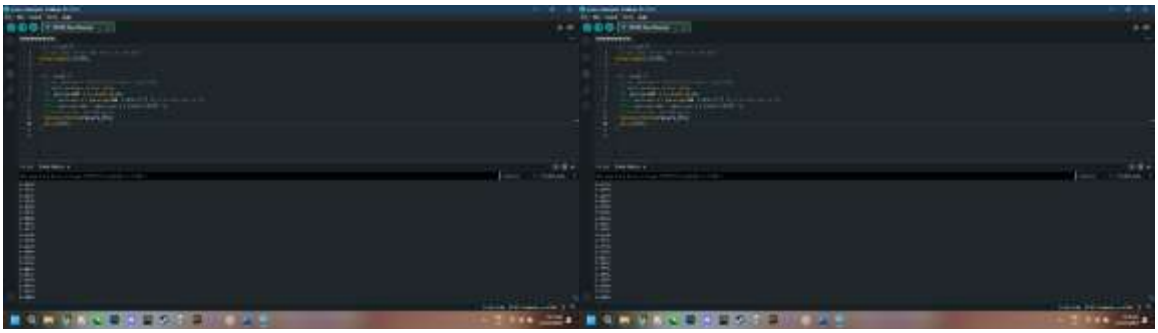

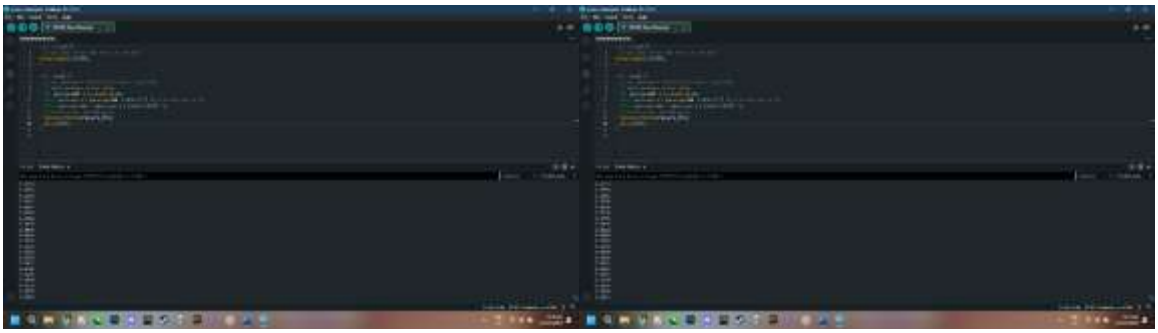

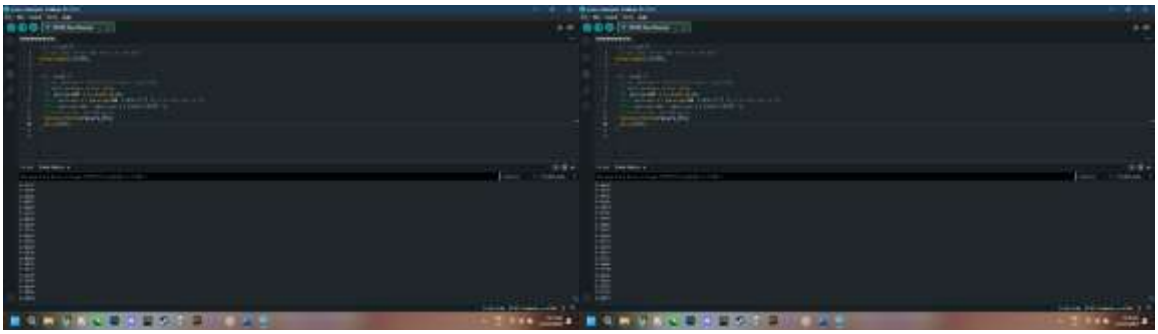

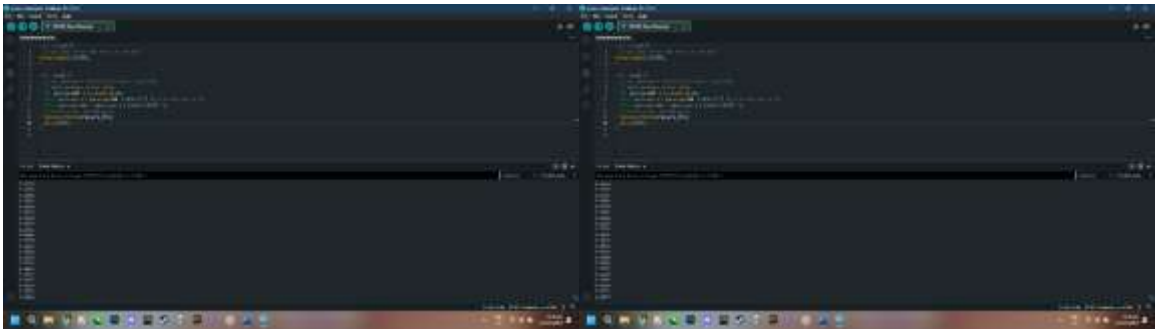

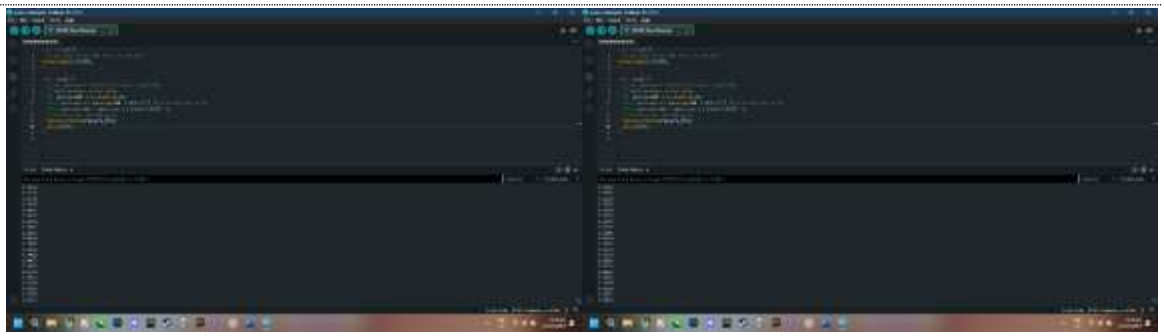

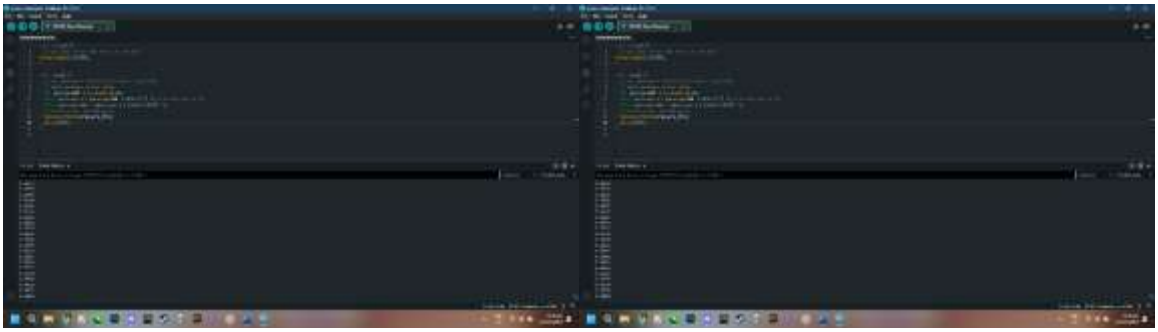

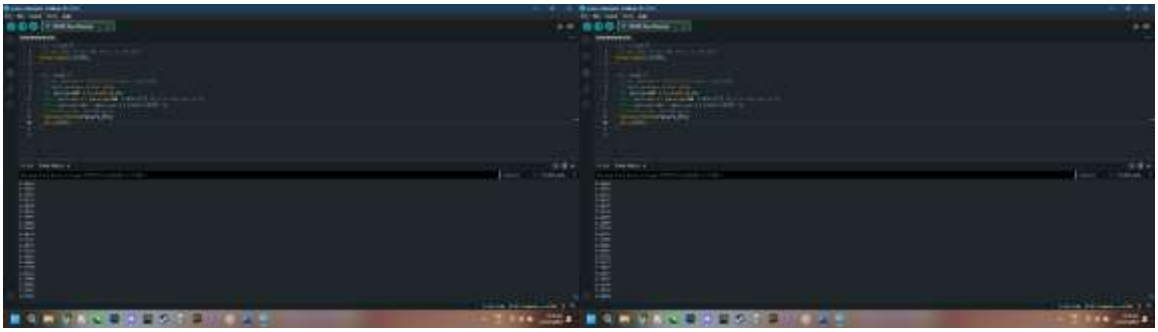

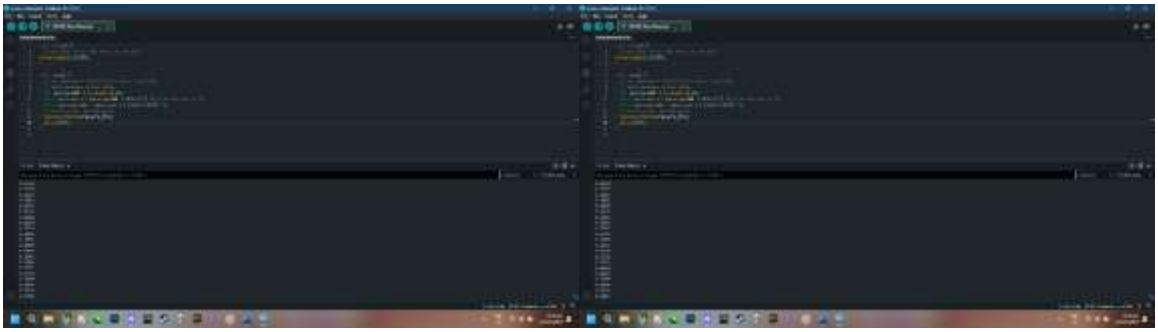

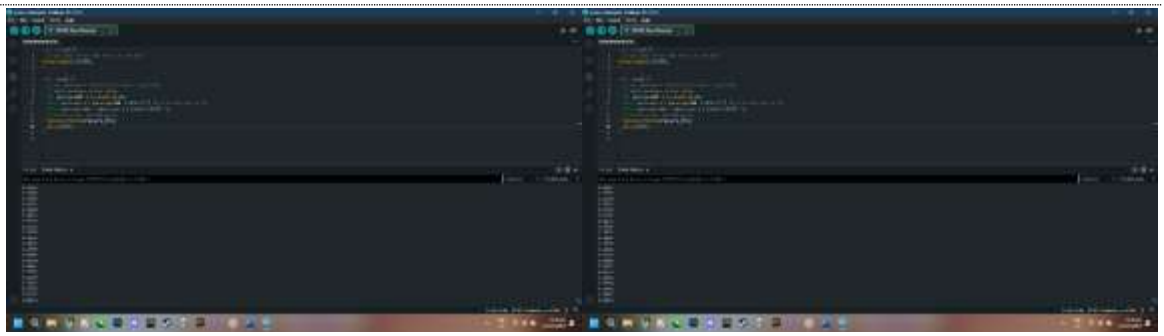

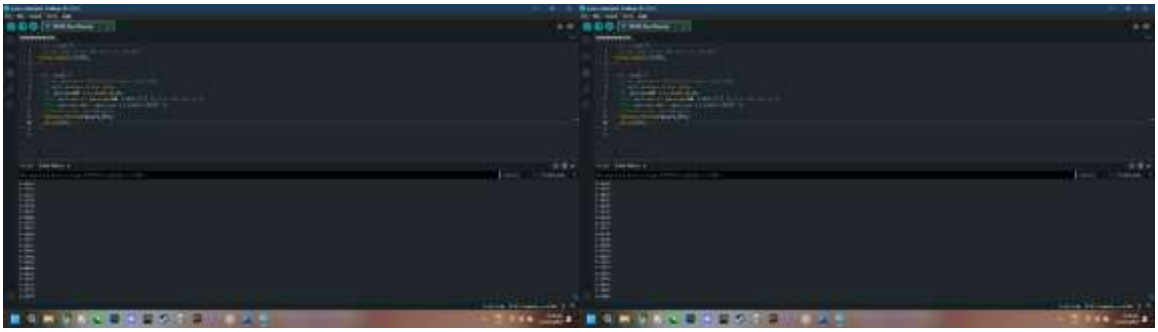

APPENDIX H

AUTO FIT MODULE RESULTS

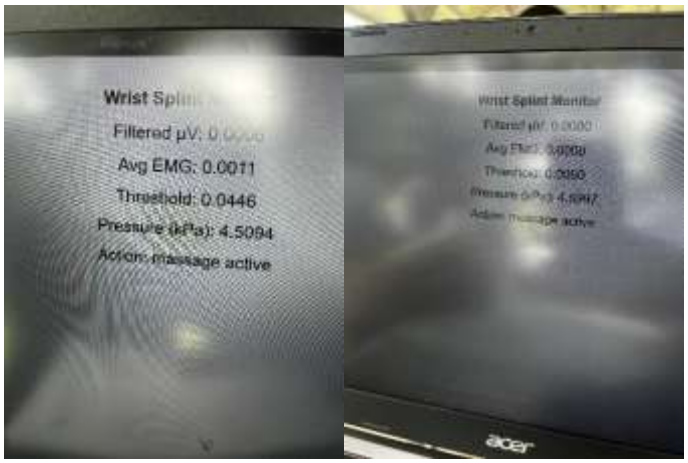

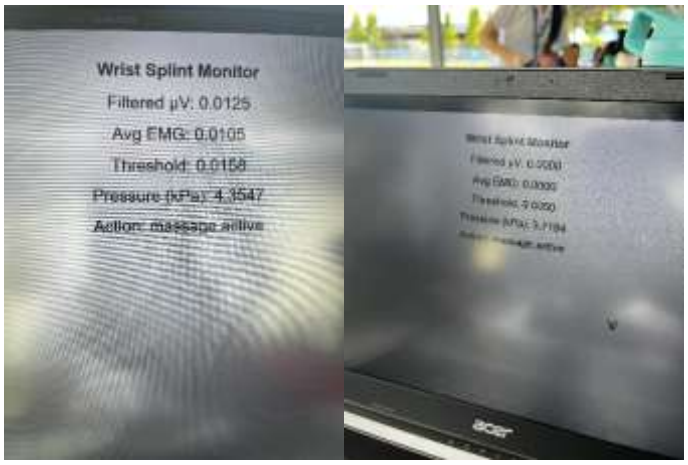

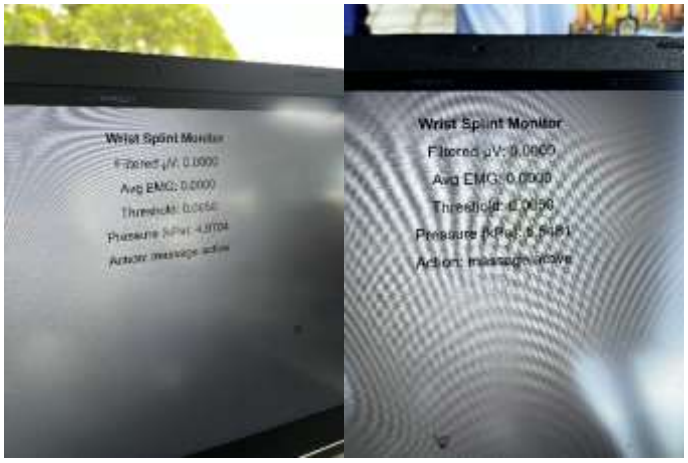


Wrist Splint Monitor
Filtered µV: 0.0000
Avg EMG: 0.0000
Threshold: 0.0050

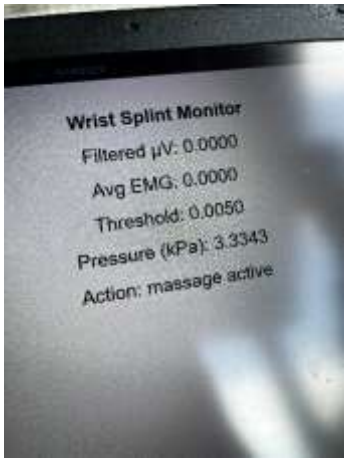
Wrist Splint Monitor
Filtered µV: 0.0000
Avg EMG: 0.0000
Threshold: 0.0050
Pressure (kPa): 3.3343
Action: massage active

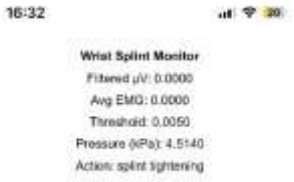
16:32
Wrist Splint Monitor
Filtered µV: 0.0000
Avg EMG: 0.0000
Threshold: 0.0050
Pressure (kPa): 4.5140
Action: splint tightening

APPENDIX I

MOTION SUPPORT MODULE RESULTS











APPENDIX J

REQUEST LETTER FOR ZCMC

• mc-chief@zcmc.doh.gov.ph
• doh9_zcmc@yahoo.com
991-2974 / 992-0052
LOCAL 002

Chezter P. Vargas
Ateneo de Zamboanga University
La Purisima Street, Zamboanga City
7000, Philippines
+63 966 044 9169

March 03, 2025

Afdal B. Kunting, MD, MPH, FPCP
Medical Center Chief II
Zamboanga City Medical Center
Dr. Evangelista St., Sta. Catalina, Zamboanga City
7000, Philippines

Dear Dr. Kunting,

Greetings of Peace!

I am Chezter Vargas, a fourth-year BS Biomedical Engineering student at Ateneo de Zamboanga University (AdZU). I am writing to formally request permission, along with my thesis partner, Mark Vincent G. Salupado, to conduct an on-site visit to the Biomedical Engineering Unit of Zamboanga City Medical Center (ZCMC) on Thursday, March 6, 2025. The primary purpose of this visit is to have a hands-on with the calibration weights and tachometer of the BME Unit, which are essential for calibrating the components of our thesis project.

Our thesis focuses on the development of an autonomous wrist splint designed to deliver therapeutic massage to individuals with Carpal Tunnel Syndrome (CTS) during periods of low muscle activity. The device integrates a lightweight massager within the splint to provide relief to individuals experiencing CTS symptoms.

We sincerely hope for your kind consideration and approval of this request. Please let us know if there are any requirements or procedures we need to fulfill before our visit. Thank you for your time and support.

Respectfully yours,

CHEZTER P. VARGAS
BS BME – IV Student

MARK VINCENT G. SALUPADO
BS CpE – IV Student

Noted by:

MUDZNAIDAN B. USAMA
Thesis Adviser

ENGR. JANET TAN
Chair, Engineering Department

RECEIVED
03-03-25
1:22 PM

APPENDIX K

PARTICIPANTS CONSENT FORM FOR BETA TESTING

Ateneo de Zamboanga University
College of Science, Information Technology, and Engineering

CONSENT FORM

I, _____, will voluntarily participate in the research project entitled "eM-Brace: Development of an Autonomous Wrist Splint with an Integrated Massage System for Alleviating Muscle Weakness Related to Carpal Tunnel Syndrome," which aims to evaluate the functionality of the developed wrist splint by gathering user feedback regarding its massage system, dynamic support, and overall usability. The purpose and procedures of the study have been explained to me by the study's proponents, and my questions have been satisfactorily answered. I understand that all data, including my name or any identifying information, collected during this study will be kept confidential and used only for research purposes.

_____ _____

Participant's Signature over Printed Name Date

Chezter P. Vargas
BSBME IV

Mark Vincent G. Salupado
BSCpE IV

APPENDIX L

PATIENT RATED WRIST EVALUATION FORM

Name: _____ Date: _____

PATIENT RATED WRIST EVALUATION

*The questions below will help us understand how much difficulty you have had with your wrist in the past week. You will be describing your **average** wrist symptoms **over the past week** on a scale of 0-10.* Please provide an answer for **ALL** questions. If you did not perform an activity, please **ESTIMATE** the pain or difficulty you would expect. If you have **never** performed the activity, you may leave it blank.

1. PAIN

Rate the **average** amount of pain in your wrist over the past week by circling the number that best describes your pain on a scale from 0-10. A zero **(0)** means that you **did not** have any pain and a **ten (10)** means that you had the **worst pain you have ever experienced** or that **you could not do the activity because of pain.**

RATE YOUR PAIN: Sample Scale →	0 No Pain	1	2	3	4	5	6	7	8	9	10 Worst Ever	
At rest	0	1	2	3	4	5	6	7	8	9	10	
When doing a task with a repeated wrist movement	0	1	2	3	4	5	6	7	8	9	10	
When lifting a heavy object	0	1	2	3	4	5	6	7	8	9	10	
When it is at its worst	0	1	2	3	4	5	6	7	8	9	10	
How often do you have pain?	0 Never	1	2	3	4	5	6	7	8	9	10 Always	

2. FUNCTION

A. SPECIFIC ACTIVITIES

*Rate the **amount of difficulty** you experienced performing each of the items listed below - over the past week, by circling the number that describes your difficulty on a scale of 0-10. A **zero** (0) means you did not experience any difficulty and a **ten** (10) means it was so difficult you were unable to do it at all.*

Sample scale →	0 No Difficulty	1	2	3	4	5	6	7	8	9	10 Unable To Do	
Turn a door knob using my affected hand	0	1	2	3	4	5	6	7	8	9	10	
Cut meat using a knife in my affected hand	0	1	2	3	4	5	6	7	8	9	10	
Fasten buttons on my shirt	0	1	2	3	4	5	6	7	8	9	10	
Use my affected hand to push up from a chair	0	1	2	3	4	5	6	7	8	9	10	
Carry a 10lb object in my affected hand	0	1	2	3	4	5	6	7	8	9	10	
Use bathroom tissue with my affected hand	0	1	2	3	4	5	6	7	8	9	10	

B. USUAL ACTIVITIES

*Rate the **amount of difficulty** you experienced performing your **usual** activities in each of the areas listed below, over the past week, by circling the number that best describes your difficulty on a scale of 0-10. By "usual activities", we mean the activities you performed **before** you started having a problem with your wrist. A **zero** (0) means that you did not experience any difficulty and a **ten** (10) means it was so difficult you were unable to do any of your usual activities.*

Personal care activities (dressing, washing)	0	1	2	3	4	5	6	7	8	9	10	
Household work (cleaning, maintenance)	0	1	2	3	4	5	6	7	8	9	10	
Work (your job or usual everyday work)	0	1	2	3	4	5	6	7	8	9	10	
Recreational activities	0	1	2	3	4	5	6	7	8	9	10	

APPENDIX M

BETA TESTING GRIP STRENGTH MEASUREMENTS

Participant 1

Participant 2

Participant 3

Participant 4

Participant 5

Participant 6

Participant 7

Participant 8

Participant 9

Participant 10

Participant 11

Participant 12

Participant 13

Participant 14

Participant 15

APPENDIX N

BETA TESTING DOCUMENTATION

Participant 1

Participant 2

Participant 3

Participant 4

Participant 5

Participant 6

Participant 7

Participant 8

Participant 9

Participant 10

Participant 11

Participant 12

Participant 13

Participant 14

Participant 15

APPENDIX O

TOTAL EXPENSES

eM-Brace Wrist Splint				
THESIS PROPOSAL BUDGET				
AUG 2024 - NOV 2024				
ITEM	**QTY.**	**UNIT**	**PRICE**	**TOTAL**
ESP32 38P	1	pc	₱349.00	₱349.00
Myoware 2.0 Muscle Sensor	1	pc	₱2,547.00	₱2,547.00
Myoware 2.0 Muscle Sensor (diff price)	1	pc	₱2,349.00	₱2,349.00
Gears	1	set	₱86.00	₱86.00
Sparkfun Surface Electrodes (10 pcs/pack)	1	pck	₱689.00	₱689.00
3D print gears	1	set	₱400.00	₱400.00
Panelist Fees	3	pax	₱700.00	₱2,100.00
3D print redesigned gears	1	set	₱750.00	₱750.00
Panelist Fees (redefense)	3	pax	₱300.00	₱900.00
JAN 2025 - APR 2025				
CTS Wrist Splint	1	pc	₱650.00	₱650.00
EMG Electrodes (10 pcs/pack)	1	pck	₱729.00	₱729.00
EMG Electrodes (50 pcs/pack)	1	pck	₱5,045.00	₱5,045.00
Pressure Sensor FSR402	1	pc	₱300.00	₱300.00
Stepper Motor	3	pairs	₱71.00	₱213.00
Strap	2	pcs	₱16.00	₱32.00
3.7V lit-ion Battery 2pcs	1	pc	₱220.00	₱220.00
Dynamometer	1	pc	₱773.00	₱773.00
Goniometer	1	pc	₱155.00	₱155.00
DRV8825 Stepper Motor Driver	3	pcs	₱57.00	₱171.00
SF45-65 Square-Shape Pressure Sensor	1	pc	₱264.00	₱264.00
3d print (overall, can change overtime)	1	pc	₱470.00	₱470.00
velcro	1	pc	₱50.00	₱50.00
Stepping Gear Motor GM1024-10BY	2	pcs	₱165.00	₱330.00
AD8226 Muscle Sensor	1	pc	₱893.00	₱893.00
Myoware Muscle Sensor Sen-13723	1	pc	₱4,077.00	₱4,077.00
N20 gear motor	2	pcs	₱192.00	₱384.00
Micro Metal Geared Stepper Motor-12V 0-6kg-cm	1	pc	₱565.00	₱565.00
TOTAL				**₱25,491.00**